

ANALYSIS OF DIVERGENT FLOW TRACER TESTS IN
FRACTURED GRANITE, NEAR ORACLE, ARIZONA

by

Alan William Aikens

A Thesis Submitted to the Faculty of the
DEPARTMENT OF HYDROLOGY AND WATER RESOURCES
In Partial Fulfillment of the Requirements
For the Degree of

MASTER OF SCIENCE
WITH A MAJOR IN HYDROLOGY

In the Graduate College
THE UNIVERSITY OF ARIZONA

1 9 8 6

STATEMENT BY AUTHOR


This thesis has been submitted in partial fulfillment of requirements for an advanced degree at The University of Arizona and is deposited in the University Library to be made available to borrowers under rules of the Library.

Brief quotations from this thesis are allowable without special permission, provided that accurate acknowledgment of source is made. Requests for permission for extended quotation from or reproduction of this manuscript in whole or in part may be granted by the head of the major department or the Dean of the Graduate College when in his or her judgment the proposed use of the material is in the interests of scholarship. In all other instances, however, permission must be obtained from the author.

SIGNED: 

APPROVAL BY THESIS DIRECTOR

This thesis has been approved on the date shown below:


Shlomo P. Neuman
Professor of Hydrology
and Water Resources

May 28, 1986
Date

ACKNOWLEDGMENTS

This thesis represents the culmination of much work. Many people have contributed to its end whom I wish to thank. Jesus Carrera developed the original computer code and is responsible for much of the theoretical development. Deepest appreciation goes out to Dr. Shlomo Neuman, my principal advisor, for his effort, guidance and understanding throughout the research period. Drs. Eugene Simpson and Daniel Evans, whose advice on the preparation of the final manuscript was invaluable, I thank. Many thanks go out to the field group: Martin Barackman, Steve Silliman, Andy Messer, Tim Leo, Jim Posedly, Joe Depner, and Gordon Wittmeyer, without whom the field work could not be done.

I wish to thank Marie Busse-Engles for preparation of the figures in the text, and Sally Adams for final preparation of this thesis. I also wish to give appreciation to the U. S. Nuclear Regulatory Commission, which provided the funding that allowed me to be part of this unique learning experience.

Finally, I thank those closest to me: my parents, who raised me with a yearning to learn and explore the unfamiliar. And lastly, Sandy, my wife, who went with me from east to west and back again, my love.

TABLE OF CONTENTS

	Page
LIST OF FIGURES	vi
LIST OF TABLES	xiii
ABSTRACT	ix
1. INTRODUCTION	1
1.1 Advective-Dispersive Processes	1
1.2 Field Applications of Advection-Dispersion Theory	6
1.2.1 Uniform Flow	7
1.2.2 Recirculation Tests	10
1.2.3 Radial Flow Tracer Tests	10
1.2.3.1 Single-well Test	12
1.2.3.2 Convergent Flow Tests	14
1.2.3.3 Divergent Flow Test	17
1.2.4 Discussion of Tracer Tests	18
1.3 Scope of Thesis	21
2. THEORY	24
2.1 Lagrangian Form of Governing Equation	24
2.2 Mixing and Sampling in the Monitoring Borehole	25
2.3 Numerical Approach	28
2.4 Stability and Convergence	34
3. DESCRIPTION OF MODEL AND SENSITIVITY STUDIES	35
3.1 The Model	35
3.1.1 Modes of Operation	35
3.1.2 Types of Input Concentration	36
3.2 Sensitivity Analyses	37
3.2.1 Effect of Grid Size	39
3.2.2 Effect of External Boundary Location	40
3.2.3 Comparison of Numerical Solution with Analytical Solutions	47
3.2.4 Effect of Velocity	52
3.2.5 Effect of Peclet Number	52
3.2.6 Effect of Mixing in Monitoring Borehole	54

TABLE OF CONTENTS--Continued

	Page
4. ANALYSIS OF DIVERGENT FLOW TRACER TEST DATA FROM ORACLE, ARIZONA	59
4.1 Site Description	59
4.2 Field Test Procedure	63
4.3 Analysis of Tracer Test Data Using DBDIV	72
4.4 Recommendations for Conducting Divergent Flow Tracer Tests	78
5. CONCLUSIONS	80
APPENDIX A: DIVERGENT FLOW TRACER TEST DATA, JULY 15-16, 1985	83
APPENDIX B: TEMPERATURE AND FLOW METER DATA	88
APPENDIX C: USERS GUIDE	94
APPENDIX D: LISTING OF COMPUTER CODE	114
REFERENCES	136

LIST OF ILLUSTRATIONS

Figure		Page
1.1	Inflow Boundary Conditions	5
1.2	Dispersion of a Solute Continuously Injected from a Well into Two-Dimensional Aquifer	8
1.3	Flow Field Established by a Recharging and a Discharging Well Pair	11
1.4	Typical Breakthrough Curve for Withdrawal Phase of Single-Well Test	13
1.5	Typical Breakthrough Curve for Method of Mandel et al. (1985)	15
1.6	Radial Flow Fields	16
1.7	Typical Breakthrough Curve at Observation Well During Injection Phase of Single-Well Test	19
2.1	Diagram of Flow Tube	27
2.2	Grid Construction	29
2.3	Dispersive Fluxes Into and Out of a Cell	31
3.1	Effect of Grid Size on Computed Breakthrough	41
3.2	Effect of External Boundary Location on Computed Breakthrough	43
3.3	Mass Accumulation at External Boundary Affecting Concentration at Monitoring Borehole, $R = 2r_I$	44
3.4	Mass Accumulation at External Boundary Affecting Concentration at Monitoring Borehole, $R = 4r_I$	45
3.5	Comparison of Analytical Solution of Raimondi et al. with Numerical Solution for $Pe = 1, 10$ and 100	48
3.6	Comparison of Analytical Solution of Hoopes and Harleman with Numerical Solution for $Pe = 1, 10$ and 100	49

LIST OF ILLUSTRATIONS--Continued

	Page	
3.7	Comparison of Analytical Solution of Dagan with Numerical Solution for $Pe = 1, 10$ and 100	51
3.8	Effect of Peclet Number	53
3.9	Effect of Mixing in Monitoring Borehole, $Pe = 10$	55
3.10	Effect of Mixing in Monitoring Borehole, $Pe = 1$	56
3.11	Effect of Mixing in Monitoring Borehole, $Pe = 0.1$	57
4.1	Topographic Map of Northern Santa Catalina Mountains . .	60
4.2	Diagram of the Oracle Site	61
4.3	Diagram of Divergent Flow Tracer Test Equipment	64
4.4	Temperature Change in H2 While Injecting into H3 (8/12/85)	66
4.5	Temperature Change in M1 While Injecting into H3 (8/12/85)	67
4.6	Vertical Flow Rates in H2 While Injecting into H3 . . .	70
4.7	Vertical Flow Rates in M1 While Injecting into H3 . . .	71
4.8	Uncorrected Curve Match	73
4.9	Corrected Curve Match	76

LIST OF TABLES

Table		Page
3.1	Standard Input Data for Sensitivity Analyses	38
3.2	External Boundary Placement Data	46
3.3	External Boundary Placement at Various Pe	46
4.1	Boreholes at Field Site	62
4.2	Results of Uncorrected Curve Match	75
4.3	Results of Corrected Curve Match	77

ABSTRACT

A computer model is extended and applied to analyze divergent flow tracer test data from a field experiment near Oracle, Arizona. The model can accommodate a pulse, step increase, and an arbitrary distribution of injection concentration with respect to time. The model is tested against three analytical solutions and is subjected to sensitivity analyses. The model is free of numerical dispersion with proper grid spacing and location of the external boundary. Analysis of field data using the model involves a curve matching procedure. An equivalent radial flow field is used to account for non-radial flow conditions by adjusting the flow rate and the mass that enters the flow field. Application of the model to field data yields a longitudinal dispersivity of 5.08 meters and a product of effective porosity and thickness of 0.009 meters. Since the test was not conducted under strict flow conditions, the above results are considered tentative.

CHAPTER 1

INTRODUCTION

Chemical movement in subsurface waters has gained attention through evidence that the quality of the groundwater supply is deteriorating as the result of human activity. Landfills, deterioration of gasoline storage tanks, municipal and industrial waste injection among other things have been identified as contributors to the problem. Now proposals have been developed to store nuclear waste deep in low permeability geologic formations. Clearly these situations provide impetus for research about the processes by which chemicals are transported through the subsurface.

This thesis deals with movement of chemical compounds that are dissolved in groundwater in a saturated medium. The chemicals are assumed to be conservative, meaning they do not react with each other nor do they adsorb onto the rock.

1.1 Advective-Dispersive Processes

Dissolved compounds are transported by several mechanisms: advection, mechanical dispersion, and diffusion. Continuity of a solute transported by groundwater requires

$$\partial C / \partial t = -\nabla \cdot \underline{J} + S \quad (1.1)$$

\underline{J} = vector of mass flux

S = source/sink term

C = concentration

t = time

\underline{J} is the combination of advective, diffusive and dispersive mass fluxes

$$\underline{J} = \underline{J}_A + \underline{J}_D \quad (1.2)$$

\underline{J}_A = advective mass flux

\underline{J}_D = diffusive and dispersive mass flux

The advective flux is

$$\underline{J}_A = \underline{V}C \quad (1.3)$$

where \underline{V} is the seepage velocity vector defined as

$$\underline{V} = \underline{q}/\phi \quad (1.4)$$

\underline{q} = Darcy flux vector

ϕ = effective porosity

Dispersive mass flux is commonly expressed in analogy to Fick's law as

$$\underline{J}_D = -\underline{\underline{D}}' \nabla C \quad (1.5)$$

Where $\underline{\underline{D}}'$ is the tensor of hydrodynamic dispersion. It combines the effects of molecular diffusion and mechanical dispersion

$$\underline{\underline{D}}' = \underline{\underline{I}}D^* + \underline{\underline{D}} \quad (1.6)$$

$\underline{\underline{I}}$ = identity matrix

D^* = coefficient of molecular diffusion

$\underline{\underline{D}}$ = tensor of mechanical dispersion

Molecular diffusion describes the movement of dissolved substance by its own thermokinetic energy. Movement is toward reduced concentration gradients of the solute. Diffusion occurs even in the absence of bulk fluid movement and whose affect ceases only when concentration gradients in space do not exist.

Mechanical dispersion is conventionally represented as the product of dispersivity and the modulus of seepage velocity

$$\underline{D} = \underline{a}V \quad (1.7)$$

where $V = |\underline{V}|$

Dispersivity, \underline{a} , is a tensor depending on the degree of heterogeneity and anisotropy of the medium, as well as on the seepage velocity.

Substitution of these equations into (1.1) yields

$$\partial C / \partial t = -\nabla \cdot [\underline{V}C - (\underline{ID}^* + \underline{a}V)\nabla C] + S \quad (1.8)$$

Expanding the first term on the right-hand side of (1.8) gives

$$\nabla \cdot (\underline{V}C) = \underline{V} \cdot \nabla C + C \nabla \cdot \underline{V} \quad (1.9)$$

$\underline{V} \cdot \nabla C$ is the projection of the velocity vector along the concentration gradient. It describes the effect of the seepage velocity in advecting the solute mass. $C \nabla \cdot \underline{V}$ describes the magnitude of the change of velocity into and out of the system. By assuming that the fluid is incompressible, flow takes place at steady state without sinks or sources, and that the effective porosity is constant, this term vanishes by virtue of mass conservation. Assuming further that there are no sinks

or sources of solute, the conventional form of the advection-dispersion equation is obtained,

$$\frac{\partial C}{\partial t} = \nabla \cdot (\underline{D}^* + a\underline{V}) C - \underline{V} \cdot \nabla C \quad (1.10)$$

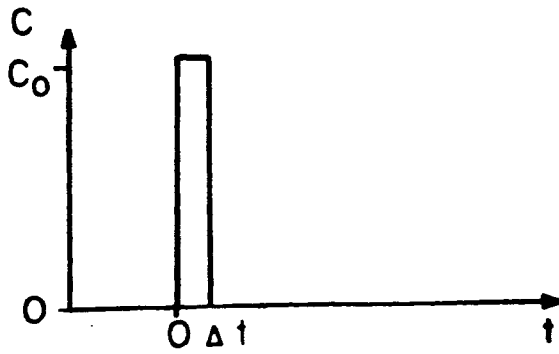
Application of (1.10) to solute transport problems requires initial and boundary conditions. Initial conditions describe the distribution of the solute in the system prior to an experiment. Often, it is assumed that the solute concentration is zero everywhere, unless the solute is known to exist in the groundwater. The known concentration distribution in space is then used to define the initial conditions. In mass transport problems two flow boundaries exist: the inflow boundary and the outflow boundary. (No-flow boundaries are of no consequence for this application.) They describe how the solute enters and exits the flow system. Three inflow boundary conditions commonly used are a square pulse, a square step increase, or an arbitrary distribution of solute concentration with respect to time. These are shown graphically in Figures 1.1 a, b, and c, respectively.

The outflow boundary is conventionally described as a non-dispersive flux boundary condition,

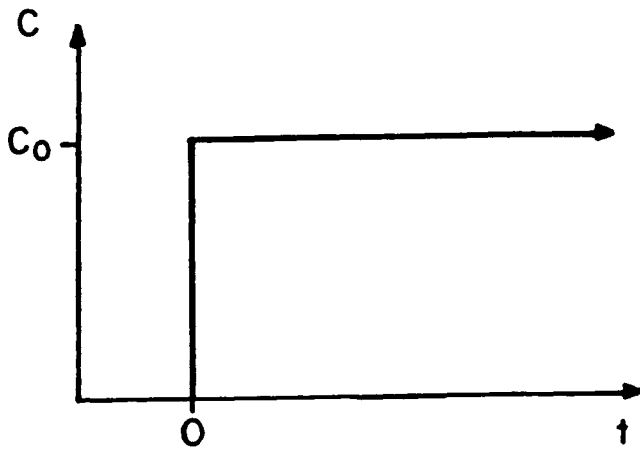
$$\underline{D} \nabla C \cdot \underline{n} = 0 \quad (1.11)$$

where \underline{n} is a unit vector normal to the boundary. The solute is advected across the boundary but not dispersed.

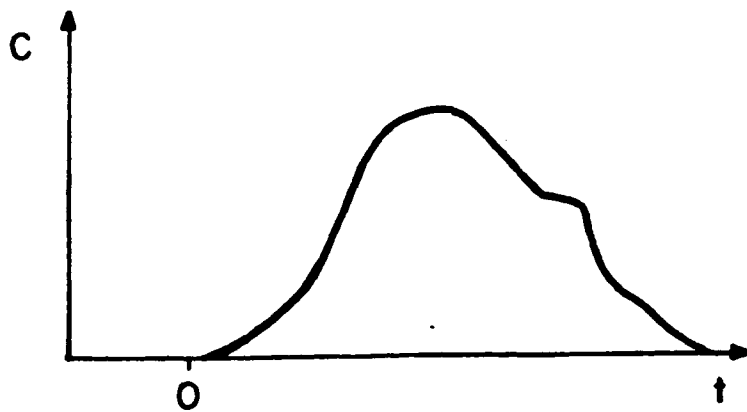
To solve the advection-dispersion equation subject to given initial and boundary conditions, the velocity field of the flow system



a. Square Pulse Inflow Boundary Condition



b. Square Step Increase Inflow Boundary Condition



c. Arbitrary Time Variation of Concentration

Figure 1.1. Inflow Boundary Conditions.

must be defined. This is usually done by applying Darcy's law when the distribution of hydraulic heads is known,

$$\underline{q} = -\underline{K}\nabla h \quad (1.12)$$

\underline{K} = hydraulic conductivity tensor

h = hydraulic head

Seepage velocity, \underline{v} , is found by applying (1.4) to (1.12).

In this section, a general form of the advection-dispersion equation was developed from conservation of mass principles. A discussion on the application of this equation was included. It is now appropriate to cite a few examples of how researchers have applied the equation to solve solute transport problems in the field.

1.2 Field Applications of Advection-Dispersion Theory

A field experiment in which man-made substances are used to quantify the transport properties of a groundwater system is called a tracer test. A tracer is introduced into a groundwater flow system at one location and the concentration of the tracer is monitored at one or more locations. Concentration data are analyzed to provide transport parameters such as dispersivity and effective porosity of the medium.

Several methods to perform and interpret tracer tests are presented in the literature. They are commonly characterized by the type of flow system prevailing in the medium. Five types of tracer tests are described in this thesis. The flow field is assumed to be at steady-state for all cases.

1.2.1 Uniform Flow

Hydrodynamic transfer of a tracer in a homogeneous, isotropic aquifer of constant thickness is described by an expansion of (1.10) in the x, y plane

$$\frac{\partial C}{\partial t} = a_L V \frac{\partial^2 C}{\partial x^2} + a_T V \frac{\partial^2 C}{\partial y^2} - V \frac{\partial C}{\partial x} \quad (1.13)$$

a_L, a_T = longitudinal and transverse dispersivity,
respectively

V = modulus of seepage velocity

Equation (1.13) assumes that the x -axis is parallel to the direction of flow and that D^* is negligible compared to mechanical dispersion.

Consider that a tracer of constant concentration, C_0 , is injected at a constant rate, Q , through a fully penetrating borehole into the aquifer. The dispersion takes place as shown in Figure 1.2. Fried (1975) provides several solutions to (1.13) for a slug injection of tracer and for continuous injection of tracer at constant concentration. However, these solutions require knowledge of the magnitude of transverse dispersivity. Harleman and Rumer (1963) give a relationship between longitudinal and transverse dispersivity

$$a_L/a_T = FR^n \quad (1.14)$$

F, n = dimensionless coefficients depending on the
pore geometry

R = Reynolds number based on seepage velocity

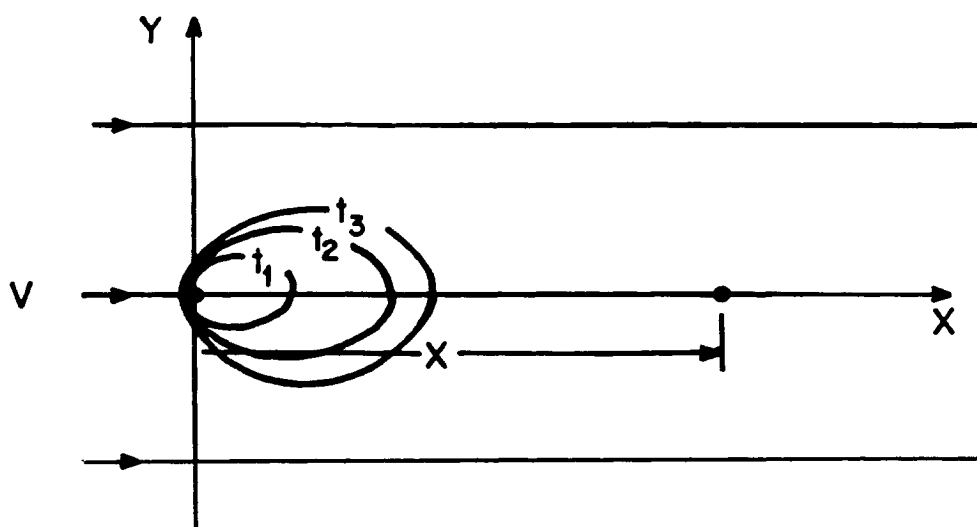


Figure 1.2. Dispersion of a Solute Continuously Injected from a Well into Two-Dimensional Aquifer.

This relationship is empirical, and field application of this concept is uncommon.

Many times researchers neglect the effect of transverse dispersion for field applications and approach the problem as one-dimensional (Sauty, 1980). The one-dimensional form of the advection-dispersion equation is

$$\partial C / \partial t = D \partial^2 C / \partial x^2 - v \partial C / \partial x \quad (1.15)$$

where $D = \alpha v$. Some authors indicate that mechanical dispersion is better described as αv^m , where m is an empirically determined constant between 1 and 2 (Freeze and Cherry, 1979).

In reality, the tracer mass is dispersed parallel and perpendicular to the direction of flow, resulting in a tracer cloud that is ellipsoidal in shape. By neglecting transverse dispersion in the one-dimensional model, longitudinal dispersion must be overestimated to describe the one-dimensional concentration front as it passes by an observation point (Domenico and Robbins, 1984). Commonly, data from uniform flow tracer tests are analyzed using analytical solutions derived from the one-dimensional form of the advection-dispersion equation, (1.15). Analytical solutions of this type are described by Rifai, et al. (1956); Ebach and White (1958); Ogata and Banks (1961); and Ogata (1970), among others, for slug and step increases of injection concentration.

1.2.2 Recirculation Tests

Tracer tests have been conducted in flow systems generated by a recharge-discharge borehole pair (hereafter called recirculation tests) by Webster, et al. (1970); Grove and Beetem (1971); Pickens and Grisak (1981); and Novakowski, et al. (1985) among others. The general approach is to subdivide the recirculating flow system into crescents formed by adjacent streamlines (Figure 1.3). The crescents are assumed to be columns of known length. The authors used the analytical solution of Brenner (1962), except Novakowski, et al. (1985) who used an analytical solution by Sauty (1980) of (1.15). Individual contributions from each crescent are summed to provide a composite breakthrough curve at the withdrawal borehole.

The method of Novakowski, et al. (1985) has the flexibility that the rate of injection and withdrawal need not be equal. Streamline, hence column, lengths and transit times are determined by a particle tracking technique. The other methods cited assume that the injection and pumping rates are equal in magnitude. Streamline lengths and transit times are found by integrating the streamline equation for the recirculating flow system presented by DaCosta and Bennett (1960).

1.2.3 Radial Flow Tracer Tests

The most common three types of tracer tests involve purely radial flow in a horizontal plane. The advection-dispersion equation in a radial coordinate system is

$$\frac{\partial C}{\partial t} = (1/r) \frac{\partial}{\partial r} [r(v + D^*) \frac{\partial C}{\partial r}] - v \frac{\partial C}{\partial r} \quad (1.16)$$

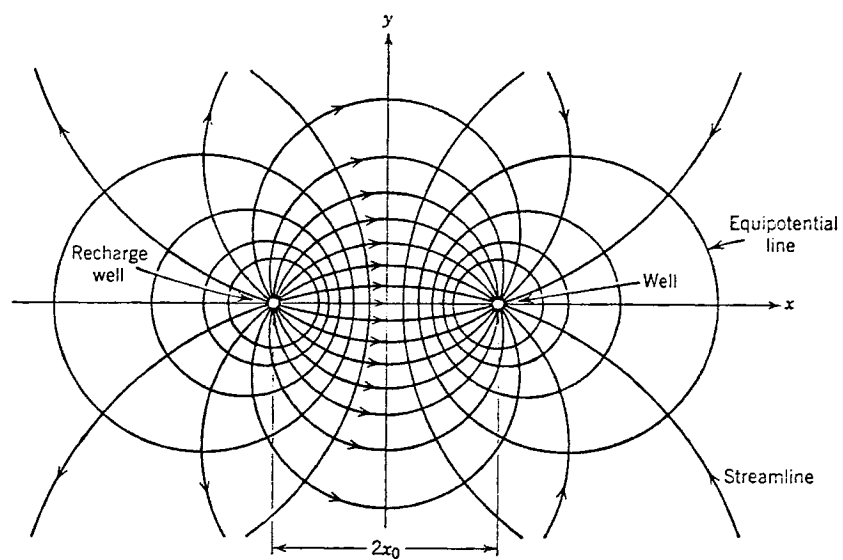


Figure 1.3. Flow Field Established by a Recharging and a Discharging Well Pair. (After Davis and De Wiest, 1966)

where $V = Q/2\pi rb\phi$

Here r is the distance along the radius from the central borehole, Q is the magnitude of the volumetric flow rate through the central borehole and b is the thickness of the zone being tested.

1.2.3.1 Single-well Test. The first of the radial flow tracer tests is the single-well injection-withdrawal test (hereafter called single-well test) described by Pickens and Grisak (1981). Water, having a constant concentration (C_0) of tracer, is injected into a borehole for a specific time period and then pumped out to recover the tracer. Water is sampled from the discharging borehole to determine the history of tracer concentration.

Mercado (1966) presented a method to graphically analyze recirculation test data. The withdrawal phase breakthrough curve is plotted as relative concentration, C/C_0 , versus the ratio of the withdrawn volume to the total injected volume, U_p/U_I . A typical breakthrough curve is presented in Figure 1.4. Dispersivity is determined by

$$a = 3U_I^{1/2}[\Delta(U_p/U_I)]^{2/3} / 32^{3/2}(\phi b)^{1/2} \quad (1.17)$$

where $\Delta(U_p/U_I)$ is determined from intercepts of a line tangent to the breakthrough curve at $C/C_0 = 0.5$ with the lines $C/C_0 = 0.0$ and 1.0 . Gelhar and Collins (1971) presented an analytical solution for relative concentration to the single-well test using the withdrawal phase concentration data. Both of these methods can accommodate unequal injection and withdrawal rates.

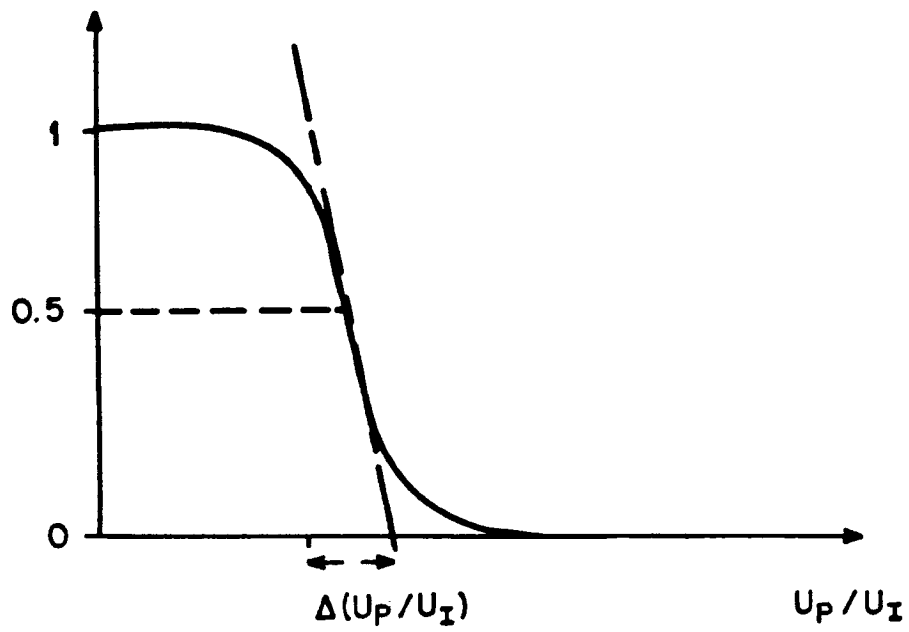


Figure 1.4. Typical Breakthrough Curve for Withdrawal Phase of Single-Well Test.

Mandel, et al. (1985) provide an alternate method to conduct a single-well test. The tracer is injected into an aquifer as a slug and is allowed to advect and disperse under natural flow conditions for a period of time, then the tracer injection borehole is pumped to recover the tracer. The method assumes that one knows the prevailing groundwater velocity and gradient, the transmissivity of the aquifer and the location of the stagnation point of the convergent flow field on the natural flow field. Dispersivity is found by using an analytical solution. Unlike the other analysis techniques for single-well tests, this method can provide an estimate of the product of the thickness of the aquifer and the effective porosity, $b\phi$, by knowing the time delay between tracer injection and the beginning of pumping, t_1 , and by determining the time for one-half of the injected mass to be recovered, t_m .

$$b\phi = \pi(TIt_1)^2/Qt_m \quad (1.18)$$

T = aquifer transmissivity

I = natural gradient of groundwater flow

Figure 1.5 shows a typical breakthrough curve and the time for one-half of the injected mass to arrive at the pumping borehole.

1.2.3.2 Convergent Flow Tests. A convergent flow tracer test is performed by pumping a central borehole at a constant rate. A tracer is introduced into the flow system through an injection borehole (Figure 1.6a). History of the tracer concentration is determined by sampling the discharged water.

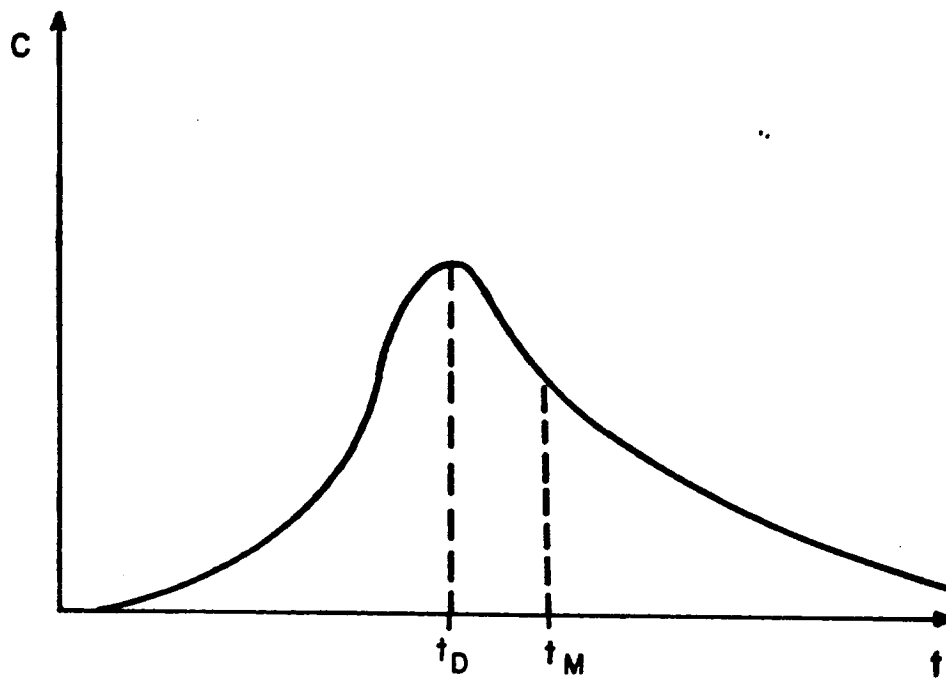
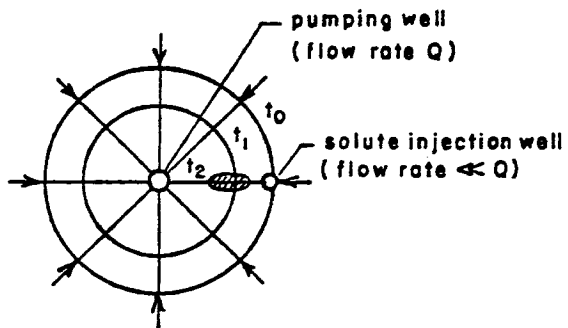
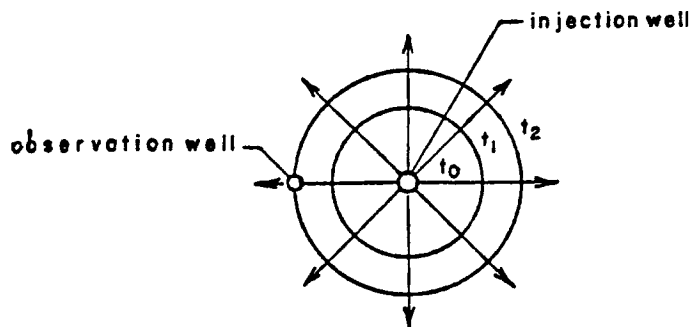


Figure 1.5. Typical Breakthrough Curve for Method of Mandel et al. (1985).



a. Convergent Flow



b. Divergent Flow

Figure 1.6. Radial Flow Fields.

Analytical solutions of (1.16) for radially convergent flow could not be found in the literature. Sauty (1977) provided a numerical scheme to solve (1.16). The method is similar to the approach used in this thesis and is detailed in Chapter 2. Cullen, et al. (1985) also employed the method of Sauty.

1.2.3.3 Divergent Flow Test. Divergent flow tracer tests are conducted by introducing traced water into an aquifer through a central injection borehole. The water and the tracer move radially away from the central borehole, tracer concentration is monitored at an observation borehole (Figure 1.6b). Tracer concentration data may be analyzed by numerous analytical and numerical techniques. Much research has been conducted in the area of waste injection; a brief overview is presented.

Analytical solutions were obtained for the case of continuous injection of water containing tracer of constant concentration. Lau, et al. (1959), Raimondi, et al. (1959), Hoopes and Harleman (1967) and Dagan (1971) provided approximate analytical solutions. Chen (1985) used the Laplace transform to obtain an exact solution to the advection-dispersion equation, (1.16), except that tracer is also allowed to migrate vertically to adjacent formations by one-dimensional diffusion. An exact solution was developed for small times and approximate solutions for intermediate and large times.

Pickens and Grisak (1981) adapted the method of Mercado (1966) to estimate dispersivity from concentration data collected at an observation borehole in a divergent flow field. A typical breakthrough

curve is shown in Figure 1.7. A line tangent to the curve is constructed through $C/C_0 = 0.5$ to intersect the lines $C/C_0 = 0.0$ and 1.0 , thereby defining Δt . Dispersivity is calculated by

$$a = (3r/16)(\Delta t/t_{0.5})^2 \quad (1.19)$$

r = distance between boreholes

$t_{0.5}$ = time for $C/C_0 = 0.5$

Effective porosity can be calculated by

$$\phi = Qt_{0.5}/\pi r^2 b \quad (1.20)$$

Sauty (1977) developed a numerical method to solve (1.16) with D^* equal to zero. This method forms the basis for this thesis and is fully developed in Chapter 2.

1.2.4 Discussion of Tracer Tests

Five types of tracer tests have been presented. Some of the advantages and disadvantages of these tests will now be discussed.

Many uniform-flow tracer tests are conducted under natural flow conditions. These tracer experiments require considerable time to complete when the velocity is low. A line of monitoring boreholes, perpendicular to the direction of flow, is necessary to provide data for mass balance.

Recirculation tests require less time than all the tracer tests described to complete (except for possibly a single-well test). By the diverging and converging nature of the streamlines of a recirculating flow system, this type of tracer test incorporates a larger volume of

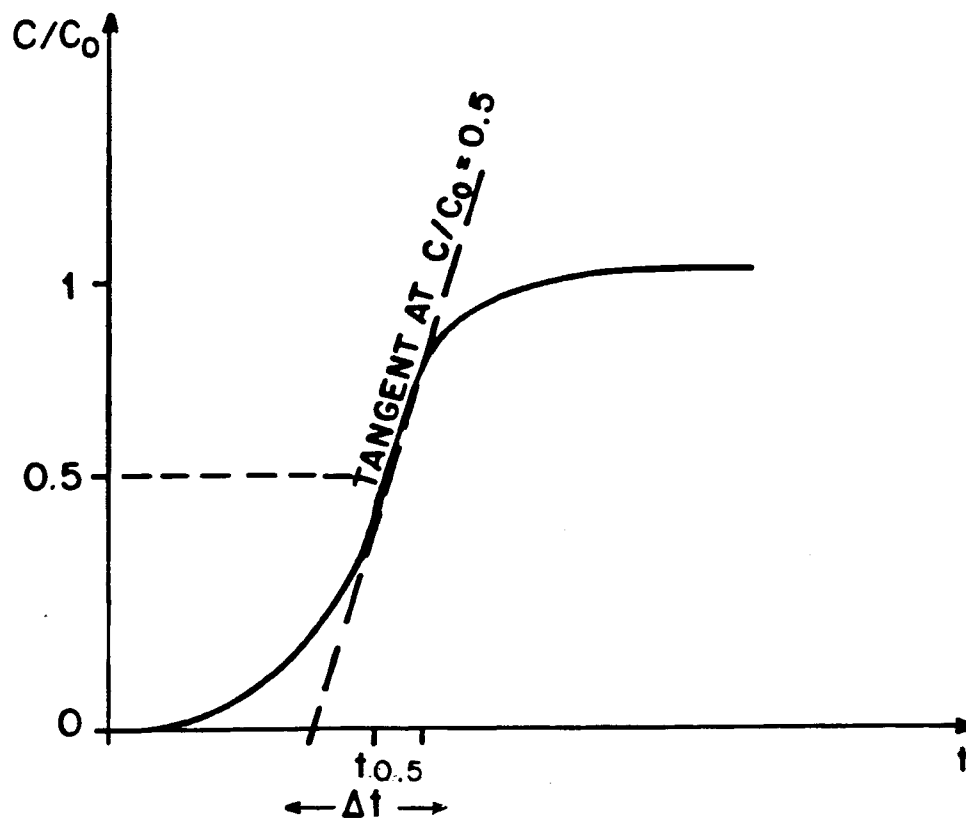


Figure 1.7. Typical Breakthrough Curve at Observation Well During Injection Phase of Single-Well Test.

the aquifer using only two boreholes than the other types of tests. A considerable amount of time is required to recover 100% of the injected mass, by virtue of the length of the outermost flow tubes.

Single-well tests require only one borehole. If monitoring boreholes are present, a divergent flow test can be conducted during the injection phase and provide another set of data for analysis. Nearly all of the injected mass is recovered after a relatively short time. However, instrumentation may be more complex because one borehole is used for injection and withdrawal.

Using convergent flow tests one can conduct multiple tracer tests simultaneously by injecting several tracers at different locations in the flow field. Using a different tracer at each injection point allows for the detection of multiple breakthrough curves at the pumping borehole. Analysis of these data may provide insight to the directional nature of the aquifer's transport characteristics. Convergent flow tests dilute tracer concentration by virtue of many flowlines converging on the pumping borehole. Thus, an integrated concentration is detected at the monitoring borehole; this is also true for recirculation tests. The implication of this is that tracer must be injected in sufficient amounts so that the detection limits of the tracer analysis equipment are not exceeded. Convergent flow tests have direct application to aquifer restoration procedures as pumping boreholes are commonly used to recover contaminated groundwater. Convergent tests allow for complete mass balance in a short time frame, relative to recirculation tests.

Divergent flow tests can provide data to examine the directional nature of dispersion in a single experiment using one tracer by monitoring several observation boreholes located spatially about the injection borehole. The data gathered from each observation borehole are analyzed separately and the results of the analyses are compared for time of arrival and shape of the breakthrough curves. In this manner the degree and direction of heterogeneity may be assessed. Divergent flow tests have the disadvantage that only a small percentage of the tracer mass is recovered, leaving much tracer in the aquifer. Environmental implications could arise. Data interpretation may be difficult because of the low percentage of recovered mass. The other tests recover a greater percentage of the injected tracer.

Divergent flow tests have direct application to waste injection practices. Many municipalities and industries dispose of treated waste through injection. These experiments also have application to the proposed deep burial of high-level nuclear waste. Injection into low permeability formations is more easily accomplished than withdrawal, as a pumping well in low permeability formations may quickly be dewatered. This is the impetus for this thesis.

1.3 Scope of Thesis

Divergent flow tracer test were conducted at the Oracle field site in low permeability fractured granitic rocks. (A description of the field site is found in Chapter 4.) A method was needed to interpret the data. Carrera and Walter (in preparation) developed a program, DBCON, to interpret data from convergent flow tracer tests. They used

the numerical method of Sauty (1977) to solve the partial differential equation with some added features: the coefficient of hydrodynamic dispersion took the form of $aV^{(m)}$ instead of aV , mixing and sampling in the monitoring borehole could be taken into account, and an inverse model was developed. DBCON was modified, in part by this author, to reverse the direction of flow and to extend the outflow boundary providing a model suitable for divergent flow, DBDIV. The dispersion coefficient was further modified to include molecular diffusion, $aV^{(m)}+D^*$.

Chapter 2 of this thesis derives the finite difference equations used in program DBDIV and provides details of the numerical approach. An algorithm is included to account for mixing in the monitoring borehole, accounting for the extraction of tracer mass during sampling.

Chapter 3 explains the modes of operation of DBDIV, as well as the types of problems that the model can simulate. This chapter also discusses the results of the model's sensitivity to grid construction, placement of the outflow boundary and parameters that are intrinsic to the advection-dispersion equation. In this chapter the numerical solution is compared to three analytical solutions.

Chapter 4 describes the Oracle field site, the test procedure and the methodology to use DBDIV for analyzing divergent flow tracer test data. It also provides the results of the divergent flow tracer test conducted during July 15-16, 1985. The model's performance and

conclusions that can be drawn from the divergent flow tracer test are included.

Chapter 5 provides the conclusions to this thesis. Included in the appendices is a users' guide to the model, listing of the code in Fortran 77, and the field data of the divergent flow tracer test.

CHAPTER 2

THEORY

Chapter 1 has provided a brief overview of the processes involved in subsurface chemical transport in the saturated zone. In this chapter, a Lagrangian form of the governing equation for mass transport in a planar radial flow system is presented with initial and boundary conditions. A finite difference equation is developed to numerically solve the governing equation. The chapter also describes a method to account for dilution of tracer concentration as water enters the monitoring borehole from the aquifer, accounting for reduction of the tracer mass due to sampling.

2.1 Lagrangian Form of Governing Equation

Expression (1.16) gives the advection-dispersion equation for plane radial flow in Eulerian coordinates. To write the same equations in Lagrangian coordinates, one defines the Lagrangian derivative

$$DC/Dt = \partial C/\partial t + V \partial C/\partial r \quad (2.1)$$

Substitution of (2.1) into (1.16) yields

$$DC/Dt = (1/r) \partial/\partial r [r(aV+D^*) \partial C/\partial r] \quad (2.2)$$

The solution of (2.2) is subject to the initial condition

$$C(r,0) = 0 \quad r > r_W \quad (2.3)$$

and the boundary conditions

$$C(r,t) = C_I(t) \quad r = r_W; t > 0 \quad (2.4a)$$

$$\partial C / \partial r = 0 \quad r = R \quad (2.4b)$$

where $C_I(t)$ is the injection concentration, r_W is the radius of the injection borehole and R is the radial distance to an arbitrary external boundary. Condition (2.4b) states that the tracer does not disperse through the outflow boundary at R , it only advects (Gershon and Nir, 1969; Bear 1979). This boundary condition has no effect on concentration at the monitoring borehole if R is sufficiently large compared to the distance between the centers of the injection and monitoring boreholes (r_I).

2.2 Mixing and Sampling in the Monitoring Borehole

The solution of (2.2) subject to the initial and boundary conditions provides the temporal distribution of tracer concentration in the aquifer at some distance r from the injection location. Typically, tracer tests are conducted in the field using boreholes to inject and monitor the tracer. Therefore, the solution process must relate tracer concentrations in the monitoring borehole to tracer concentrations in the aquifer.

For this, we assume that at the distance r_I from the injection borehole, the streamlines are essentially parallel passing through the monitoring borehole, except in its immediate vicinity where they are deflected toward the borehole. Under these conditions, the width of

the streamtube feeding into the monitoring borehole is twice the diameter of this borehole, as shown in Figure 2.1.

The flow rate, Q_M , through the flow tube passing through the monitoring borehole is

$$Q_M = 4r_M b \phi V \quad (2.5a)$$

or

$$Q_M = 2r_M Q / \pi r_I \quad (2.5b)$$

where r_M is the radius of the monitoring borehole. To write a mass balance expression for the tracer in the borehole, we assume that it mixes completely in the borehole and that it does not disperse as it crosses the borehole wall. Then

$$S_M \frac{dC_M(t)}{dt} = C(t)Q_M - C_M(t)Q_M - C_M Q_S \quad (2.6a)$$

$$S_M = \pi r_M^2 h_M$$

where $C(t)$ is the concentration in the aquifer immediately upstream of the monitoring borehole, C_M is the concentration in the monitoring borehole, Q_S is the volumetric sampling rate, and h_M is the height of the mixing column in the borehole. Expression (2.6a) can be rewritten as

$$\frac{dC_M(t)}{dt} = wC(t) - (w+z)C_M(t) \quad (2.6b)$$

$$\text{where } w = 2Q / \pi^2 r_I r_M h_M$$

$$z = Q_S / \pi r_M^2 h_M$$

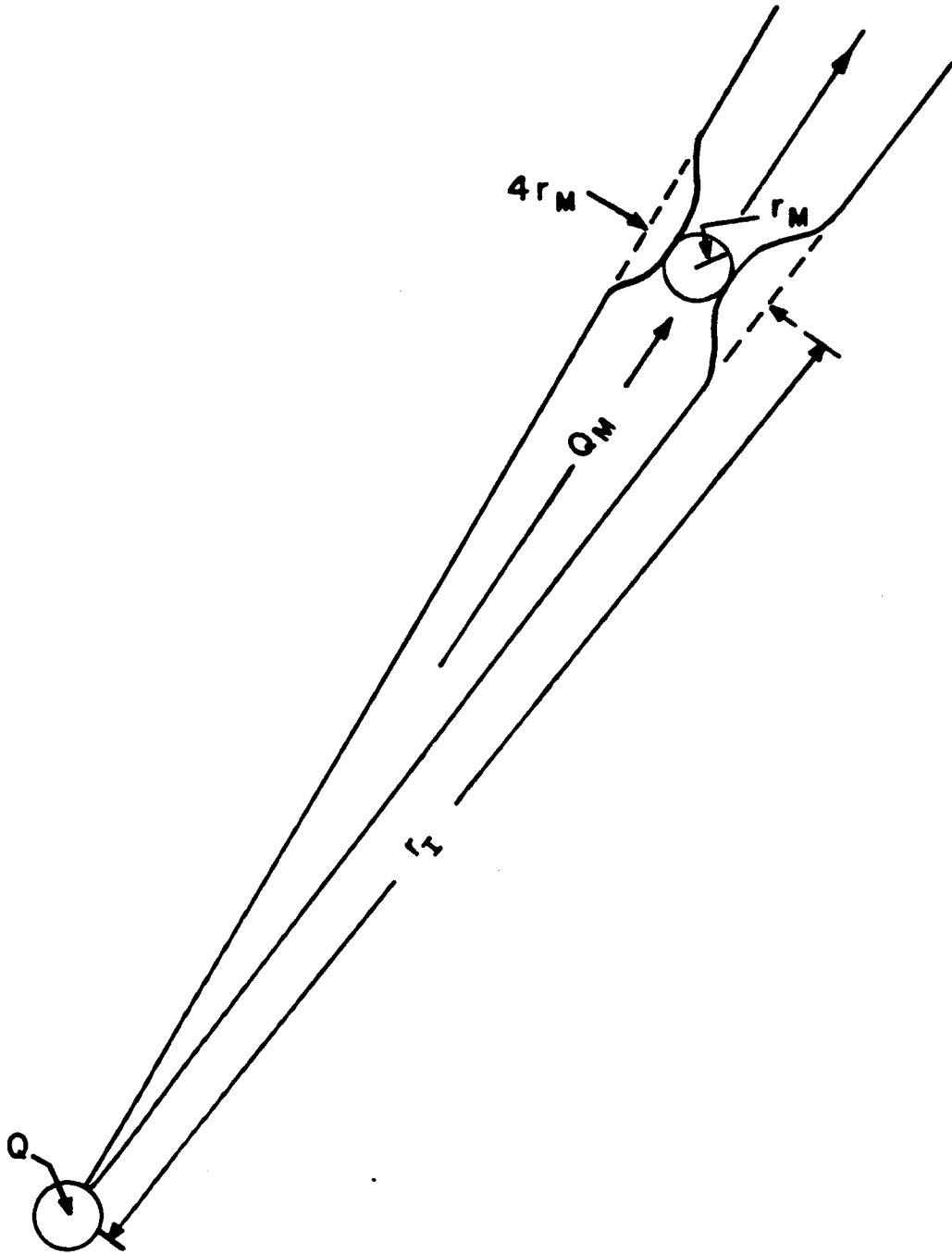


Figure 2.1. Diagram of Flow Tube.

This is an ordinary differential equation which can be solved for $C_M(t)$ if $C(t)$ is given. Note that water balance is not maintained for the sampling correction.

2.3 Numerical Approach

The numerical solution of (2.2) - (2.5) uses a grid consisting of node centered cells. Except at the inflow and outflow boundaries where only half cells are present. Here, the nodes are on the boundary. As Sauty (1977), the method employs a synchronic grid, such that a particle moves from node i to node $i+1$ (Figure 2.2) in exactly one time step. An equation relating the duration of a time step to the distance between neighboring nodes is found by integrating the expression for the seepage velocity. Let

$$V = B/r = Dr/Dt \quad (2.7)$$

where $B = Q/2\pi b\phi$

so that

$$\int_{r_i}^{r_{i+1}} r \, Dr = B \int_t^{t+\Delta t} Dt$$

where r_i = radial distance to node i

Δt = duration of a time step

and

$$(r_{i+1}^2 - r_i^2)/2 = B\Delta t \quad (2.8)$$

The relationship between the duration of a time step and the number of nodes, N , is

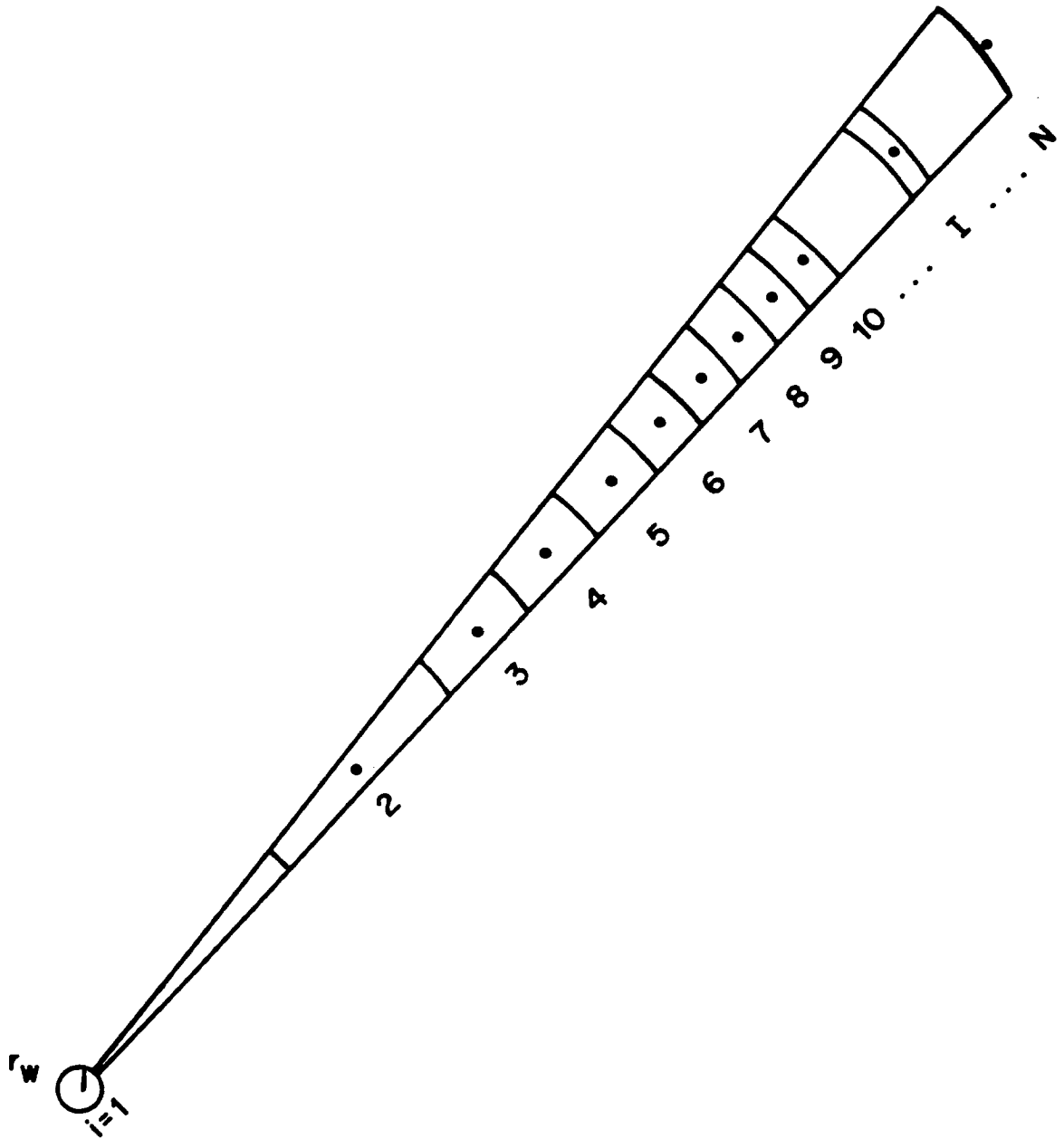


Figure 2.2. Grid Construction.

$$\Delta t = (R^2 - r_w^2) / 2B(N-1) \quad (2.9)$$

where N represents the total number of nodes. The grid is constructed such that the first node is on the wall of the injection borehole, node N is on the external boundary, and the axis of the monitoring borehole coincides with node 1 (Figure 2.3). Thus, $N-1$ cells are within the space from $r = r_w$ to R .

By construction all the cells have identical volumes, equal to $Q\Delta t$, the volume of water transferred between cells during a time step. The change in mass of the dissolved tracer due to advection from cell $i-1$ to cell i during time step k is $Q(C_i^k - C_{i-1}^{k-1})\Delta t$, where subscripts indicate location and superscripts indicate time steps. Therefore, mass flux due to advection is

$$DC/Dt = Q\Delta t(C_i^k - C_{i-1}^{k-1})/\Delta t = Q(C_i^k - C_{i-1}^{k-1}) \quad (2.10)$$

In the model, expressions for dispersive flux are centered about the cell boundaries. The net dispersive flux within a cell is

$$DC/Dt \sim J_{in} - J_{out} \quad (2.11)$$

as shown in Figure 2.3. Discretizing (2.2), the advection-dispersion equation, between nodes $i-1$ and i for J_{in} and nodes i and $i+1$ for J_{out} yields

$$J_{in} = -(1/r_{i-1/2})D'_{i-1/2}r_{i-1/2}A_{i-1/2}(C_i^k - C_{i-1}^k)/(r_i - r_{i-1}) \quad (2.12a)$$

$$J_{out} = -(1/r_{i+1/2})D'_{i+1/2}r_{i+1/2}A_{i+1/2}(C_{i+1}^k - C_i^k)/(r_{i+1} - r_i) \quad (2.12b)$$

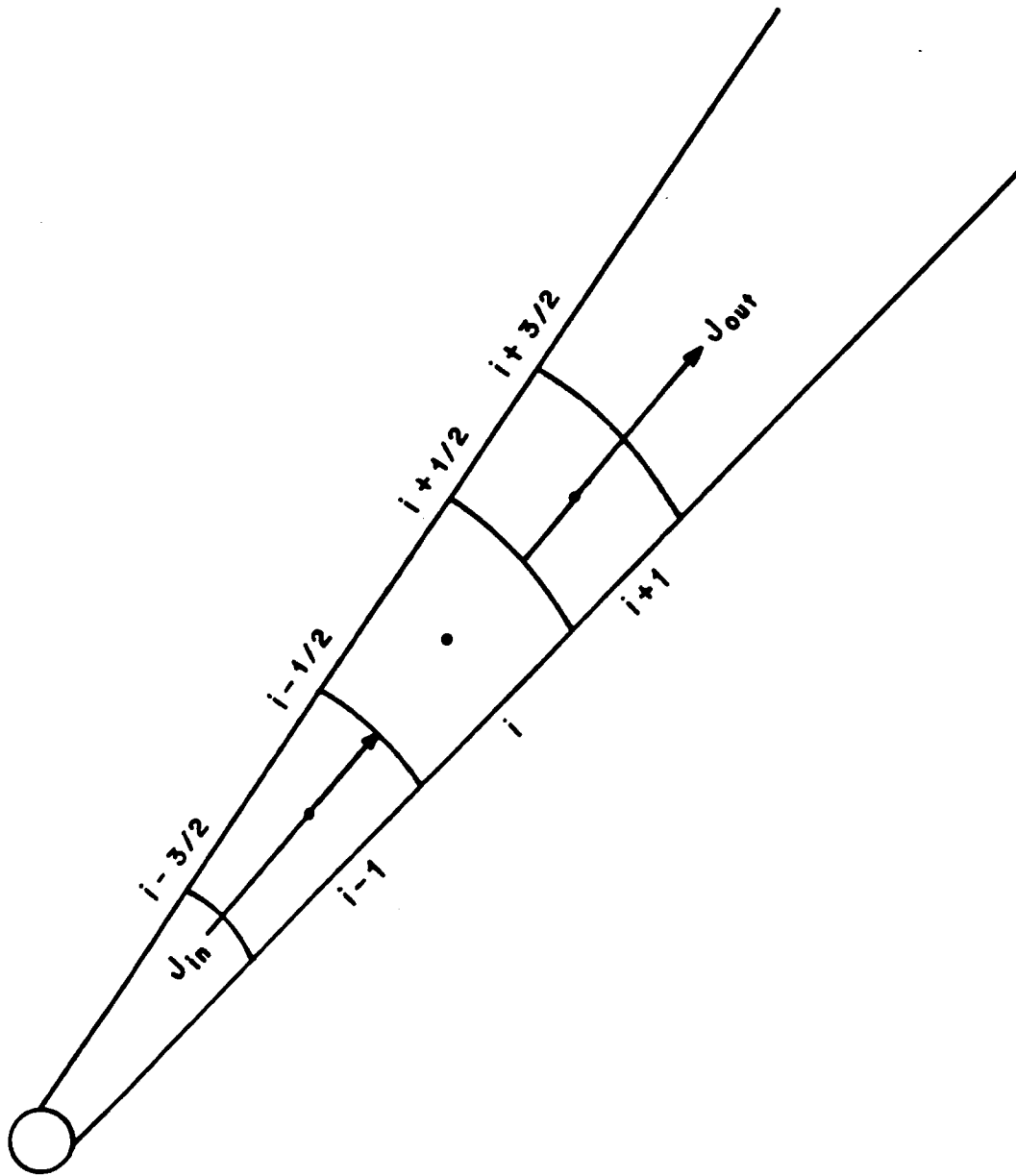


Figure 2.3. Dispersive Fluxes Into and Out of a Cell.

$$A_i = 2\pi r_i b \phi$$

where the half-nodal subscripts indicate the locations of the cell boundaries. The quantity A_i/r_i is Q/B , a constant, and is substituted into (2.12a) and (2.12b). Equating the advected mass flux (2.10) and the net dispersive flux (2.11) provides the mass balance expression

$$C_i^k - C_{i-1}^{k-1} = -[r_{i-1/2} D'_{i-1/2} (C_i^k - C_{i-1}^k) / (r_i - r_{i-1}) - r_{i+1/2} D'_{i+1/2} (C_{i+1}^k - C_i^k) / (r_{i+1} - r_i)] / B \quad (2.13)$$

Substitution of the general form of the coefficient of hydrodynamic dispersion ($aV^{(m)+D^*}$) for D' and the seepage velocity (V_i) at the cell boundary for B/r_i , according to (2.7), into (2.13) gives, after rearrangement,

$$-F_{i-1} C_{i-1}^k + (1 + F_{i-1} + F_i) C_i^k - F_i C_{i+1}^k = C_{i-1}^{k-1} \quad (2.14)$$

where $F_i = (aV_{i+1/2}^{(m)+D^*}) / V_{i+1/2} (r_{i+1} - r_i)$

(Note that the parentheses around m indicate that it is an exponent, not a superscript.) Expressions (2.14) represents a linear system of equations

$$\underline{\underline{A}} C^k = \underline{C}^{k-1} \quad (2.15)$$

where $\underline{\underline{A}}$ is the matrix of coefficients which is symmetric and tridiagonal, \underline{C}^k is the vector of unknown nodal concentrations, and \underline{C}^{k-1} is the vector of known nodal concentrations from the previous time step.

Solution of (2.15) involves decomposing the matrix using the Cholesky algorithm and employing forward and backward substitution, repeating the substitution process while stepping through time. The numerical solution approximates the solution of the partial differential equation, (2.2), and provides concentrations for all the nodes. The concentrations for the node representing the monitoring borehole, I, must be adjusted to reflect concentrations in the monitoring borehole.

Discretizing (2.6b) we obtain

$$(C_M^k - C_M^{k-1})/\Delta t = wC_{I-1}^{k-1} - (w+z)C_M^k \quad (2.16)$$

which assumes that mixing and sampling occur in the present time step. The method uses the concentration at the node immediately upstream of the monitoring borehole at the previous time step, C_{I-1}^{k-1} , because the tracer does not disperse across the borehole wall it only advects. Solving for the present concentration in the monitoring borehole, C_M^k , yields

$$C_M^k = (C_M^{k-1} + wC_{I-1}^{k-1})/(1+w+z) \quad (2.17)$$

where $W = w\Delta t$

$Z = z\Delta t$

W and Z are dimensionless quantities representing mixing and sampling effects, respectively. Chapter 3 assesses the influence of W on the numerical solution.

2.4 Stability and Convergence

The finite difference scheme (2.14) is consistent by formulation. The method is unconditionally stable because it is fully implicit. By Lax's equivalence theorem (Huyakorn and Pinder, 1983) the solution of the approximation converges to the solution of the partial differential equation for arbitrary initial data as the time step, Δt , and the largest grid spacing, Δr , approach zero.

CHAPTER 3

DESCRIPTION OF MODEL AND SENSITIVITY STUDIES

3.1 The Model

Chapter 3 describes the types of problems that the model, DBDIV, can handle and the manner in which it does it. The chapter explores the sensitivity of the numerical solution to grid size, placement of the outflow boundary, and various dimensionless parameters. The validity of the model is ascertained by comparing results with three analytical solutions. The fundamental parameters of the solution are C/C_0 or C_D , t_D , Pe , W and r_{WD} , the dimensionless injection borehole radius.

3.1.1 Modes of Operation

DBDIV has three operational modes: standard simulation, type curve production and parameter estimation. Input which is common to all three modes includes the injection rate, aquifer thickness, distance between injection and monitoring boreholes, and the radius of the injection borehole. In the standard simulation mode, DBDIV calculates a breakthrough curve for given values of effective porosity, dispersivity, and inflow concentration versus time.

In the type curve production mode, the model calculates a suite of breakthrough type curves for given values of the effective porosity, the inflow concentration and a sequence of Peclet numbers. The Peclet

number, Pe , is a dimensionless quantity expressing the ratio between advective and dispersive transport. For our purposes it is defined as

$$Pe = Vr_I/D' \quad (3.1)$$

Whereas the standard and type curve production modes represent forward problems, the parameter estimation mode represents an inverse problem. In this latter mode, one specifies the inflow concentration and a breakthrough curve obtained in a field or laboratory experiment and the model estimates the dispersivity, effective porosity, and/or injected mass using a maximum likelihood approach. The inverse mode is beyond the scope of this thesis and is not discussed further.

3.1.2 Types of Input Concentration

Three types of input concentration can be accommodated by DBDIV for the injection well: 1) a square pulse, 2) a step increase and 3) an arbitrary time variation of concentration. A square pulse of concentration is the numerical equivalent of a Dirac pulse. The magnitude of the pulse is

$$C_0 = M/Q\Delta t \quad (3.2)$$

where M = injected mass

The entire tracer mass is taken to enter the aquifer from the injection borehole during the first time step.

In the case of a step increase of concentration, the magnitude of this step is given by

$$C_0 = M/QT \quad (3.3)$$

where $T = NT \times \Delta t$, T being the total simulation time and NT the corresponding number of time steps. The step increase option is appropriate for simulations where tracer is injected into the aquifer at a constant rate during the entire test period.

The third option applies when the input concentration is arbitrarily distributed in time, as is the case in most field tracer tests. The model must be supplied with a discretized version of the known input concentration at constant time intervals, Δt . This latter option will be used to analyze the tracer test performed at the Oracle field site.

3.2 Sensitivity Analyses

In this section we assess the sensitivity of the computed breakthrough curve to various grid and physical parameters. We begin by exploring the effects of grid size and location of the external boundary on the breakthrough curve. We then compare the numerical solution to several analytical solutions. Finally, the effect of various dimensionless parameters on the functional form of the computed breakthrough curve is examined.

Table 3.1 lists the standard values of the variables used in the sensitivity analyses. The sensitivity analysis consists of systematically varying some of these variables while keeping the others at their standard values. All the simulations were done with pulse tracer injection.

Table 3.1 Standard Input Data for Sensitivity Analyses

Variable	Value
r_I	5.0 m
R	10.0 m
Q	10.0 m ³ /min
b	10.0 m
M	10.0 gm
ϕ	0.1
a	0.5 m
D^*	0.0
r_M	0.05 m
h_M	0.0
m	1.0

One of the dimensionless parameters that control the breakthrough curve is dimensionless time, t_D , defined as

$$t_D = Qt/\pi r_I^2 b \phi \quad (3.4)$$

It is half the ratio between the real time required for the tracer to reach the monitoring well by advection, and the time it would take to reach the same well at the velocity prevailing at r_I .

Another important parameter is the dimensionless concentration

$$C_D = \pi r_I^2 b \phi C/M \quad (3.5)$$

where C is the concentration measured in the monitoring borehole. It represents the ratio between the mass of tracer that would exist within a cylindrical aquifer of radius r_I and thickness b if the concentration was everywhere equal to C , and the total mass of tracer, M , injected. We shall plot C_D versus t_D on double logarithmic paper to highlight the peak of the curves. The early rising limb and the late tail of the breakthrough curve are of less importance for tracer test interpretation than the shape and location of the peak. The comparisons with the analytical solutions are plotted on arithmetic paper.

3.2.1 Effect of Grid Size

We recall from (2.9) that the number of nodes in the finite difference grid is proportional to the square of the grid radius. It follows that nodes are spaced farther apart near the injection borehole than near the monitoring borehole, and more closely near the external

boundary when the latter extends beyond r_I . Whereas accuracy demands that the number of nodes within a grid of a given radius be made large, the need to minimize computer time dictates that the number of nodes be kept within a reasonable limit. To find an acceptable compromise between these two conflicting requirements, we performed six simulations for $Pe = 10$ with the external boundary placed at r_I and the number of nodes, N , varying according to $N = 12, 25, 37, 50, 100$ and 200 . The results are shown in Figure 3.1. In the case of a coarse grid with $N = 12$, the peak is too high. As N increases, the computed breakthrough curves converge toward a stable shape. The latter is achieved when $N = 100$. Experiments with $Pe = 100, 1$ and 0.1 also yield stable shapes when $N \geq 100$. We will therefore maintain 100 nodes between the injection and monitoring boreholes. This question was also investigated for a step increase injection with the exact same results: the grid must contain at least 100 nodes between the injection and the monitoring boreholes.

3.2.2 Effect of External Boundary Location

The condition (2.4b) states that mass advects across the external boundary without dispersion. Since a non-zero dispersive mass flux is allowed to exist upstream of the boundary yet is not allowed to cross the boundary, an artificial accumulation of tracer behind the external boundary results. To prevent this from affecting C at the monitoring well, the external boundary must be removed from this well. The question how far must the external boundary be moved is investigated next.

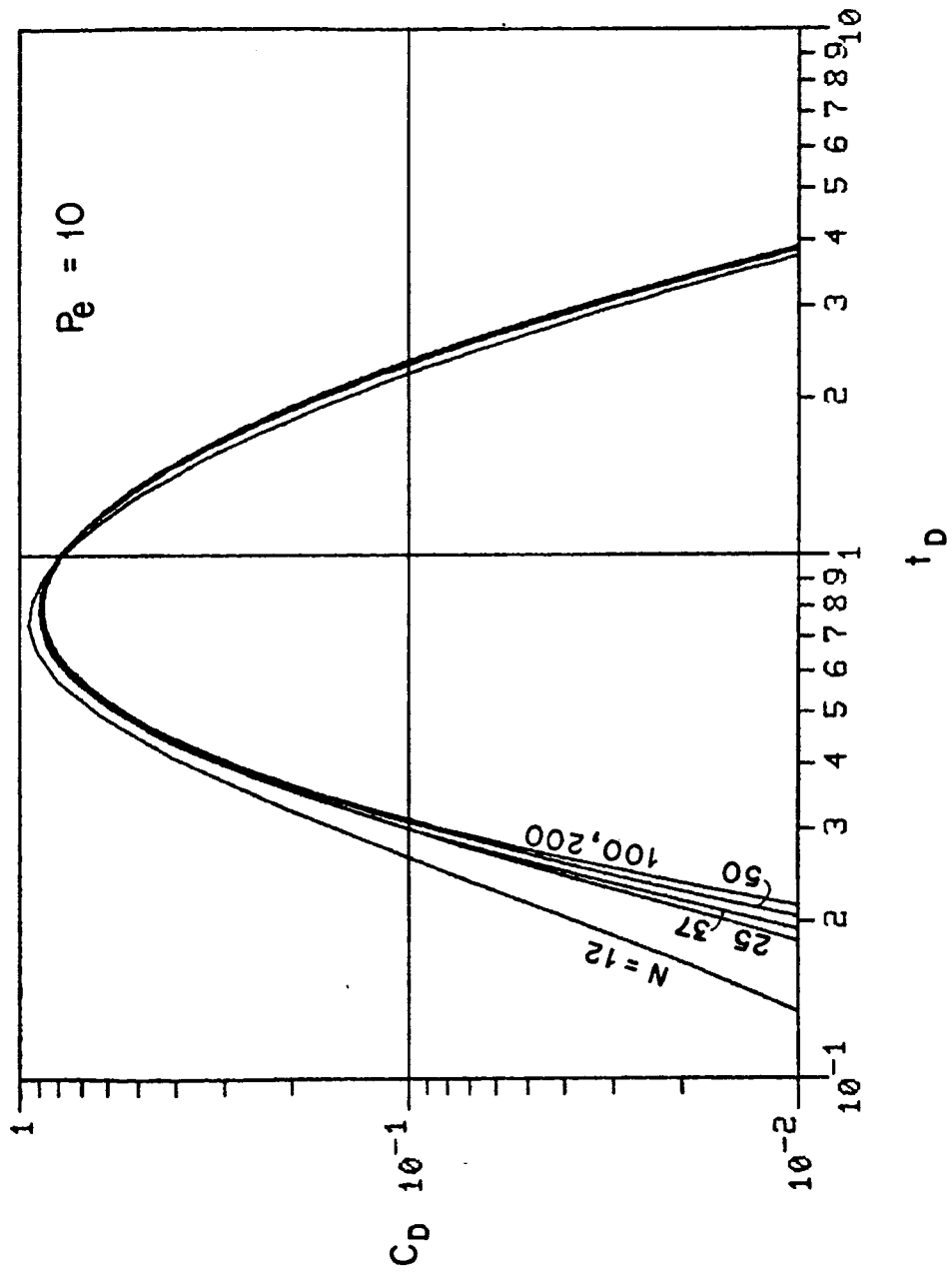


Figure 3.1. Effect of Grid Size on Computed Breakthrough.

As the external boundary is moved farther from the monitoring well, the number of nodes between it and the monitoring borehole increases by the factor

$$\text{MULT} = R^2/r_I^2 \quad (3.6)$$

where R is the external radius. R is chosen such that the total number of nodes is an integer. The total number of nodes in the grid, NN , is thus

$$NN = N \times \text{MULT} \quad (3.7)$$

where N represents the number of nodes between the injection and the monitoring boreholes.

Figure 3.2 displays the effect of placing the outflow boundary at successively larger distances from the monitoring borehole when $Pe = 10$. The corresponding grid data are listed in Table 3.2. When $R = r_I = 5.0\text{m}$, the breakthrough curve shows an effect of mass accumulation at the boundary: the breakthrough occurs too early and its peak is too high. Moving the boundary out to $R = 7.08, 8.67$ and 10.0 m eliminates this effect. Experiments with $Pe = 100, 1$ and 0.1 indicate that as Pe decreases, the outflow boundary must be placed farther and farther from the monitoring borehole. Experiments using a step input lead to identical conclusions.

The effect of placing the outflow boundary at various distances is illustrated in Figures 3.3 and 3.4 for $Pe = 0.1, 1, 10$ and 100 . The figures show what happens when the boundary is placed at $R = 2r_I$ and

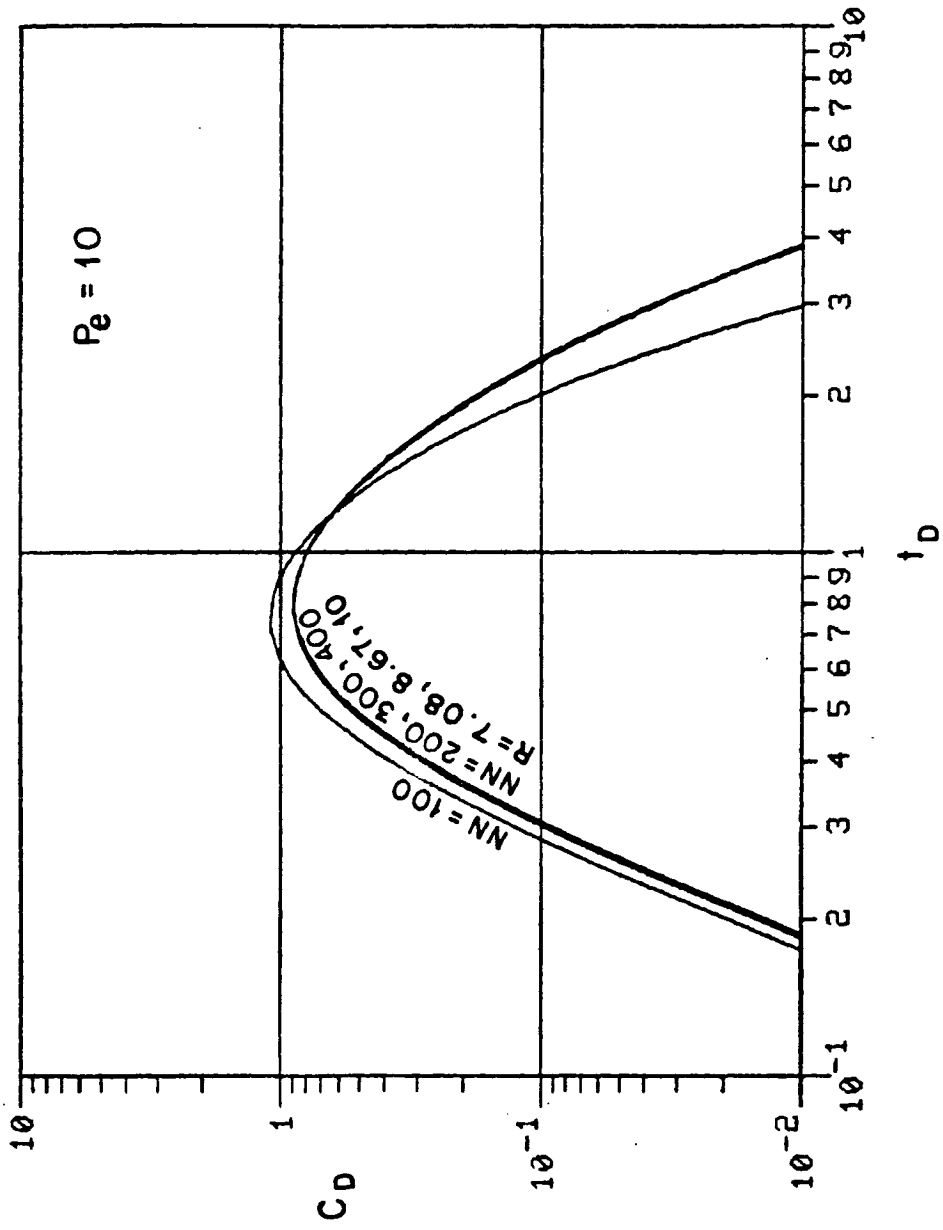


Figure 3.2. Effect of External Boundary Location on Computed Breakthrough.

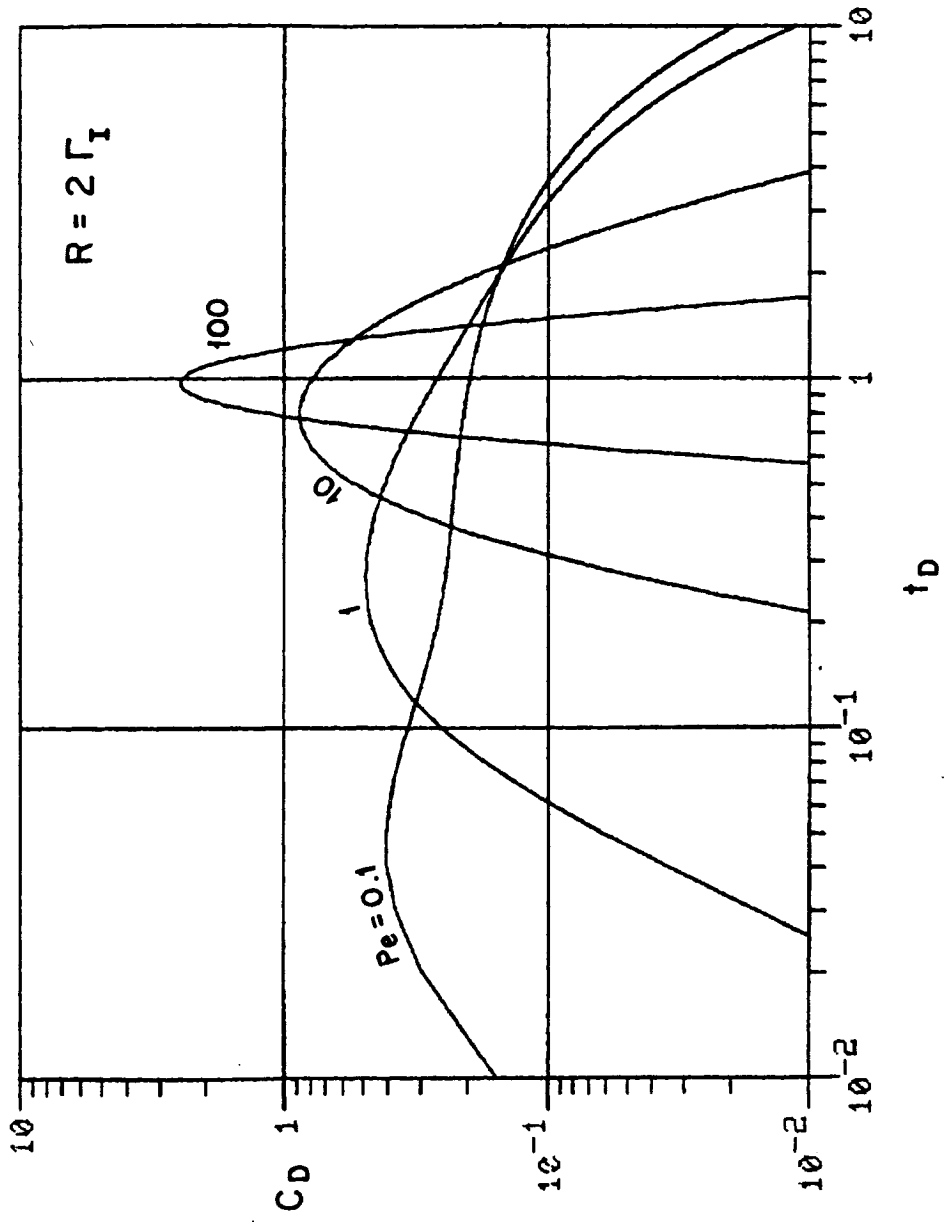


Figure 3.3. Mass Accumulation at External Boundary Affecting Concentration at Monitoring Borehole, $R = 2r_I$.

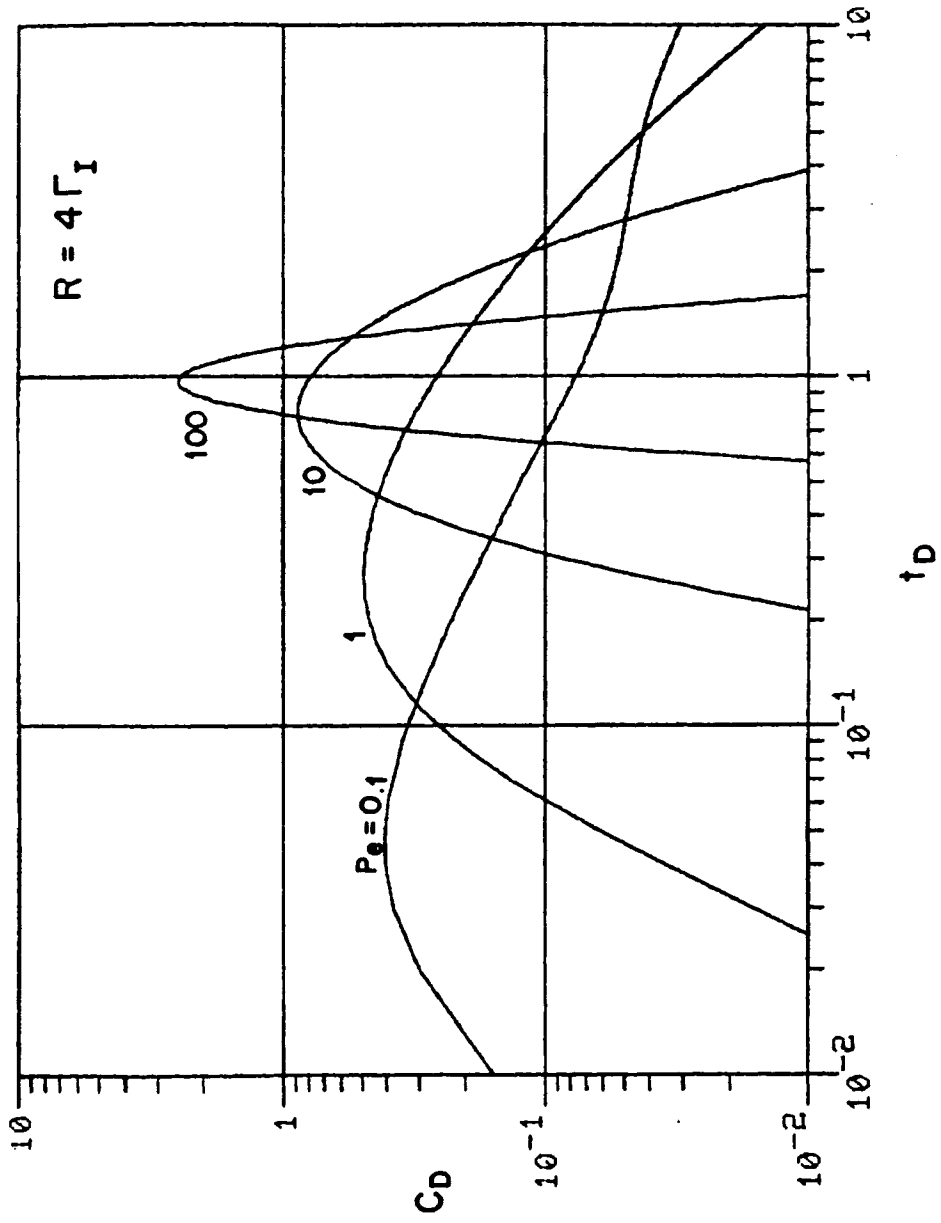


Figure 3.4. Mass Accumulation at External Boundary Affecting Concentration at Monitoring Borehole, $R = 4r_I$.

$R = 4r_I$, respectively. The curves for $Pe = 10$ and 100 are identical in both cases. However, the receding limb of the curves for $Pe = 0.1$ and 1 are seen to be too high when the boundary is close. This additional height is due to artificial mass accumulation behind the outflow boundary, which is reflected in the monitoring borehole. Acceptable external boundary distances for various Peclet numbers are listed in Table 3.3.

Table 3.2 External Boundary Placement Data
($r_I = 5.0$ m, $Pe = 10$)

R (m)	MULT	NN
5.0	1	100
7.08	2	200
8.67	3	300
10.0	4	400

Table 3.3 External Boundary Placement at Various Pe

Distance to Boundary From Injection Borehole	Pe
$R = 2^{1/2} r_I$	$Pe \geq 10$
$R = 2r_I$	$10 > Pe > 1$
$R = 4r_I$	$1 \leq Pe < 0.1$
$R \geq 32^{1/2} r_I$	$Pe = \leq 0.1$

3.2.3 Comparison of Numerical Solution with Analytical Solutions

In this section we compare the numerical solution to three analytical solutions from the literature, all of which assume a step increase of concentration in the injection borehole while disregarding mixing in the monitoring borehole. The solutions of Raimondi, et al. (1959) and Hoopes and Harleman (1967) assume a line source of constant strength while the solution of Dagan (1971) provides for a well of finite radius and a step increase of concentration in this well. The first solution is due to Raimondi et al. The original paper could not be obtained, so this author is unable to describe the method of solution and the approximations it involved. However, it is known that the solution assumes large Pe (Hoopes and Harleman, 1967), which leads to

$$C/C_0 = 0.5 \operatorname{erfc} [(3Pe)^{1/2}(1-t_D)/4t_D^{3/4}] \quad (3.8)$$

A comparison with our numerical solution for a step increase of concentration with Pe = 1, 10 and 100 is shown in Figure 3.5. At Pe = 100 and at Pe = 1 it is poor.

Hoopes and Harleman (1967) provide another analytical solution which theoretically should be valid for large Pe. Their solution is given by

$$C/C_0 = 0.5 \operatorname{erfc} [(3Pe)^{1/2}(1-t_D)/4] \quad (3.9)$$

As shown in Figure 3.6, this solution does not agree with the numerical results at any of the Pe tested.

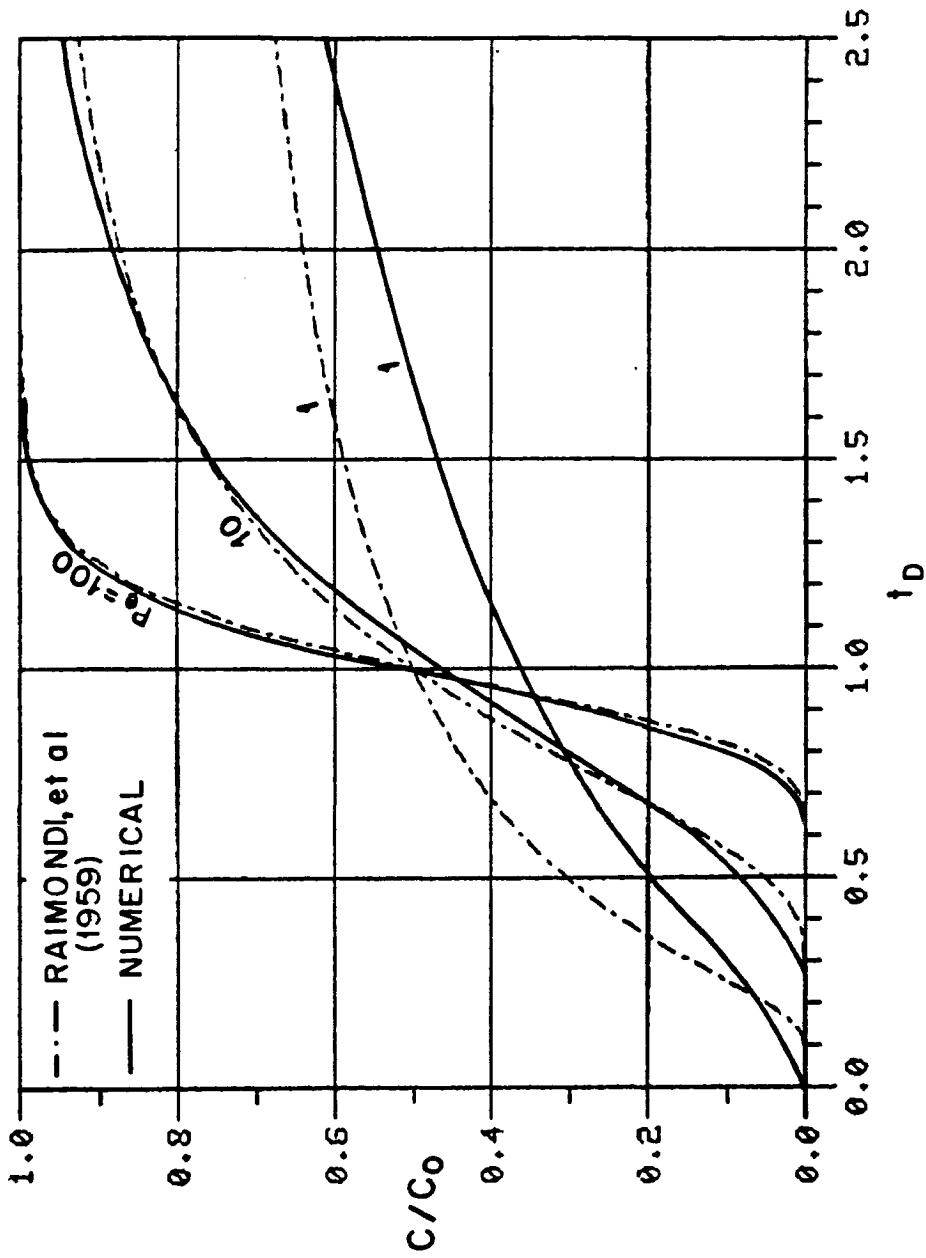


Figure 3.5. Comparison of Analytical Solution of Raimondi et al. with Numerical Solution for $Pe = 1, 10$ and 100 .

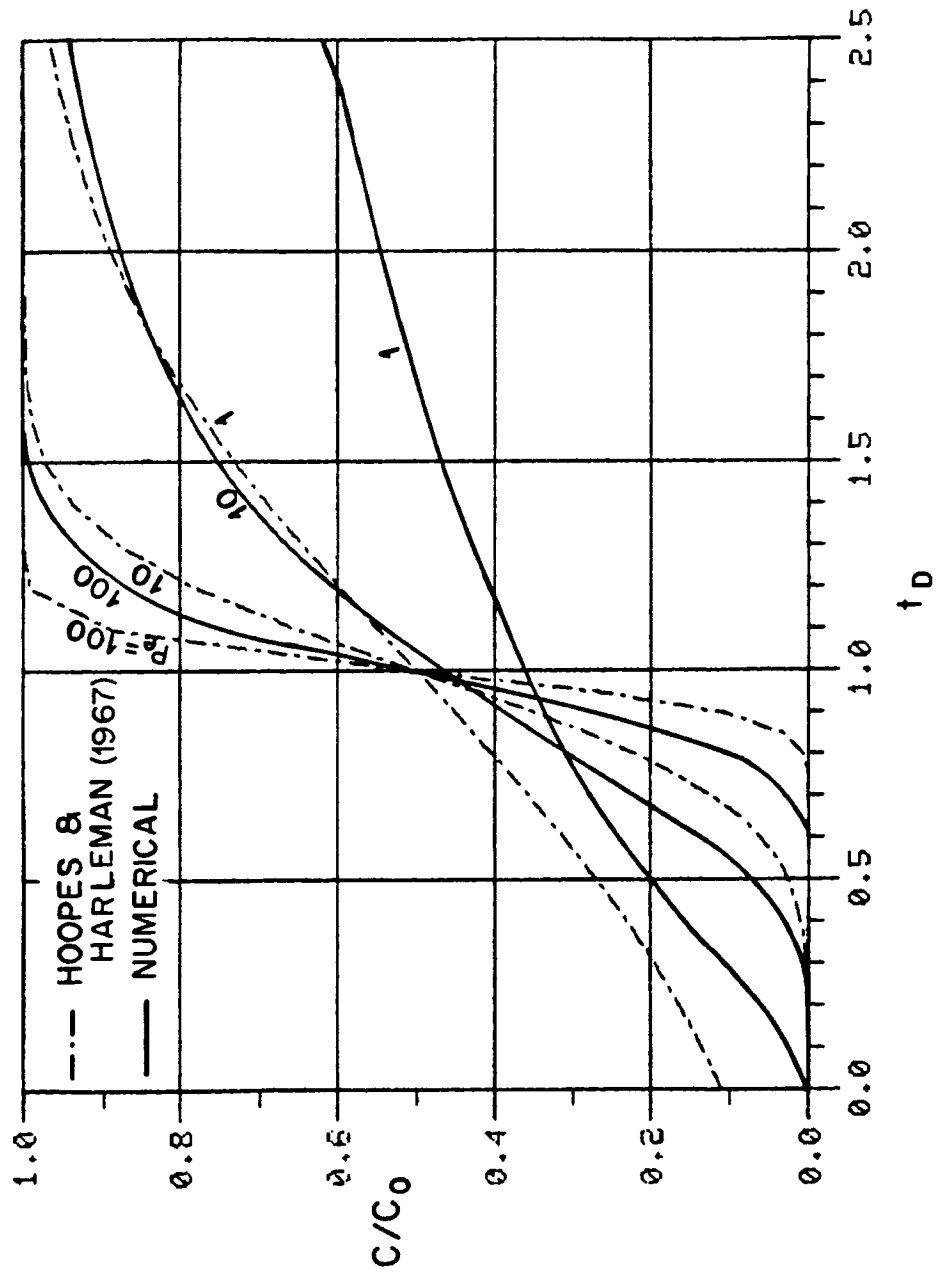


Figure 3.6. Comparison of Analytical Solution of Hoopes and Harleman with Numerical Solution for $Pe = 1, 10$ and 100 .

Dagan (1971) develops yet another analytical solution for large Pe by perturbation expansions, his solution is

$$C/C_0 = 0.5 \operatorname{erfc} \left\{ (3Pe)^{1/2} (\ln r' - 0.5 \ln t'_R) (t'_R) / [2(t'_R)^{3/2} - r'_W]^2 \right\} \quad (3.10)$$

$$r'_W = r_W/R$$

$$t'_R = t_D + r'_W{}^2$$

It is compared with the numerical solution in Figure 3.7. As in the case of the solution by Raimondi et al. the agreement is good at Pe = 100, less good at Pe = 10, and poor at Pe = 1. Overall, the solution of Raimondi, et al. appears to be the best among the three analytical solutions, and that of Hoopes and Harleman to be the worst. All three solutions fail at Pe smaller than 10.

Furthermore, the analytical solutions consistently pass through the point $t_D = 1.0$ and $C/C_0 = 0.5$. This is due to the underlying assumption that Pe is large, i.e., that advection dominates over dispersion and the center of mass travels with the average seepage velocity. While this true in uniform velocity fields, in radially divergent flow the velocity is greatest near the injection borehole and diminishes as $1/r$ with distance from this borehole increases. Since dispersion is proportional to velocity, it is more pronounced when the concentration front is near the injection borehole than at later times. As a result, the front is skewed downstream and the center of mass lags behind. As dispersion is greatest at small Pe, this is where the lag

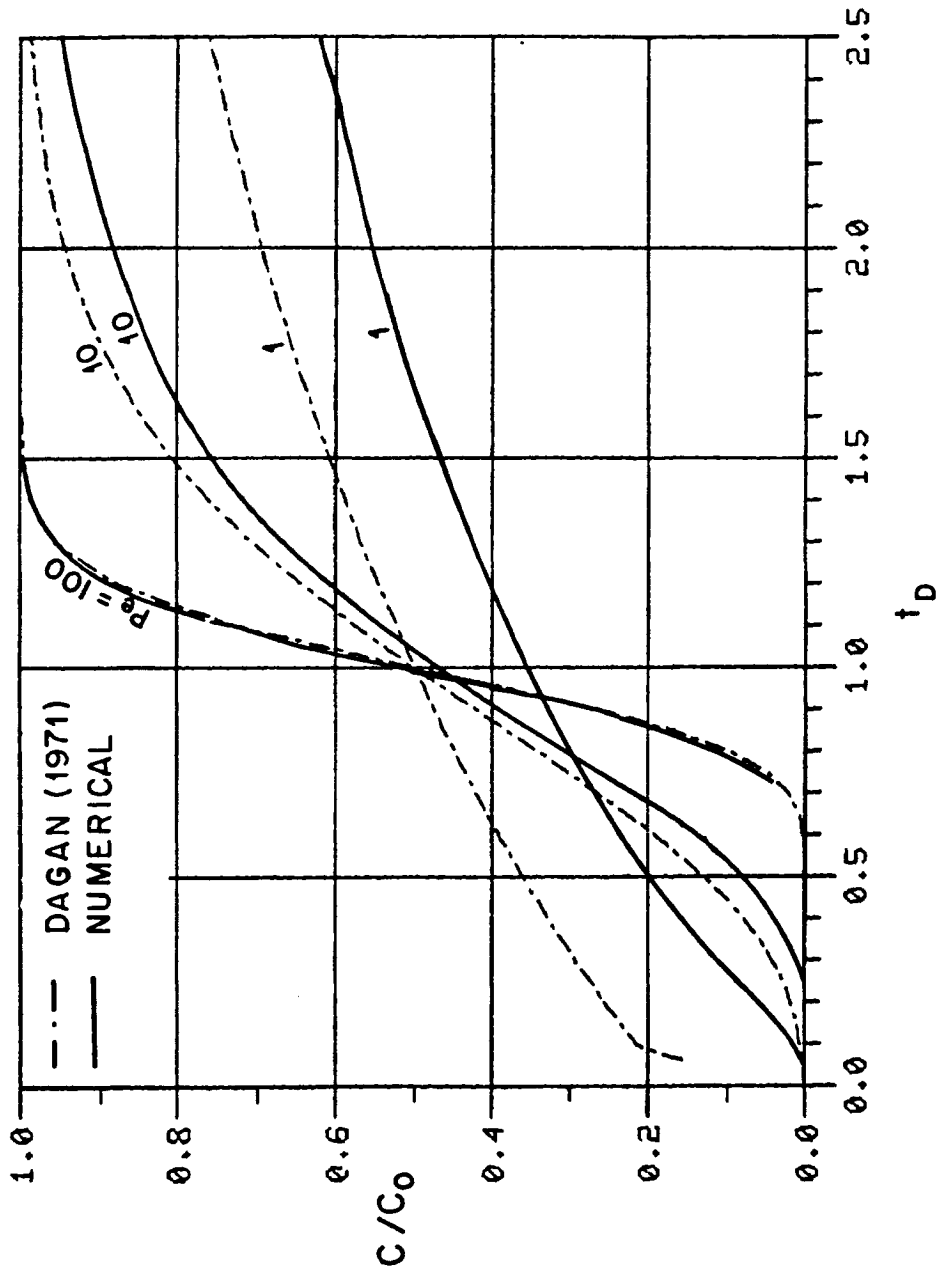


Figure 3.7. Comparison of Analytical Solution of Dagan with Numerical Solution for $Pe = 1, 10$ and 100 .

is most pronounced, as our numerical solution clearly demonstrates. The analytical solutions fail to accurately reproduce this phenomenon at small Pe.

3.2.4 Effect of Velocity

One would expect velocity to have no effect on the form of the numerical solution except due to numerical errors. Experiments with Pe = 0.1, 1, 10 and 100 and with velocities varying over four orders of magnitude have confirmed that the solution is not sensitive to velocity.

3.2.5 Effect of Peclet Number

Since in all our sensitivity analyses $m = 1$ and molecular diffusion is zero, the Peclet number reduces to

$$Pe = r_I/a \quad (3.11)$$

Figure 3.8 shows the breakthrough curves for Pe = 0.1, 1, 10, 100. As the Peclet number increases, the breakthrough curve becomes more peaked and the peak increases and moves to the right. In deriving these curves the external boundary was placed according to Table 3.3. The curve Pe = 0.1 shows an effect of mass accumulation at the external boundary at its tail end. Here the boundary was located at $R = (32)^{1/2}r_I$ and further expansion of the grid was not possible due to computer storage limitations. The dashed line is our estimate of how the tail may look if the external boundary were properly located.

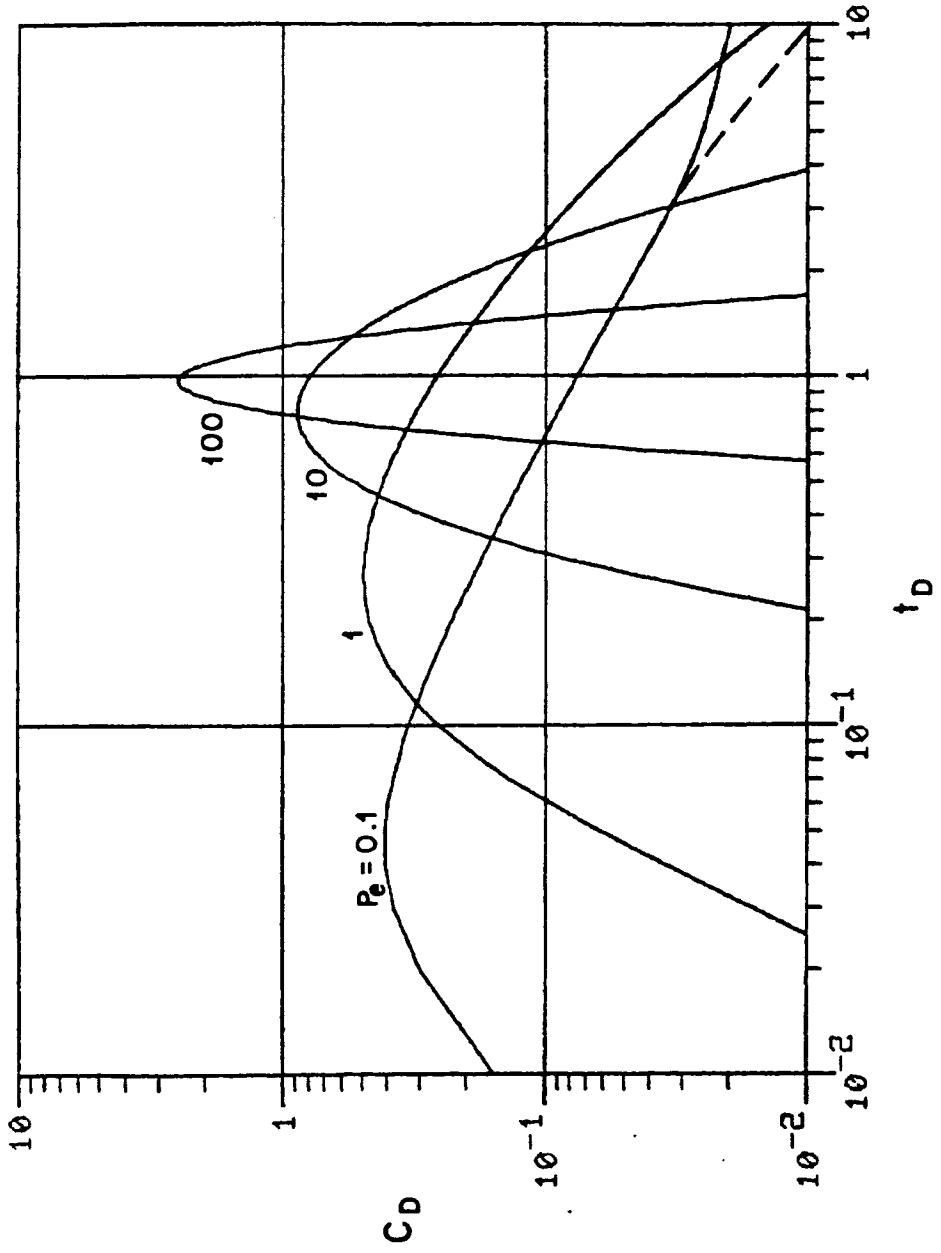


Figure 3.8. Effect of Peclet number.

The distinct shapes of the curves for various Pe in Figure 3.8 suggests that one should be able to identify this parameter with relative ease from field breakthrough data.

3.2.6 Effect of Mixing in Monitoring Borehole

An algorithm accounting for mixing in the monitoring borehole was described in Section 2.3. A dimensionless mixing parameter, W , was defined as

$$W = D/h_M \quad (3.12)$$

where $D = 2Q_M t / \pi^2 r_I r_M$

To assess the effect of mixing on the numerical solution, the reciprocal of W as varied according to $1/W = 0, 1/10D, 1/D$ and $10/D$. The results for $Pe = 10, 1$ and 0.1 are shown in Figures 3.9, 3.10 and 3.11, respectively. Figure 3.9 shows that at $Pe = 10$, mixing in the monitoring borehole does not significantly affect the shape and placement of the breakthrough curve until $1/W$ exceeds $1/D$. As Pe decreases, the effect of mixing becomes progressively more pronounced (Figures 3.10 and 3.11, Figure 3.11 reflects mass accumulation at the external boundary beyond $t_D = 3$).

To conclude this chapter, we found that the numerical solution converges to a stable shape when the grid contains at least 100 nodes between the injection and the monitoring boreholes for this application; that the external boundary must be far enough from the monitoring borehole to avoid artificial mass buildup in this borehole

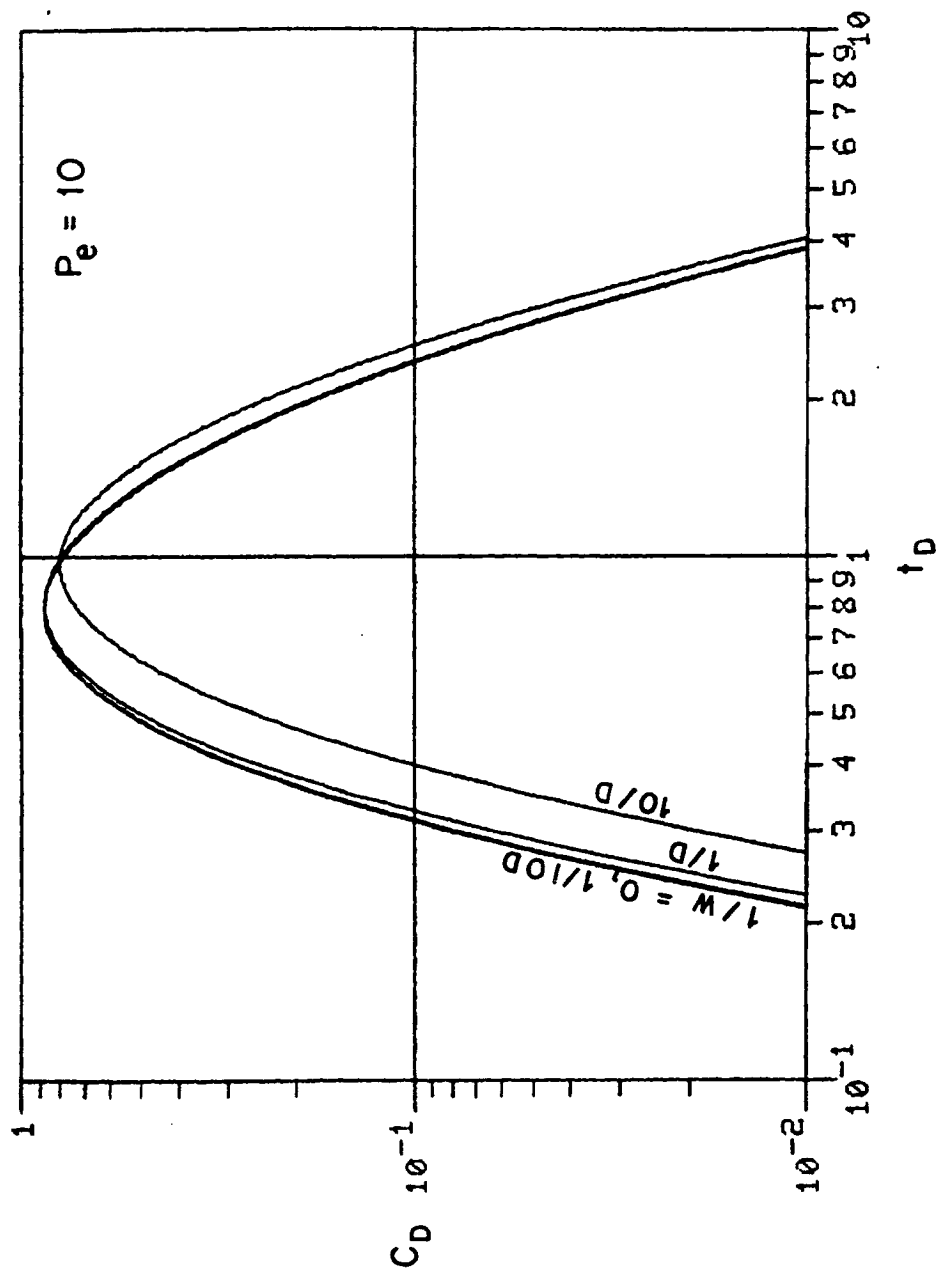


Figure 3.9. Effect of Mixing in Monitoring Borehole, $Pe = 10$.

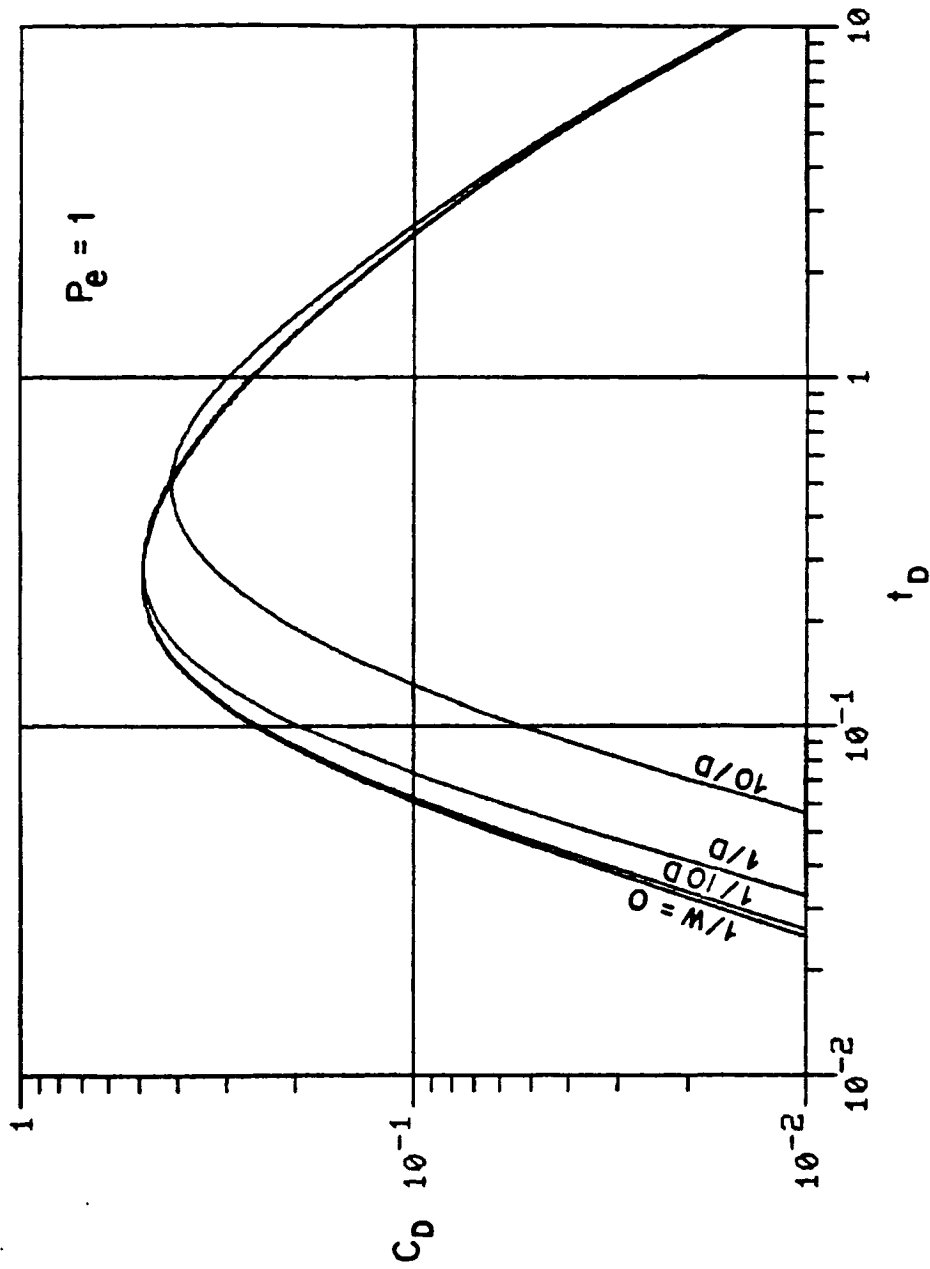


Figure 3.10. Effect of Mixing in Monitoring Borehole, $Pe = 1$.

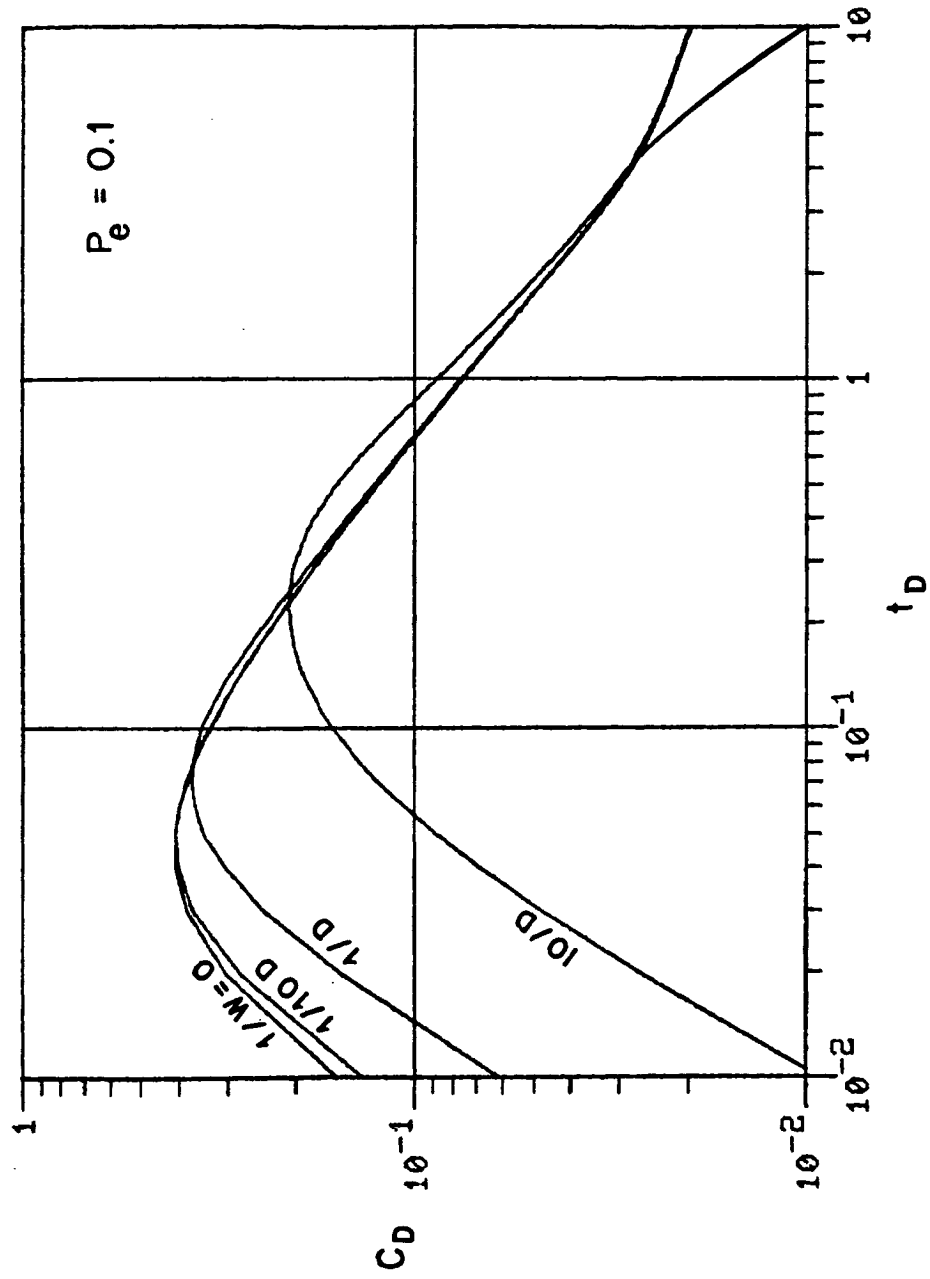


Figure 3.11. Effect of Mixing in Monitoring Borehole, $Pe = 0.1$.

at small Pe ; that available analytical solutions for step input perform poorly at low Pe ; that breakthrough curves are very sensitive to Pe , and become increasingly sensitive mixing in the monitoring borehole as Pe decreases and W goes down. Having thus established confidence in our model we are ready to use it for the analysis of field tracer tests.

CHAPTER 4

ANALYSIS OF DIVERGENT FLOW TRACER TEST DATA FROM ORACLE, ARIZONA

The Oracle field site has been host to numerous hydraulic and tracer tests funded by the U.S. Nuclear Regulatory Commission. Efforts have been focused to develop methodologies to characterize various flow and transport properties of fractured crystalline rocks. Work at the site began in January 1981 and continued through November 1985. This chapter describes the Oracle field site, the divergent flow tracer test procedure, and the manner in which DBDIV was used to analyze the data from the test of July 15-16, 1985.

4.1 Site Description

The Oracle field site is located about five miles southeast of Oracle, Arizona, on a granitic pediment of the northwest portion of the Santa Catalina Mountains (Figure 4.1). Jones, et al. (1985) give a geologic description of the site. The site includes eight boreholes, an analytical equipment shed and a hydraulics and electronicc shed (Figure 4.2). The latter houses tools and supplies to service the tracer test equipment. Table 4.1 contains data pertinent to borehole construction.

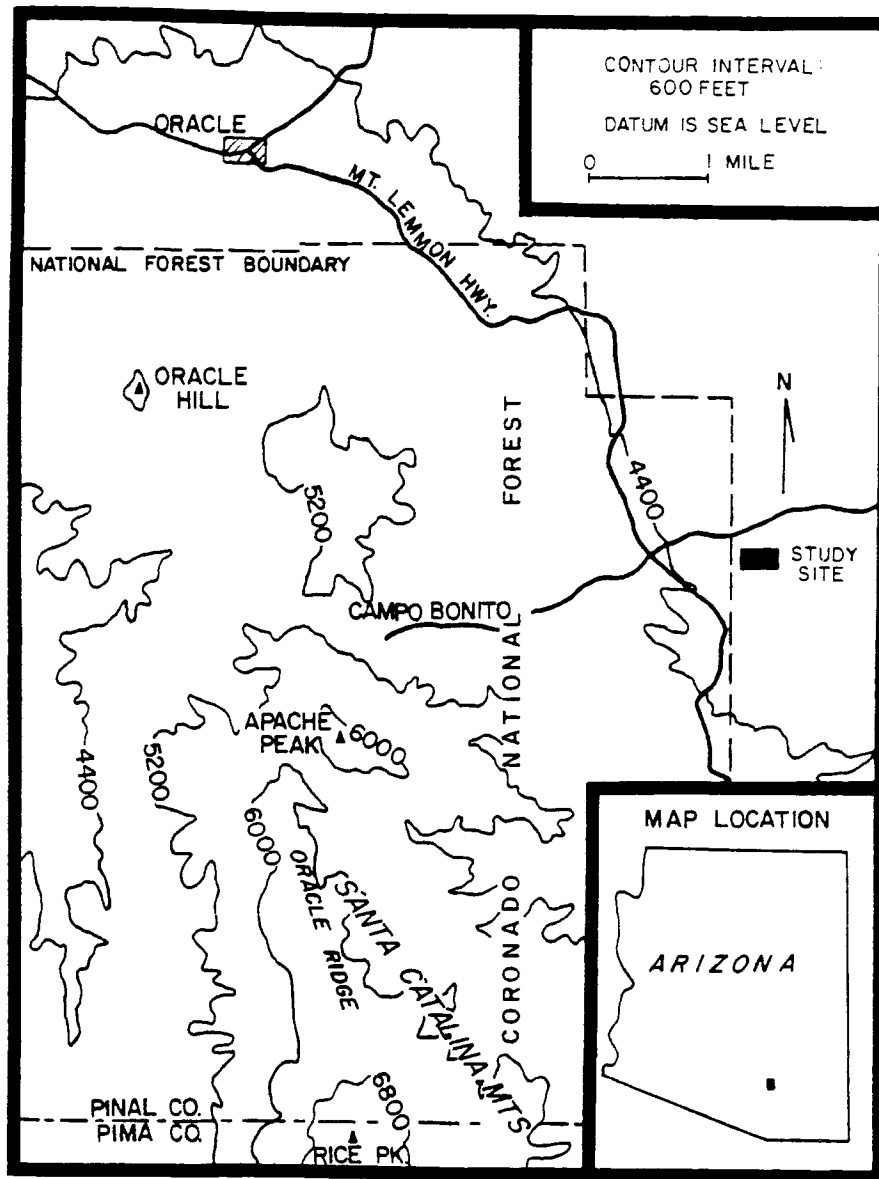


Figure 4.1. Topographic Map of Northern Santa Catalina Mountains.
(After Jones et al., 1985)

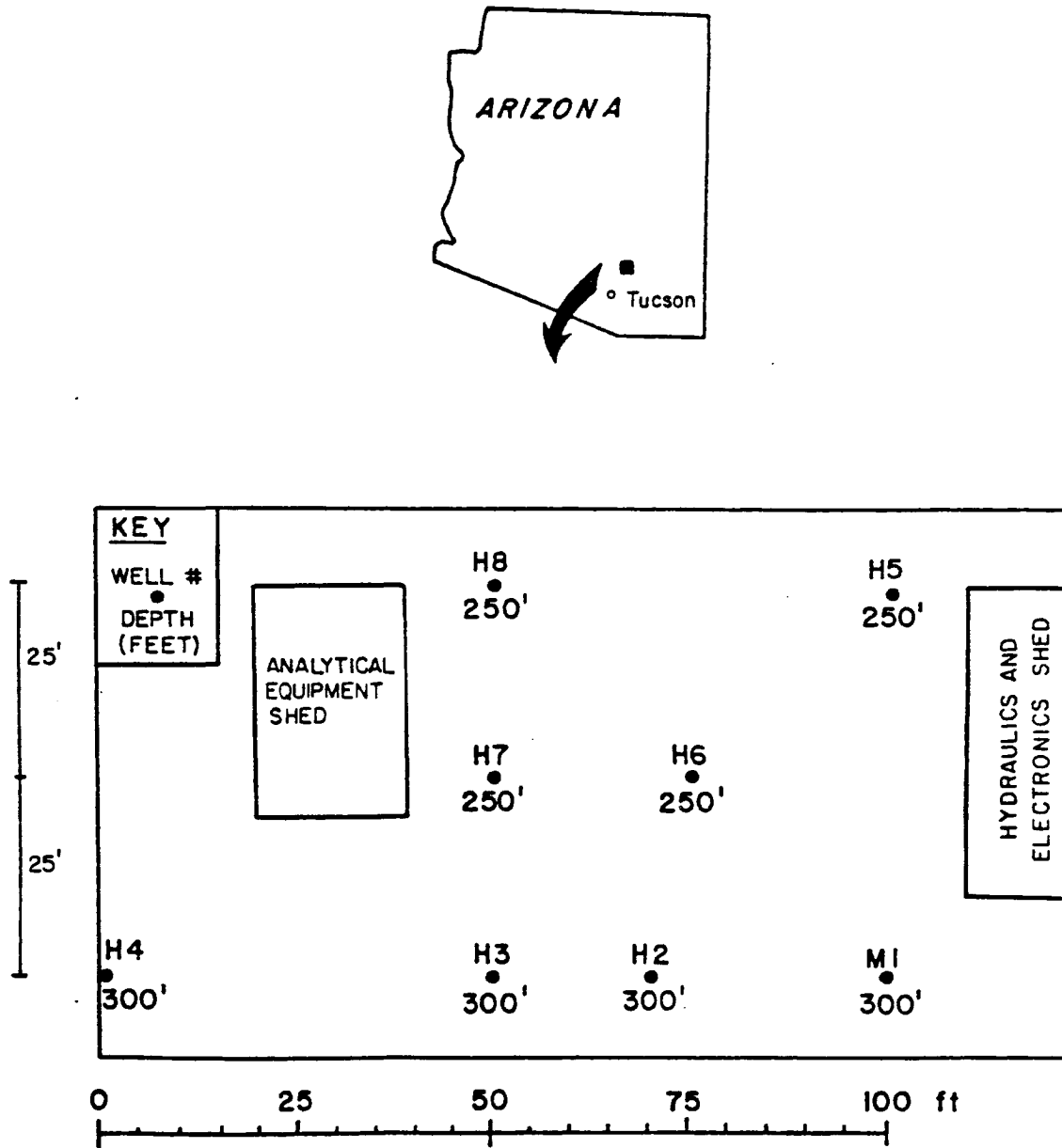


Figure 4.2. Diagram of the Oracle Site.

Table 4.1. Boreholes at Field Site

BOREHOLE NO.	TOTAL DEPTH (METERS)	CASING DEPTH (METERS)	NOMINAL CASING DIAMETER (METERS)	NOMINAL BOREHOLE DIAMETER (METERS)	DRILLING METHOD ** (METERS)
M1	91.5	17.7	0.20	0.17	0-17.7 MR 17.7-32.3 C 32.3-91.5 AH
H2	91.5	18.0	0.13	0.11	0-18.0 MR 18.0-91.5 AH
H3	91.5	17.7	0.18	0.17	0-17.7 MR 17.7-91.5 AH
H4	87.8	13.1	0.13	0.11	0-13.1 MR 13.1-87.8 C
H5	76.2	18.6	0.13	0.11	0-76.2 AH/F
H6	76.2	19.2	0.13	0.11	0-76.2 AH/F
H7	76.2	20.1	0.13	0.10	0-20.1 AH/F 10.2-76.2 C
H8	76.2	18.0	0.13	0.10	0-18.0 AH/F 18.0-76.2 C

** AH/F - air hammer/foam
 AH - air hammer
 MR - mud rotary
 C - cored

After Jones, et al. (1985)

4.2 Field Test Procedure

The divergent flow tracer test was conducted on July 15 and 16, 1985, injecting into borehole M1 and sampling in H2. We isolated the depth interval of 80.8-86.0 meters below land surface (BLS) for injection using straddle packers. The hydraulic conductivity of this interval is given as being on the order of 10^{-6} m/sec by Depner (1985). Point samplers were positioned in H2 at depths of 77.4, 78.9 and 80.5 meters BLS. Figure 4.3 shows a diagram of the test equipment. Barackman (1985) provides information on point sampler construction and operation.

Untraced water was injected between the packers for 1 3/4 hours at $0.0057 \text{ m}^3/\text{min}$. (1.5 gpm) to create a steady state velocity field. The injection equipment was then switched to a tank containing the tracer solution: 234 grams of Pentafluorobenzoic acid dissolved in approximately 570 liters of water. Tracer was first detected in a sample extracted from the injection zone ten minutes after tracer injection began. Here, the sampling interval was approximately 5 minutes. The tracer solution was injected for about 1.5 hours then the injection system was switched back to a fresh water tank; all of the tracer solution had been injected. Water continued to be injected at $0.0057 \text{ m}^3/\text{min}$. for the duration of the test. The pressure within the injection interval in M1 was estimated to be 800 kPa above ambient.

Three point samplers, one above, one between and one below the packers monitored tracer injection. The sampler between the packers provided water samples which after analysis indicated the tracer

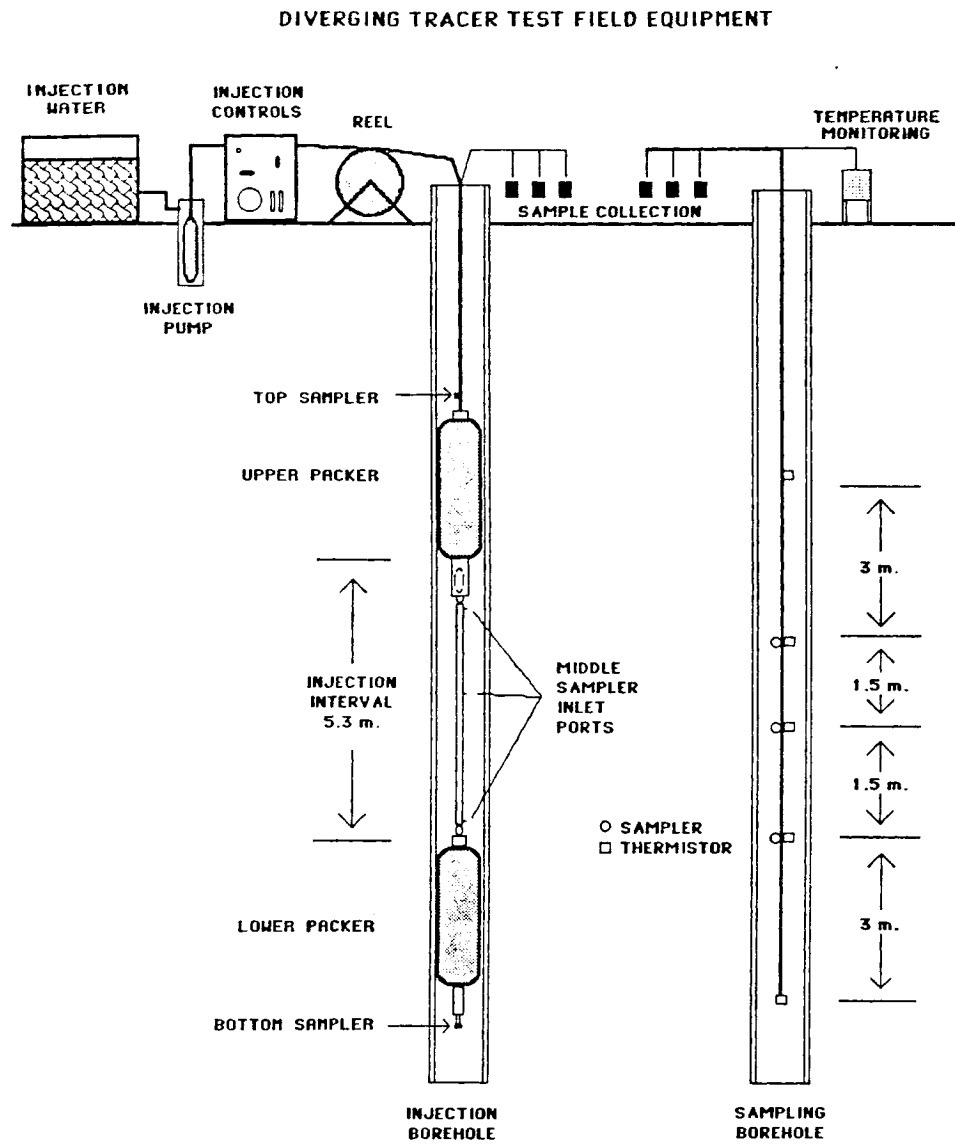


Figure 4.3. Diagram of Divergent Flow Tracer Test Equipment.

injection concentration. Samplers above and below the packer string were used to indicate leakage of tracer around the packers. The bottom sampler did not function properly during the test, so data were not available to determine leakage around the bottom packer.

Three point samplers were used in the monitoring borehole to collect water samples to analyze for tracer breakthrough. Locating the samplers near the zone of inflow into H2 was essential for accurate tracer monitoring. Two methods were developed to locate inflow in the monitoring borehole. The need to develop these methods arose from several earlier unsuccessful attempts at a divergent tracer test. The first method relies on temperatures in a borehole, the second on flow velocity measurements using a heat-pulse flow meter. The first is described by Silliman, Barackman and Messer (1985), the second by Messer (1985). Both were developed as part of this NRC-sponsored project.

An experiment was conducted on August 6, 1985, to test the method based on temperature data. A string of thermistors was used to measure temperature deviations from ambient in H2 and M1 while injecting untraced water into H3 at $0.0019 \text{ m}^3/\text{min}$ (0.5 gpm) over the interval 74.3 - 79.6 meters BLS. We investigated the zones 76.2 - 85.4 meters BLS in H2 and 61.0 - 88.4 meters BLS in M1. The resulting deviations of temperature from their ambient values prior to injection are shown in Figures 4.4 and 4.5, respectively. The thermistors used in H2 were not calibrated so the temperature deviations are not known accurately, but the directions of change in the water temperature were

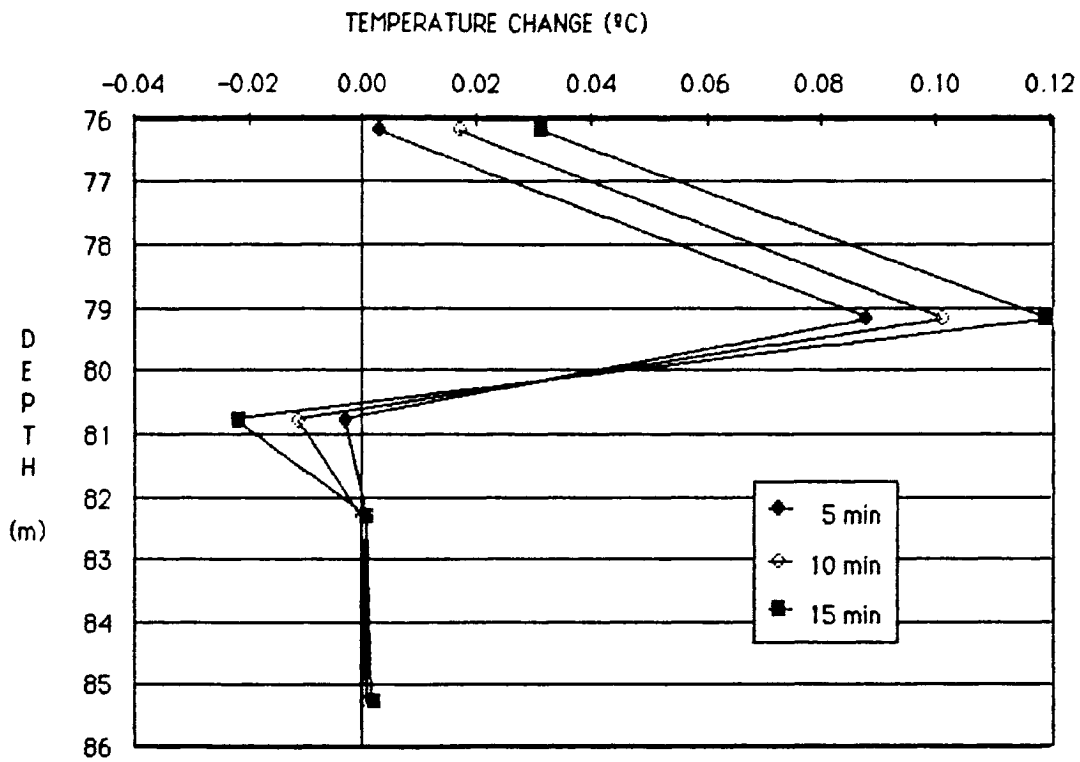


Figure 4.4. Temperature Change in H2 While Injecting into H3 (8/12/85).
(Silliman unpublished data)

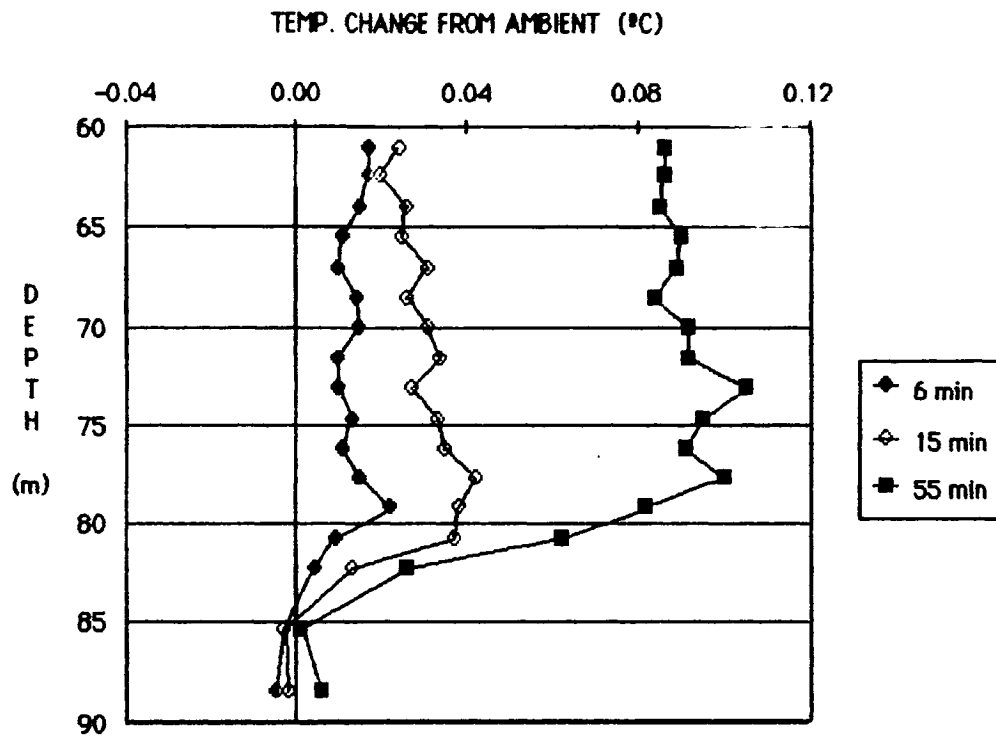


Figure 4.5. Temperature Change in M1 While Injecting into H3 (8/12/85).
(Silliman, unpublished data)

correctly recorded at a given point in time. Figure 4.4 shows that from 80.8 to 83.2 meters BLS water enters H2 from a higher elevation, where, under the prevailing geothermal gradient, ambient temperatures are lower. From 79.2 to 80.8 meters BLS water enters the hole from below, resulting in a temperature increase above ambient.

Figure 4.5 indicates that little disturbance took place in M1 below 85.4 meters BLS. Water appeared to be entering the hole at a fairly uniform rate over the interval 79.3 to 85.4 meters BLS shown by a consistent shift of the curves as time progressed. The zone from 61.0 to 79.3 meters appeared to be inactive relative to the lower zone. These temperature deviations were measured using a single thermistor, therefore the deviations at various levels can be compared to one another. Each curve on the figure corresponds to a single run of the thermistor up the hole. A run consisted of placing the thermistor at 85.4 meters BLS and taking a resistance measurement, then moving the thermistor up the hole in increments of 1.5 meters and measuring the resistance. This continued until the thermistor was at 61.0 meters BLS. Resistance measurements were then converted into temperature using a polynomial equation. The time of each curve indicates the starting time of a run. The data is listed in Appendix B.

The second method uses a heat-pulse flowmeter to measure vertical water velocities in a borehole, as described by Messer (1985). The flow meter consists of a wire grid which when an electrical current is pulsed across the grid produces a heat pulse. The heat pulse is transported by vertical movement of water in the borehole. Thermistors

are positioned above and below the grid to detect the passage of the heated water. Vertical velocity is indicated by the elapsed time required for the pulse to pass by the thermistors. The method was tested in experiments conducted on August 12 and September 13, 1985. Figures 4.6 and 4.7 show the results for H2 and M1, respectively. Injection into H3 at 74.3 - 79.6 meters BLS occurred at 0.0019 and 0.0038 m³/min. (0.5 and 1.0 gpm) during the test of August 12. The flow data graphed in Figure 4.6 indicate that most of the water entered H2 between 80.0 and 82.3 meters BLS and the rest of the hole received relatively little inflow. Some outflow occurred at 30.8 meters BLS.

Figure 4.7 shows a graph of the test data collected while injecting into H3 at 0.0019 m³/min and monitoring M1 during two experiments, one on August 12 and the other on September 13. The graph of the August 12 test indicates that water was entering M1 over the interval 83.8 to 82.3 meters (275-270 feet) BLS and exited over the interval 79.3 to 76.2 meters (260-250 feet) BLS. These are the only data that are of interest because injection during the divergent tracer test in M1 occurred only over the interval 80.8-86.0 meters BLS. The test of September 13 indicated that water entered M1 over the interval 85.4 to 73.2 meters BLS. These conflicting results cannot be explained within the scope of this thesis and the reader is referred to Messer (1985) for possible explanations. The data are given in Appendix B.

From the above results it appears that a number of conducting fractures extends from M1 and converge toward a narrow fracture zone in H2. When water was injected into M2, it flows through numerous

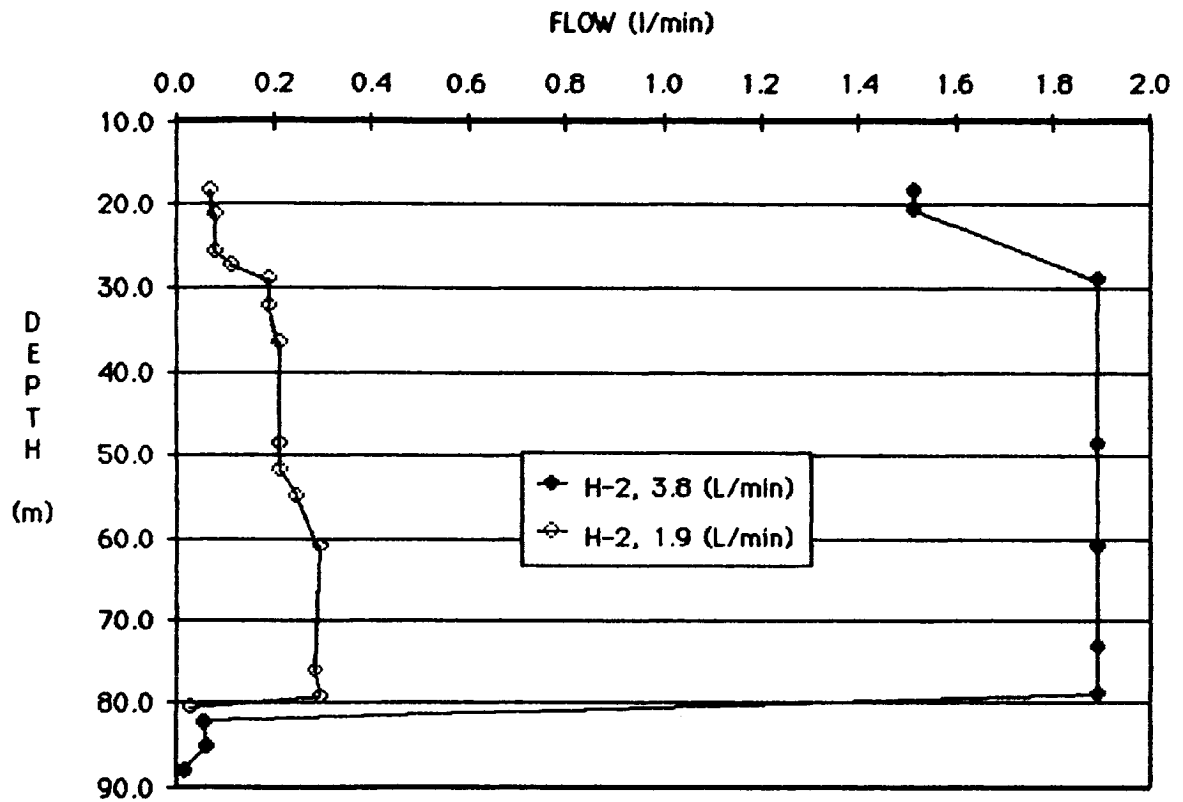


Figure 4.6. Vertical Flow Rates in H2 While Injecting into H3. (After Messer, in preparation)

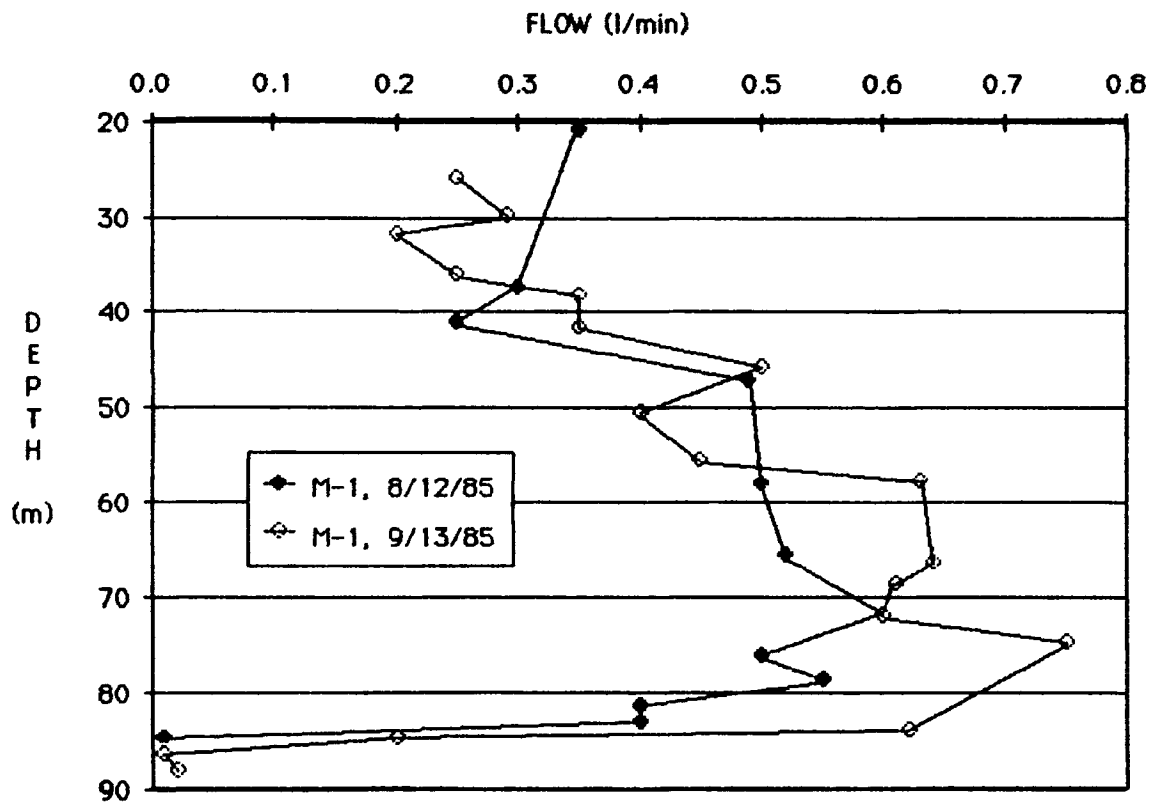


Figure 4.7. Vertical Flow Rates in M1 While Injecting into H3. (After Messer, in preparation)

fractures which conveyed it toward a narrow outlet in H2. It is this outlet that was packed off in our tracer test.

During the tracer test of July 15-16, water samples were extracted from H2 and spot analyzed in the field using high performance liquid chromatography (HPLC) to indicate the progress of the experiment. Sampling was initially done at 10 minute intervals, then the sampling interval was reduced to five minutes when the peak of tracer concentration appeared to approach the monitoring interval, as indicated by rapidly increasing concentration levels of successive samples. Once the tracer concentration peak had passed, the time interval between samples was increased, and by the end of the test samples were extracted every 30 minutes. The test continued until the concentration dropped to approximately 5% of the peak concentration of 131 gm/m^3 . All the samples were analyzed in the laboratory using HPLC to fully define the breakthrough curve. Injection and breakthrough concentration data are listed in Appendix A.

None of the boreholes, excluding the injection hole, contained packers. As a result, water overflowed borehole H2 before tracer was injected into M1. Water levels were recorded from all the boreholes at various times during the test and the data are presented in Appendix A.

4.3 Analysis of Tracer Test Data Using DBDIV

Figure 4.8 shows the breakthrough data from the test, plotted as C/C_{max} (C_{max} being the peak concentration measured in borehole H2) versus the log of t . To obtain a match with a theoretical breakthrough curve, it is convenient to obtain a rough estimate of the parameter ϕb

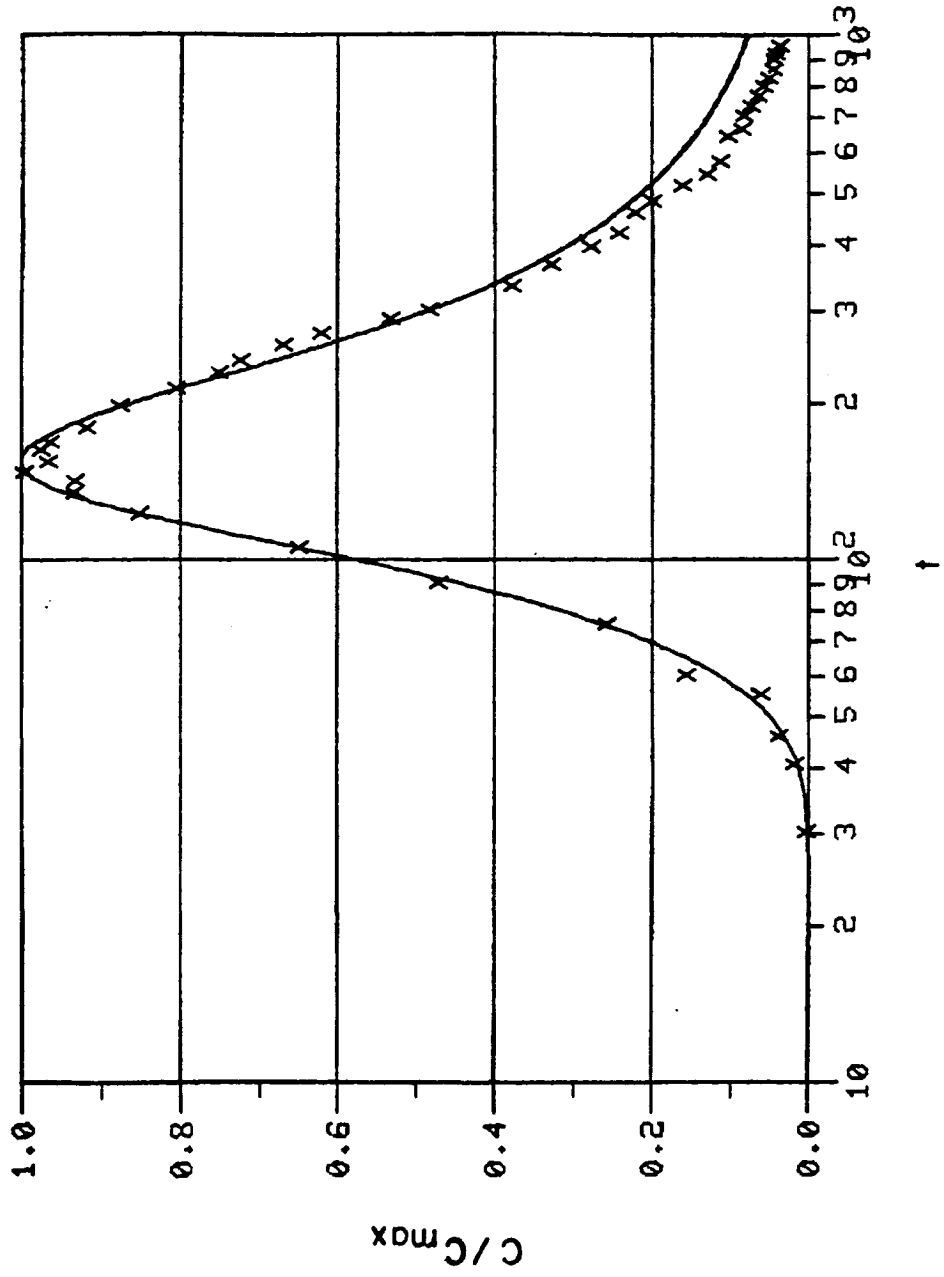


Figure 4.8. Uncorrected Curve Match.

(the product of effective porosity and thickness) from the time, t_I , it takes the center of mass to arrive at the monitoring borehole. If this center of mass travels with the water seepage velocity, then

$$\begin{aligned} t_I &= \int_{r_W}^{r_I} dr/V(r) = \int_{r_W}^{r_I} 2rb\phi Q\pi dr \\ &= \pi(r_I^2 - r_W^2)b\phi/Q \end{aligned} \quad (4.1)$$

from which $b\phi$ can be estimated. In our case, $r_I - r_W = 5.02$ m, $Q = 0.0057$ m³/min, $t_I = 235$ min, and thus a first estimate of ϕb is 0.016 m. Starting from this value and using a trial and error procedure, we obtain the match in Figure 4.8 with $\phi b = 0.007$ m, $a = 7.26$ m and $h_M = 0.15$ m. This match corresponds to $Pe = 0.7$. These and additional data are listed in Table 4.2.

When the data are replotted as concentration, C , versus time, the peak falls about 18% above that of the corresponding theoretical curve from Figure 4.8. While this may have numerous causes, we will assume for simplicity that the flow diverges out of M1 not in all directions, but only through a horizontal angle α ($< 2\pi$). If this is the case, the velocity in the numerical solution is given not by $Q/(2\pi rb\phi)$, but rather by $Q/(\alpha rb\phi)$, and the concentration increases by the factor $2\pi/\alpha$. Trial and error shows that a consistent match (Figure 4.9) can be obtained with $\phi b = 0.009$ m and $Q = 0.0075$ m³/min, the same a and h_M as before, and with other parameters as listed in Table 4.3.

That water was being diverted toward H2 is evidenced by the fact that it was overflowing during the test. As seen in Appendix A,

Table 4.2 Results of Uncorrected Curve Match

Variable	Value
Q	0.0057 m ³ /min
r _I	5.08 m
R	20.32 m
∅ _b	0.007 m
a	7.26 m
h _M	0.15 m
r _M	0.057 m
C _{max}	111 g/m ³
N	100 nodes
Δt	1 min

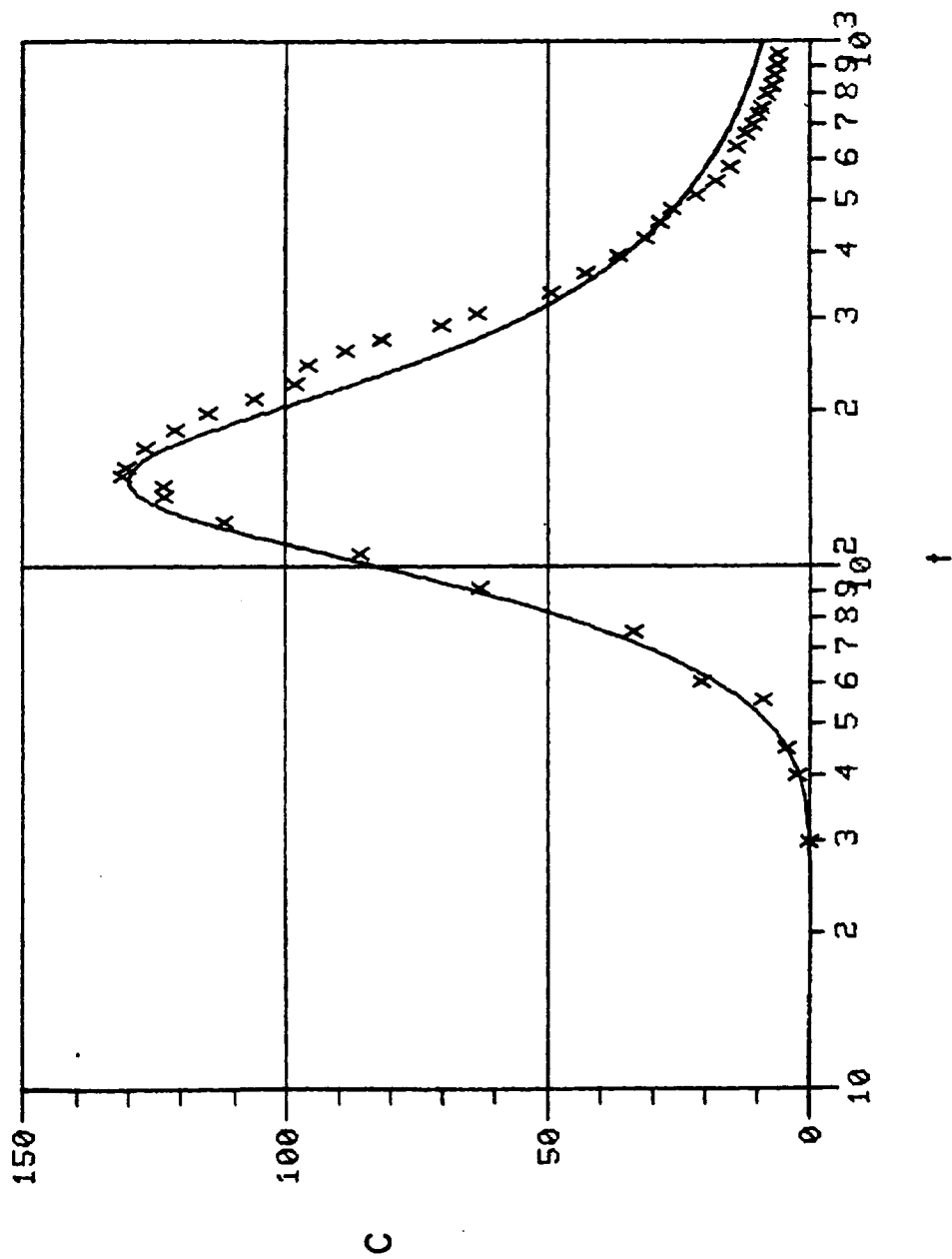


Figure 4.9. Corrected Curve Match.

Table 4.3 Results of Corrected Curve Match

Variable	Value
Q	0.0075 m ³ /min
r _I	5.08 m
R	20.32 m
∅b	0.009 m
a	7.26 m
h _M	0.15 m
r _M	0.057 m
C _{max}	129 g/m ³
N	97 nodes
Δt	1 min

water levels in other boreholes were also rising during the test; approximately 40% of the injected water appeared in the boreholes. This suggests that we are not dealing with a true radially divergent flow situation, but rather a multiple-well test in which M1 acts as an injection well and other boreholes (especially H2) act as sinks. This may account for the relatively large dispersivity of 7.26 m that we calculated in the above analysis. The same test data are currently being reanalyzed using a model which treats H2 as a pumping well. We expect the dispersivity from this analysis to be smaller than 7.26 m, as much of the dilution indicated by our breakthrough data is probably due to a variability in velocities within, and lengths of, various streamtubes running from M1 to H2. The ϕb product calculated by us could also be in error for the same reason. The assumptions of isotropy and uniformity made in our model are also not met at the Oracle site.

4.4 Recommendations for Conducting Divergent Flow Tracer Tests

From the experience of past divergent flow tests, one could suggest several improvements to be implemented in future work: 1) The hydraulic properties of the aquifer and the hydraulic connections between the boreholes should be clearly understood. This can be achieved by conducting injection tests and employing the thermistor and flow meter methods to define the zones in the monitoring boreholes that are hydraulically connected to the pumping or injecting well. 2) One must be able to monitor the tracer concentration as the tracer enters

the formation at one borehole and exits the formation at another hole. We have done this at the Oracle site; A future modification would include installing a mixing pump on the injection equipment within the injection interval to insure that tracer concentration is uniform throughout the injection zone. 3) A modification of the test procedure would be to place packers in the other boreholes to isolate those zones that are in connection with the injection zone from the remainder of each borehole in an attempt to maintain radial flow. 4) The test should be continued until the breakthrough curve is adequately defined. Our tracer test was continued until the concentration in the monitoring borehole was less than 5% of the peak concentration.

CHAPTER 5

CONCLUSIONS

In this thesis a numerical model for the analysis of radially divergent tracer test data has been used and perfected. The model results were compared with three analytical solutions from the literature. The model was subjected to sensitivity analyses of the controlling parameters and used to analyze field data from a tracer test near Oracle, Arizona. From this work we conclude:

1) The numerical model provides an accurate solution to the governing transport equation at both high and low Peclet numbers, Pe . The model is free of numerical dispersion. However, constraints on grid construction and outflow boundary placement must be adhered to: in our case the grid must contain at least 100 nodes between the injection and the monitoring boreholes and the external boundary also must be far enough from the monitoring borehole, this distance increasing with decreasing Pe .

2) The three analytical solutions examined assume that Pe is large and therefore do not accurately describe transport at small Pe . The solutions of Raimondi, et al. (1959) and Dagan (1971) compare well with each other and with the numerical solution at $Pe > 10$. As Pe decreases the solution of Dagan deviates from the numerical solution more rapidly than does the solution of Raimondi, et al. The solution of Hoopes and Harleman (1967) does not agree well with any of the other

solutions (including numerical) over the entire range of Pe examined, $0.1 \leq Pa \leq 100$.

3) The numerical solution is very sensitive to Pe , and sensitive to the mixing volume at small Pe . Variations in the porosity-thickness product cause the breakthrough curve to shift along the time axis. Variations in Pe cause these curves to open or close, and the peak concentration to increase or decrease for noncontinuous injection. Mixing in the monitoring borehole may affect the curve in both ways. Hence, one can rarely guarantee a unique fit between the theoretical curve and the given field data.

4) To properly conduct a divergent tracer test in the field, it is preferable to know the hydraulic properties of the rock and hydraulic connections between the boreholes. One must be able to describe accurately how and where the tracer enters and exits the aquifer. The tracer test should be continued until the breakthrough curve is fully defined, in our case the test was continued until chemical analysis of the samples extracted from the monitoring borehole indicated that the concentrations were <5% of the peak concentration. All zones in the other boreholes that are hydraulically connected to the injection interval should be isolated by packers in order to maintain a radial flow field. Packers were not available to isolate these zones in the other boreholes, as such the unpacked boreholes were locations of high storage for water, relative to the formation. Thus boreholes behaved as hydraulic sinks that distorted the flow field. This may explain why we computed what appears to be an inordinately

high dispersivity for the site. The data are currently being analyzed with the aid of another model which accounts for the nonradial nature of the flow field.

APPENDIX A

DIVERGENT FLOW TRACER TEST DATA, JULY 15-16, 1985

Table A.1. Injection Concentration Data (M1)

Top Sampler		Middle Sampler	
Time(min.)*	Conc.(g/m ³)	Time(min.)*	Conc.(g/m ³)
80	0.5	10	1.34
90	0.22	14	4.25
270	1.10	20	79.7
		26	169.
		32	262.
		38	308.
		44	341.
		50	358.
		56	373.
		62	400.
		68	425.
		74	426.
		80	443.
		86	428.
		98	398.
		104	337.
		110	249.
		116	115.
		122	74.4
		128	39.6
		130	29.1
		134	51.1
		165	15.6
		180	9.1
		210	3.28
		270	3.0
		330	0.44

* time since beginning of tracer injection

Table A.2. Breakthrough Concentration Data (H2)

Time *	Concentration 80.5 meters	Concentration 80.0 meters
(minutes)	(g/m ³)	(g/m ³)
40	2.22	
45	4.21	
55	7.97	
60	20.2	15.2
75	33.6	38.0
90	62.3	53.8
105	85.1	79.5
120	112.0	102.0
135	123.0	122.0
140	123.0	
145	131.0	
150	130.0	124.0
155	127.0	123.0
165	127.0	127.0
170		125.0
180	121.0	120.0
195	115.0	119.0
205		111.0
210	106.0	105.0
225	98.1	101.0
240	95.3	92.4
255	87.9	90.8
270	81.3	80.1
285	69.7	70.7
300	63.2	63.8
330	49.0	51.4
360	42.3	46.4
390	36.2	40.9
420	29.5	31.3
450	26.7	28.7
480	26.3	27.0
510	21.0	23.1
540	17.1	19.2
570	14.8	17.0

Table A.2--Continued

Time *	Concentration 80.5 meters	Concentration 80.0 meters
(minutes)	(g/m ³)	(g/m ³)
600		16.0
630	13.3	
660	11.6	
690	11.1	
720	9.34	
750	8.98	
780	7.61	
810	6.83	
840	6.25	
870	5.78	
900	5.99	
930	5.30	

* time since beginning of tracer injection

Table A.3. Water Level Data

Borehole	Time **	Water Level (meters BLS)
M1	2213	7.74
	2218	7.67
	2222	7.62
	2224	7.59
	2228	7.56
	2345	7.10
H2	2147	8.22
	2220	6.34
	2225	5.12
	2230	4.30
	2235	3.35
	2249	1.68
	2255	0.91
	2306	overflow
H3	2150	9.42
	0002	6.01
	1115	2.37
	1445	2.56
H5	2156	8.84
	0007	8.63
	1110	7.59
	1443	7.39
H6	2154	9.33
	2247	8.72
	2323	7.88
	2355	7.79
	1104	7.10
	1442	3.90
H7	2359	9.39
	1106	5.01
	1438	4.54
H8	1107	6.78
	1441	6.10

** time of day on a 24-hour clock
 (Note: the tracer injection began at 2400 hours)

APPENDIX B

TEMPERATURE AND FLOW METER DATA

Table B.1. Temperature Change in M1, Injecting into H3

Depth (m)	Temp. Change* t=6min.	Temp. Change t=15 min.	Temp. Change t=55 min.
88.4	-0.005	-0.002	0.006
85.4	-0.003	-0.003	0.001
82.3	0.004	0.013	0.026
80.8	0.009	0.037	0.062
79.3	0.022	0.038	0.082
77.7	0.015	0.042	0.100
76.2	0.011	0.035	0.091
74.7	0.013	0.033	0.095
73.2	0.010	0.027	0.105
71.6	0.010	0.034	0.092
70.1	0.015	0.031	0.092
68.6	0.014	0.026	0.084
67.1	0.010	0.031	0.089
65.5	0.011	0.025	0.090
64.0	0.015	0.026	0.085
62.5	0.017	0.020	0.086
61.0	0.017	0.024	0.086

* Degrees Celsius

After Silliman unpublished data

Table B.2. Temperature Change in H2, Injecting into H3

Depth (m)	Temp. Change [*] t=5 min	Temp. Change t=10 min	Temp. Change t=15 min
84.5	0.001	0.001	0.002
82.3	0.001	0.000	0.001
80.8	-0.003	-0.011	-0.022
79.3	0.088	0.101	0.115

* Degrees Celsius

After Silliman unpublished data

Table B.3. Flow Meter Results in M1, Injecting
into H3 8/12/85

Depth (m)	Flow (gpm)
84.8	0.010
83.1	0.150
81.4	0.150
78.7	0.125
76.2	0.110
71.6	0.235
65.5	0.200
57.9	0.200
47.3	0.160
41.2	0.100
37.5	0.110
21.0	0.120

After Messer (in preparation)

Table B.4. Flow Meter Results in M1, Injecting
into H3 9/13/85

Depth (m)	Flow (gpm)
88.1	0.008
86.6	0.008
84.8	0.050
83.8	0.220
74.7	0.240
72.0	0.200
68.6	0.210
66.5	0.212
57.6	0.135
50.6	0.125
45.7	0.155
41.5	0.108
38.1	0.110
36.0	0.082
31.7	0.045
29.9	0.090
25.9	0.075

After Messer (in preparation)

Table B.5. Flow Meter Results in H2 Injecting into H3

Injection Rate=0.1 gpm		Injection Rate=0.5 gpm	
Depth (m)	Flow (gpm)	Depth (m)	Flow (gpm)
88.1	0.005	80.5	0.008
85.4	0.017	79.3	0.078
82.3	0.015	76.2	0.074
79.0	0.500	61.0	0.078
73.2	0.500	54.9	0.065
61.0	0.500	57.8	0.055
48.8	0.500	48.8	0.055
29.0	0.500	36.6	0.055
20.7	0.400	32.0	0.050
18.3	0.400	29.0	0.050
		27.4	0.030
		25.9	0.020
		21.3	0.020
		18.3	0.018

After Messer (in preparation)

APPENDIX C

USERS GUIDE

C.1 Introduction

DBDIV is a program of the analysis of divergent flow tracer tests. It is written in FORTRAN 77. The analytical part of the program is self-contained (i.e., it does not require any system library.) However, the program uses the plotting package PLOT-10 (both the Terminal Control System and the Advanced Graphing II) for graphic output. The theory behind the program is described in this M.S. thesis Analysis of Divergent Flow Tracer Tests in Fractured Granite, Near Oracle, Arizona.

DBDIV can be used for simulation and for parameter estimation. For simulation purposes, the program can handle a wide range of alternatives with regard to boundary conditions at the injection well, initial conditions, and dispersion coefficient. Regarding the injection well, the program can simulate an instantaneous slug injection of finite or infinitesimal size into the formation. Arbitrary input concentrations over time can also be simulated. The outflow boundary is a non-dispersive flux boundary. The internal boundary, representing the injecting well, is treated as non-dispersive, implying that all the transport across the borehole wall is due to the advective movement of water. An option is provided to account for mixing in the monitoring borehole. Initial conditions are taken, by default, to be zero concentration throughout the flow domain; however arbitrary initial conditions can be defined by the user.

Finally, the dispersion coefficient can be of the form

$$D' = aV^n + D^* \quad (C.1)$$

D^* = molecular diffusion

where D is the dispersion coefficient, a is the dispersivity and n is an arbitrary constant between one and two. By default, the program takes $n = 1$.

In the parameter estimation mode, DBDIV uses the method of Newton to estimate the porosity, dispersivity and/or mass injected into the formation that best fit measured data. These can be computed in conjunction with any of the options discussed in the previous paragraph.

Following is the input description, listing of the code, a flow chart, list of subroutines and arrays, as well as three examples which are included.

C.2. Input Description

To run DBDIV on the Data General MV 10000, one must type:

```
X DBDIV
```

The program will ask the input and output file names. These must be typed with quote symbols. If the input data is such that a plotting file is created, the user may want to execute PLOT after DBDIV.

The program also asks for two output files. The first prompts the user with "enter output file name." This file contains a copy of the input data and all of the output data. The second output file is

Prompted with "enter output file name for cmax values." This output file contains information of grid construction (Δt , NT, NN, MULT), Peclet number, dispersivity, maximum concentration, and if pertinent, maximum concentration after mixing in the monitoring well. Following is the description of the input data file.

Card	Cols	Format	Name	Description
1	PROBLEM NAME 1-80	A60	HED	Problem name. Up to 60 characters, it is printed at various stages in output.
2	PROBLEM INDICES 1-5	I5	IPROB	Type of problem index 0. Standard simulation 1. Type curves production 2. Parameter estimation
	6-10	I5	IPL	Plotting index 0. No plot produced 1. Plot produced
	11-15	I5	INJ	Input concentration at injection well 1. Pulse injection followed by constant concentration 2. Arbitrary 3. Step increase
	16-20	I5	IBND	Boundary condition at monitoring well 0. No dispersion 1. Prescribed conc. 2. Mixing with borehole volume (no dispersion)

Card	Cols	Format	Name	Description
21-25	I5		INIT	Initial conditions index 0. Slug at injection well 1. Arbitrary initial condition plus slug at injection well
26-30	I5		IDIS	Index controlling form of dispersion coefficient 0. Dispersion proportional to V , $D=aV+D^*$ 1. Constant dispersion 2. D proportional to V^2 3. D of the form $D=aV^n+D^*$
31-35	I5		ISOL	Index controlling solution method 0. Equations derived from mass balance 1. Equations derived from Finite Element method NOTE: if $IDIS \neq 0$, then $ISOL$ must be 0. The option $ISOL=1$ is not verified.
36-40	I5		IRAD	Index controlling grid construction 0. First cell is centered in the wall of injection well. 1. Wall of injection well coincides with edge of first cell.
41-45	I5		IGRID	Controls the manner in which the grid is generated. 0. Grid is such that time interval is approximately t 1. Grid has NN nodes
46-50	I5		NN	Number of nodes
51-55	I5		NT	Number of time intervals

Card	Cols	Format	Name	Description
	56-65	F10.3	AT	(Ignore if IPROB=1) If IGRID=1, AT=maximum simulation time. If IGRID=0, AT=time increment

If IPROB=1, then IGRID should be set equal to 1, which is usually the best choice, unless time dependent inputs are specified.

3	PHYSICAL DESCRIPTION			
	1-10	F10.0	RI	Distance between centers of monitoring and injec- tion wells
	11-20	F10.0	RW	Radius of injection well
	21-30	F10.0	Q	Injection rate
	31-40	F10.0	THK	Aquifer thickness
	41-50	F10.0	RAQ	Distance from center of injection well to boundary
	51-60	F10.0	XMS	Mass of tracer injected (If IPROB=1)
4	HYDRODYNAMIC PARAMETERS (Omit if IPROB=1)			
	1-10	F10.3	POR	Porosity
	11-20	F10.3	ALP	Longitudinal dispersivity.
	21-30	F10.3	XMS	Mass of tracer injected.
	31-40	F10.3	DISEX	Exponent of velocity in the dispersion coefficient
	41-50	F10.3	DMOL	Coefficient of molcular diffusion

NOTE: If IPROB=0, POR, ALP, XMS, and DISEX are the hydrodynamic parameters. If IPROB=2, then they are the initial values for the iterative search of the optimum parameters.

Card	Cols	Format	Name	Description
5	BOUNDARY CONDITIONS IN INJECTION WELL (Omit if INJ=2,3)			
	1-10	F10.3	CO	Prescribed concentration
	11-20	F10.3	XMAS	Mass of solute at the injection well borehole at the beginning of the simulation.
	21-25	I5	INJBC	0. No dispersion through $r=RW$ 1. Prescribed concentration
6	BOUNDARY CONDITION AT INJECTION WELL (Omit if INJ=0,1)			
	1-60	6F10.3	CI(N)	For $N=1, \dots, NT$ CI(N) is concentration at injection well, at N-th time step.
NOTE:	Give six values per card and repeat as many cards as needed until completion. In order to assign realistic values to CI(N), it may be necessary to define IGRID=0 in Card 2.			
7	BOREHOLE AT MONITORING WELL (Omit if IBND \neq 2)			
	1-10	F10.3	RM	Radius of monitoring well
	11-20	F10.3	HM	Height of water in monitoring well
8a	INITIAL CONDITIONS-I (Omit if INIT=0)			
	1-5	I5	N1	Number of first node for which initial conditions are to be specified.
	5-10	I5	N2	Number of last node for which initial conditions are to be specified.
8b	INITIAL CONDITIONS-II (Omit if INIT=0)			
	1-60	6F10.0	C1(N)	For $N=N1, \dots, N2$, C1(N) is the initial concentration.

This card must be repeated as many times as needed to specify the initial concentration at all nodes between N1 and N2. Concentration is assumed to be zero at all other

Card	Cols	Format	Name	Description
nodes. In assigning the initial concentrations, it is convenient to bear in mind that all cells have the same constant volume of water: $Q t$.				
9	TYPE CURVES PARAMTERS (Omit if IPROB#1)			
	1-5	I5	NCM	Number of type curves.
	6-10	I5	ITC	Index of Peclet numbers generation 0. Same sequence as Sauty 1. Exponential increment 2. Arbitrary Peclet sequence defined in next card
	11-20	F10.3	TRMIN	Minimum reduced time.
	21-30	F10.3	TRMAX	Maximum reduced time.
	31-40	F10.3	PCIN	(Omit if ITC#1) Minimum Peclet number for which curves are to be produced.
	41-50	F10.3	FAC	(Omit if ITC#1) Incremental factor. Curves will be produced for Peclet numbers of: $Pe=PCIN*(FAC)^N$ $N=0,1,\dots,NCM-1$
	51-60	F10.3	DMOL	Coefficient of molecular diffusion
	61-70	F10.3	DISEX	Exponent of velocity in dispersion coefficient
9b	PECLET NUMBERS LIST (Omit if IPROB#1 or ITC#2)			
	1-60	6F10.3	PE(N)	For $N=1,\dots,NCM$ PE(N) is the Peclet number of Nth curve.

Card	Cols	Format	Name	Description
10	PLOTTING PARAMETERS (Omit if IPL=0)			
	1-10	F10.3	SMAX	Maximum concentration
	11-20	F10.3	SMIN	Minimum concentration
	21-30	F10.3	TMIN	Minimum time.
	31-40	F10.3	TMAX	Maximum time.
	41-45	I5	IFLPL	Hard copy index. 0. Plot to screen 1. Binary output file 2. Output in CS.DAT
	46-50	I5	ILOG	Type of scaling index. 0. Arithmetic scaling for time axis. 1. Logarithmic scaling for time axis. 2. Log-log scaling
	51-55	I5	IMASS	Vertical axis index. 0. Vertical axis represents concentrations. 1. Vertical axis represents mass.
	56-60	I5	ISCAL	Scaling index. 0. Real time, real concentration. 1. Real time, concentrations scaled by the maxima. 2. Dimensionless time, real concentrations. 3. Dimensionless time, concentrations scaled by the maxima. 4. Dimensionless time, dimensionless concentration

Card	Cols	Format	Name	Description
11	PARAMETERS ESTIMATION (Omit if IPROB#2)			
	1-5	I5	NINT	Number of measurements
	6-10	I5	IW	Weighting option. 0. Equal weight to all measurements. 1. Arbitrary weight matrix 2. Autoregressive process
	11-15	I5	MB	Bandwidth of weight matrix (Ignore if IW=0 or 2)
	16-20	I5	IALP	1. Dispersivity is to be estimated. 0. Otherwise
	21-25	I5	IPOR	1. Porosity is to be estimated. 0. Otherwise
	26-30	I5	IMAS	1. Injected mass is to be estimated. 0. Otherwise
	31-35	I5	ITMX	Maximum number of iterations (default, 20).
	36-45	F10.3	OBMIN	Stop if sum of squared residuals < OBMIN.
	46-55	F10.3	RATIO	Stops if maximum relative change in parameter value is smaller than RATIO for three consecutive iterations.
	56-65	F10.3	AUTO	Autocorrelation coefficient (omit if IW#2)
12	MEASUREMENTS			
	1-10	F10.3	TM(N)	Times corresponding to Nth measurement.
	11-20	F10.0	CM(N)	Measured concentration.

Card	Cols	Format	Name	Description
21-80	6F10.0	W(N,M)		For M=1...MB, enter the N-Mth components of weighting matrix W.

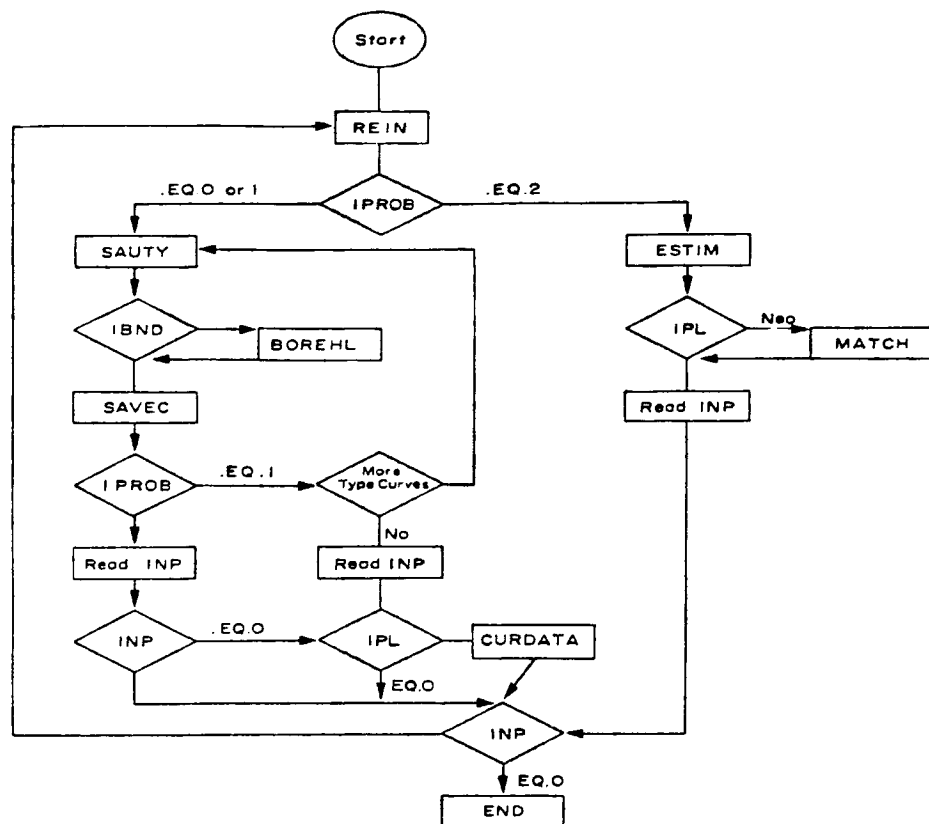
Card 4 must be repeated NINT times, one for each data point.

WARNING: Inasmuch as the bulk of the data is entered with this card and it is much easier to change a format card than the format of all data, it is likely that the actual format in the program is different from the one shown here. Therefore, the author suggests that the user check what the actual format is (FORMAT #235 in subroutine REIN).

13	END CARD (Restart)			
1-5	I5	INP	0.	Stop execution.
			n.	(1<n<12) continue execution reading cards n-12 (if necessary)
			-n.	(1<n<12) continue execution re-reading card n and changing parameters as indicated

NOTE: Once the bulk of cards 1-12 has been read, one can stop the execution (INP=0), or change the parameters in card #n (INP=-n) and execute the problem thus defined, or change the parameters in cards #n-12 (INP=n).

C.3 Flow Chart



C.4. List of Subroutines

REIN	Reads and prints input data.
SAUTY	Computes output concentrations.
MBLC	Computes mass in system at a given moment.
MESH	Computes values of NN, NT, and/or AT.
RADIUS	Computes radii array.
MATRIX	Computes F.D. matrix (ISOL=0, IRAD=0, IDIS=0).

SOLTRI	Forward and backward substitution in tridiagonal symmetric linear system.
DECTRI	Triangular decomposition of tridiagonal symmetric matrix.
DERIV	Computes concentrations and Jacobian matrix.
BOREHL	Mixing effect in pumping well borehole.
TMINT	Time interpolator.
ESTIM	Computes a , ϕ and M so as to match measured and computed concentrations.
CHOLES	Cholesky decomposition.
FORBAC	Forward and backward substitution.
WTDRES	Weighted residuals and objective functions.
CFMTR	Matrix of coefficients (on normal equations).
RHS	Right-hand side of normal equations.
SAVEC	Stores computed concentrations in CS array.
FMAX	Finds maximum of array.
MATREL	Builds finite element matrix.
DETRUN	Triangular decomposition of tridiagonal non-symmetric matrix.
SOTRUN	Forward and backward substitution in nonsymmetric tridiagonal matrix.
FMIN	Finds minimum value of an array.
MODBND	Modifies the matrix of coefficients for boundary conditions.
MATDIS	Builds matrix for arbitrary dispersion ($D=aV^n+D^*$).
CURDATA	Prepares data for CURVA to plot sets of curves.
CURVA	Plots curves.

C.5. List of Arrays

<u>Symbol</u>	<u>Dimension</u>	<u>Description</u>
A	NNA,2	Finite differences matrix
R	NNA	Radius coordinates
C	NNA	Concentrations at nodes
CT	NTA	Concentrations at monitoring well
C1	NTA	Initial concentration (over space)
CI	NTA	Injection concentrations
X	NTA	Working space
CM	NMA	Measured concentrations
TM	NMA	Measured times
CC	NMA	Computed concentrations at measurement times
W	NMA,3	Weighting matrix
CW	NMA	Weighted concentration (and residuals)
HW	NMA,3	Weighted sensitivity matrix
H	NMA,3	Sensitivity matrix (Jacobian)
A	3,3	Normal equations matrix
P	3	Vector of model parameters
P1	3	Vector of model parameters in previous iteration
B	3	R.H.S. vector of normal equations
PE	NPA	Peclet numbers
CS	NTA,NPA	Computed concentrations in a maximum of NPA problems

<u>Symbol</u>	<u>Dimension</u>	<u>Description</u>
TS	NPA	Time increment
STAY	NTA	Vector of mass remaining in the system
GONE	NTA	Vector of accumulated output mass

C.6. Examples

Three examples are presented to illustrate some of the capabilities of the program. The first two examples deal with the type curve production mode, example 1 employs a step increase of injection concentration, while example 2 uses a square pulse injection boundary condition. The third example is in the standard simulation mode. It describes the use of DBDIV'S ability to generate multiple simulations in this mode. It also incorporates mixing in the monitoring well. The results of all simulations are shown as real concentration versus time.

An example of the parameter estimation mode is not presented. If the reader wishes to use this mode, he is referred to Carrera and Walter at Hydro Geo Chem, Inc. in Tucson, Arizona. Also the finite element option is not verified.

All of the examples are of the same basic problem; the physical conditions of the problem are shown in Table C.6.1.

Example 1

Example 1 illustrates the use of the program to simulate five type curves using a step increase of injection concentration. Five

Table C.6.1. Physical Conditions

Parameter	Value
RI	10. m
RW	0.05 m
Q	0.01m ³ /min
b	10 m
RAQ	14.15 m
M	1000 gm
Ø	0.1
D*	0.0

Peclet numbers are used: 100, 50, 10, 5, 1. Figure C.6.1a provides the input file and Figure C.6.2 shows the breakthrough curves.

Example 2

Example 2 shows the use of DBDIV to simulate five type curves using a square pulse injection concentration. The same sequence of Peclet numbers as Example 1 is used. The input file and breakthrough curves are shown on Figures C.6.1b and C.6.3 respectively.

Example 3

Example 3 simulates the same problem as Example 2 except this example uses the standard simulation mode using the repeat feature of card 13 for multiple simulations. This example also illustrates the use of mixing in the monitoring well, $r_M=0.05m$, $h_M=10.m$. Figures C.6.1c and C.6.4 provide the input file and simulation curves.

STEP INCREASE OF CONCENTRATION

1	1	3	0	0	0	0	0	1	2000	100	10.
10.		.05		.01		10.		14.15		1000.	
1	2	0.0		3.5						0.0	1.0
1.											
1.		0.		0.		2.5		0	0	0	3
0											

a. Example 1, Step Increase Injection

SQUARE PULSE OF CONCENTRATION

1	1	0	0	0	0	0	0	1	200	100	10.
10.		.05		.01		10.		14.15		1000.	
0.						0					
5	2	0.0		3.5						0.0	1.0
1.		5.		10.		50.		100.			
8.		0.		1000.		100000.		0	1	0	0
0											

b. Example 2, Pulse Injection

STANDARD SIMULATION OF SEVERAL CURVES (PULSE INPUT & MIXING)

0	1	0	2	0	0	0	0	1	200	100	100000.
10.		.05		.01		10.		14.15		1000.	
.10		10.		1000.		1.		0.			
0.						0					
.05		10.									
8.		0.		1000.		100000.		0	1	0	0
-4											
.10		2.		1000.		1.		0.			
-4											
.10		1.		1000.		1.		0.			
-4											
.10		.2		1000.		1.		0.			
-4											
.10		.1		1000.		1.		0.			
0											

c. Pulse Injection with Mixing in the Monitoring Borehole

Figure C.6.1. Input Files for Examples.

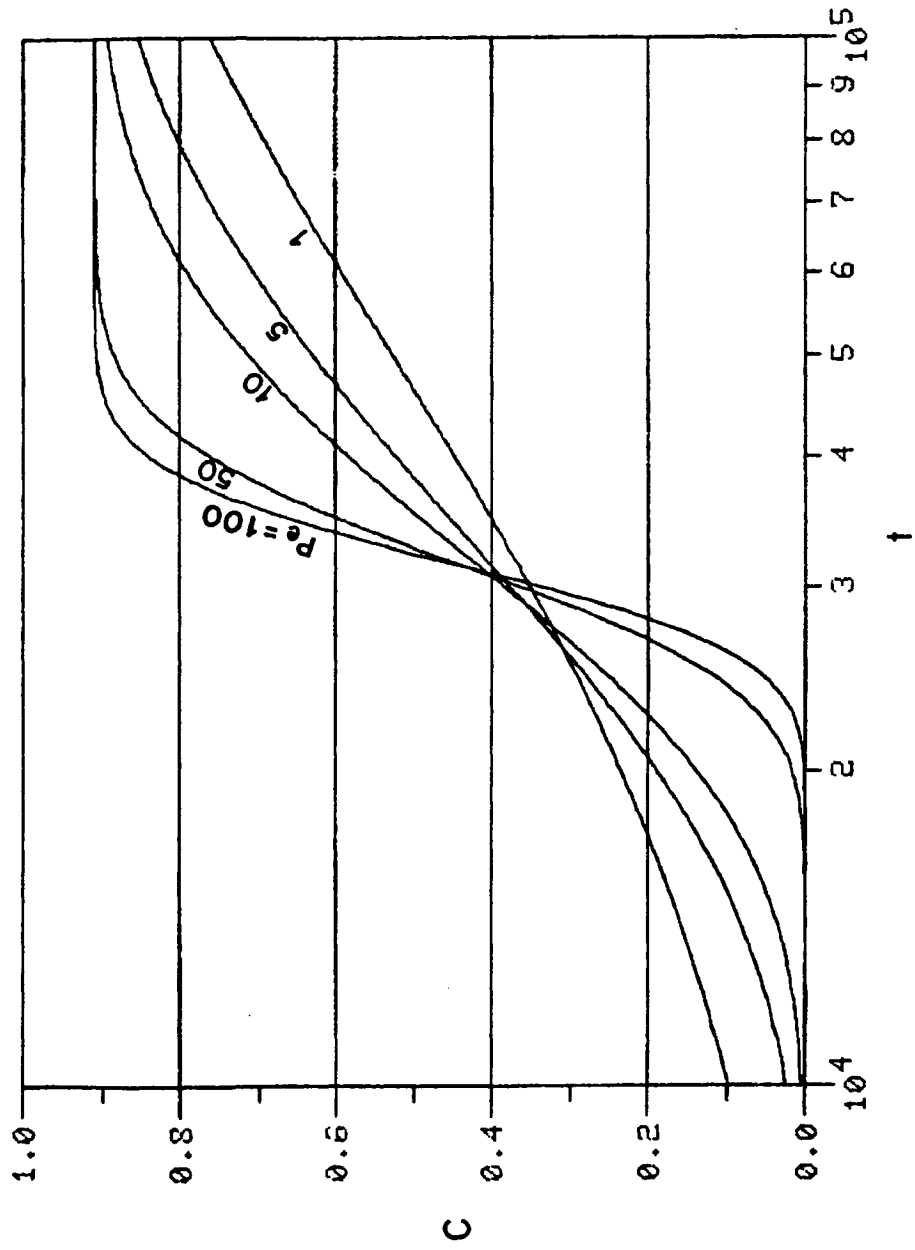


Figure C.6.2. Breakthrough Curves for Example 1, A Step Increase of Concentration.

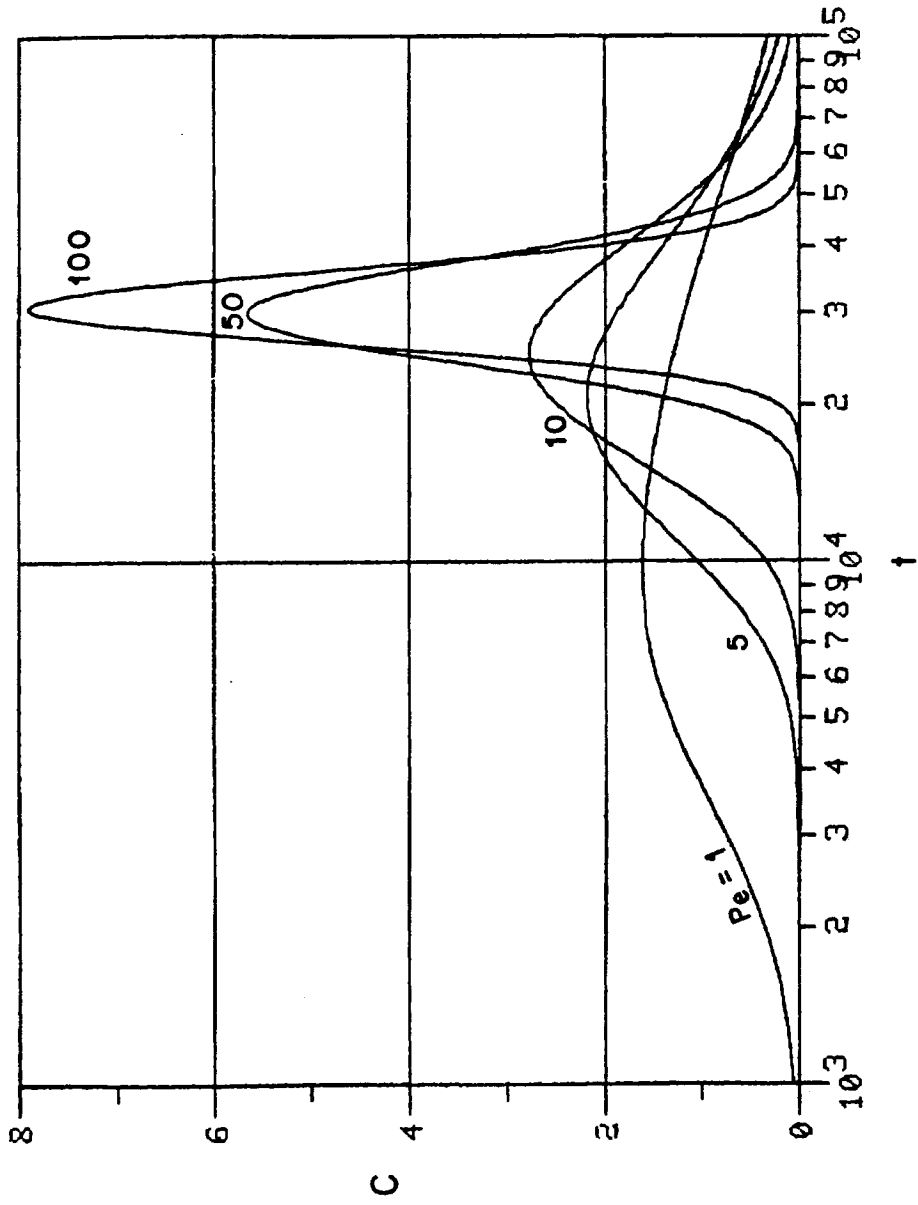


Figure C.6.3. Breakthrough Curves for Example 2, Pulse Injection.

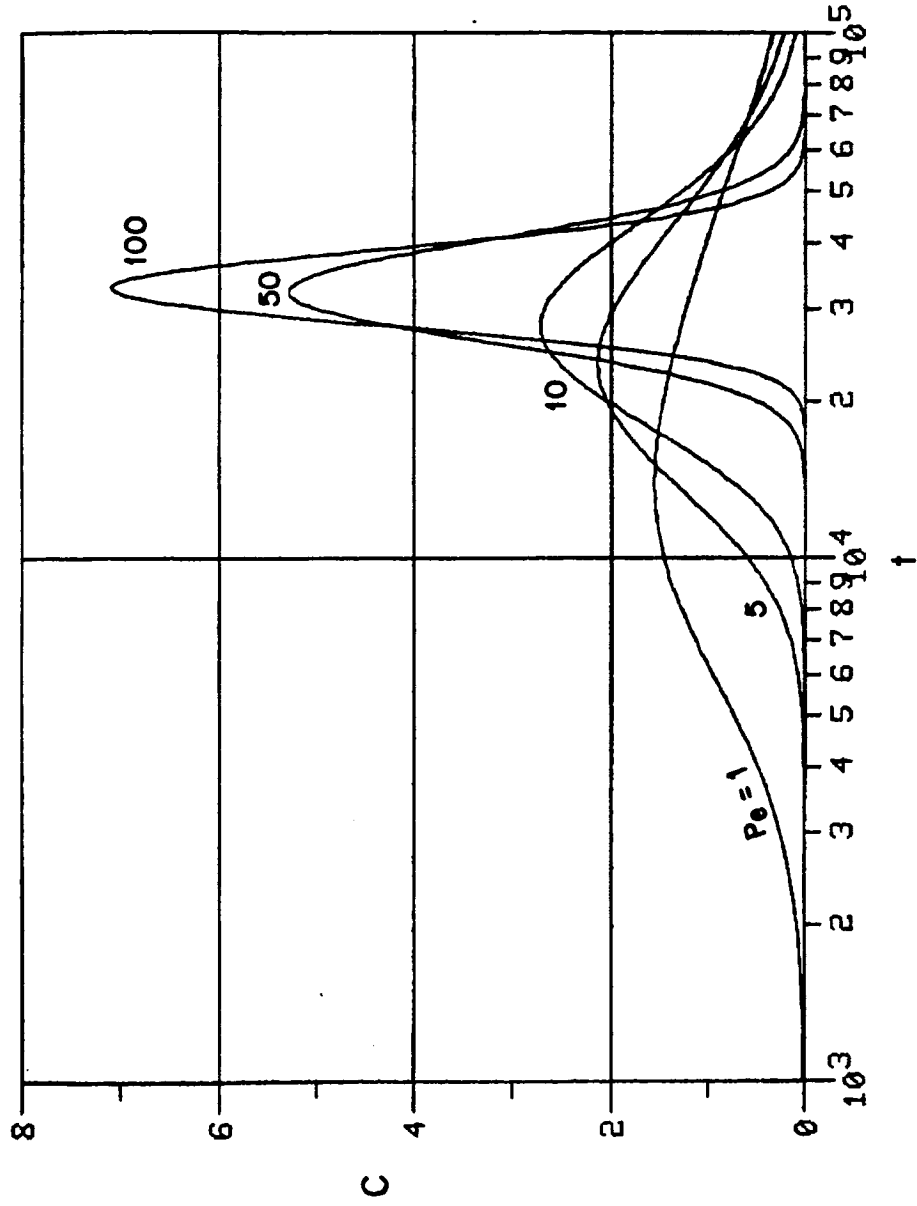


Figure C.6.4. Breakthrough Curves for Example 3, Pulse/Injection with Mixing in the Monitoring Borehole.

APPENDIX D

LISTING OF COMPUTER CODE

```

***
*** SIMULATES DIVERGENT FLOW TRACER TEST
***
*** LIST OF VARIABLES
*** RI-DISTANCE TO SAMPLING WELL
*** RW- RADIUS OF INJECTION WELL
*** THK-AQUIFER THICKNESS
IMPLICIT DOUBLE PRECISION(A-H,O-Z)
CHARACTER*20 HED
PARAMETER(NNA=4000)
PARAMETER(NTA=4000)
PARAMETER(NMA=200)
PARAMETER(NPA=12)
DIMENSION A(NNA,3),R(NNA),C(NNA),CT(NTA),C1(NNA),CI(NTA),
1 X(NTA),CM(NMA),TM(NMA),CC(NMA),W(NMA,3),CW(NMA),
2 HW(NMA,3),H(NMA,3),PE(NPA),CS(NTA,NPA),TS(NPA)
3 ,STAY(NTA),GONE(NTA)
COMMON /DATA/ IRAD,IFLPL,THK,RI,RW,POR,ALP,XMS,Q,AT,NN,NT,NC,
1 CO,NCM,ITC,TRMIN,TRMAX,SMAX,SMIN,TMIN,TMAX,TTMAX,NN1,NT1,
2 AT1,DIS,IMASS,ILOG,DISEX,ISCAL,INJBC,IMSD,RM,RAQ,MULT,FM,QS
3 ,DMOL
COMMON /EST/ P(5),P1(5),AA(5,5),B(5),IALP,IPOR,IMAS,MB,ITMAX,
1 NINT,OEMIN,RATIO,AUTOC
COMMON /INDI/ ISOL,IR,IP,IPOB,IPL,INJ,IBND,IGRID,INIT

*** INITIALIZATION

Z=-1.
PI=DACOS(Z)
IR=15
IP=16
ISCR = 99
IPE=0
INP=1
DO 5 I=1,NTA
  CT(I)=0.
  GONE(I)=0.
  STAY(I)=0.
  DO 5 J=1,NPA
    CS(I,J)=0.
5 CONTINUE
INC=1
*
* OPEN FILES
*
  WRITE(6,11)
11 FORMAT(' ENTER INPUT FILE NAME')
  READ(5,*) HED
  OPEN(IR,FILE=HED,IOSTAT=IOS,ERR=900,STATUS='OLD',PAD='YES')

  WRITE(6,12)
12 FORMAT(' ENTER OUTPUT FILE NAME')
  READ(5,*) HED
  OPEN(IP,FILE=HED,IOSTAT=IOS,ERR=900,STATUS='FRESH',PAD='YES')

  WRITE(6,13)
13 FORMAT(' ENTER OUTPUT FILE NAME FOR CMAX VALUES')
  READ(5,*) HED
  OPEN(12,FILE=HED,IOSTAT=IOS,ERR=900,STATUS='FRESH',PAD='YES')

*** READS AND PRINTS INPUT DATA

10 CALL REIN(INP,C1,CI,PE,CM,TM,W,NMA,NNA,NTA,NPA)
  IF(IPROB.EQ.2) GOTO 800

```

```

      IPE=IPE+1
      IF (IPROB.EQ.1)IPE=0
*** SOLVES DIRECT PROBLEM

400 UC=Q/((RI*R1-RW*RW)*THK*POR*PI)
      UM=UC*XMS/Q
      IF(IPROB.EQ.1) THEN
          IPE=IPE+1
          ALP=RI/PE(IPE)
          TMAX=TRMAX/UC
      END IF
      PC=RI/ALP
      CALL SAUTY(STAY,GONE,A,R,C,CT,C1,CI,NNA,NTA,ISCR,PI,PC)
      CALL FMAX(CT,CMAX,NT,NT)
      IF(IBND.EQ.2) THEN
          CALL BOREHL(CT,NTA,NT,Q,AT,RM,RI,HM,QS,PI)
          CALL FMAX (CT,CMIX,NT,NT)
      ENDIF
      WRITE(IP,450) ALP,POR,XMS,PC
450 FORMAT('1'/' DISPERSIVITY=',F10.3,' POROSITY      =',F8.3//
1 ' INJ. MASS      =',F10.3,' PECTLET NUMBER =',F8.3/
2 ' INT. TIME RED.TIME CONCENTRATION RED.CON.'
3 ' STAY GONE' /
3 ' -----'
5 ' -----')
      WRITE(IP,500) (N,AT*N,UC*AT*N,CT(N),CT(N)/UM,
1 STAY(N),GONE(N),N=1,NT)
500 FORMAT(I5,F10.3,F12.3,F15.5,E10.3,2F10.3)
      IF (IPROB.EQ.2) CALL FMAX(CT,CMAX,NTA,NT)
      IF(IPROB.NE.2) THEN
          WRITE(12,510)PC,ALP,CMAX
510 FORMAT(' PECTLET NO.....=',F10.5,/,
1 ' DISPERSIVITY....=',F10.5,/,
2 ' CMAX.....=',E11.4,/)
          IF (IBND.EQ.2) WRITE(12,515)CMIX
515 FORMAT(' CMAX AFT MIX....=',E11.4,/)
      ENDIF
      IF(IPL.NE.0) THEN
          IF(IMASS.EQ.0) CALL SAVEC(INC,NT,TS,AT,ISCAL,UM,UC,CT,CS,
1 NTA,NMA)
          IF(IMASS.NE.0) CALL SAVEC(INC,NT,TS,AT,ISCAL,UM,UC,GONE,CS,
1 NTA,NMA)
      END IF
      IF(IPROB.EQ.1.AND.IPE.LT.NCM) GOTO 400
      READ(IR,520) INP
520 FORMAT(I5)
      IF((INP.EQ.0.OR.INC.GE.NPA).OR.IPROB.EQ.1) THEN
          IF(IPL.NE.0)THEN
              CALL CURDATA(CS,TS,NTA,NPA,TMIN,TMAX,SMAX,SMIN,ILOG,NT,IPE,
1 ISCR,IMSD,TM,CM,NINT,IFLPL,ISCAL,POR,THK)
              IF(INP.NE.0) GOTO 10
              CALL FINITT(0,700)
          ENDIF
          INC=1
          IPE=0
      END IF
      IF(INP.NE.0) GOTO 10
*** STOPS EXECUTION
      STOP

*** SOLVES INVERSE PROBLEM

800 CALL ESTIM(A,R,C,CT,C1,CI,X,CM,TM,CC,W,CW,HV,H,
1 NNA,NTA,NMA,STAY,GONE)

```

```

      READ(IR,520) INP
      IF(IPL.GT.0) THEN
        IF(IMASS.EQ.0) CALL MATCH(CT,AT,CM,TM,NT,NINT,TMIN,TMAX,ILOG)
        IF(IMASS.GT.0) CALL MATCH(GONE,AT,X,TM,NT,NINT,TMIN,TMAX,ILOG)
        IF(INP.GT.0) GOTO 10
        CALL FINITT(0,700)
      END IF
      IF(INP.GT.0) GOTO 10
*** STOPS EXECUTION
      STOP
*
*   ERROR CHECKING
*
900  WRITE ( 5,901 ) IOS
901  FORMAT(1X,'ERROR IN OPEN OF FILE',I5)
1000 STOP
      END
*****
      SUBROUTINE REIN(INP,C1,C1,PE,CM,TM,W,NMA,NNA,NTA,NPA)
      IMPLICIT DOUBLE PRECISION(A-H,O-Z)
      DIMENSION CI(NTA),C1(NNA),PE(NPA),CM(NMA),TM(NMA),W(NMA,3)
*****
*** READS AND PRINTS INPUT DATA
*****
      COMMON /DATA/ IRAD,IFLPL,THK,RI,RW,POR,ALP,XMS,Q,AT,NN,NT,NC,
1     CO,NCM,ITC,TRMIN,TRMAX,SMAX,SMIN,TMIN,TMAX,TTMAX,NN1,NT1,
2     AT1,IDIS,IMASS,ILOG,DISEX,ISCAL,INJBC,IMSD,RM,RAQ,MULT,HM,QS
3     ,DMOL
      COMMON /EST/ P(5),P1(5),AA(5,5),B(5),IALP,IPOR,IMAS,MB,ITMAX,
1     NINT,OBMIN,RATIO,AUTOC
      COMMON /INDI/ ISOL,IR,IP,IPOB,IPL,INJ,IBND,IGRID,INIT
      CHARACTER*60 HED
      IF(INP.LT.0) THEN
        INP=-INP
        I1=1
      ELSE
        I1=0
      END IF
      GOTO (10,30,50,70,90,110,130,150,170,190,210,230) INP
*
*** TITLE(CARD 1)
*
10  READ(IR,20) HED
    WRITE(IP,25) HED
20  FORMAT(A60)
25  FORMAT('1'//1X,70('*')/1X,A60/1X,70('*'))
    IF(I1.EQ.1) RETURN
*
*** PROBLEM INDICES(CARD 2)
*
30  READ(IR,60) IPOB,IPL,INJ,IBND,INIT,IDIS,ISOL,IRAD,IGRID,NN,NT,AT
    WRITE(IP,65) IPOB,IDIS,IPL,INJ,IBND,INIT,ISOL,IRAD,IGRID,
1     NN,NT,ISOL,AT
    NN1=NN
    NT1=NT
    AT1=AT
    IF(IDIS.GT.0) ISOL=0
    IF(IGRID.EQ.1) TTMAX=AT
    IF(IGRID.EQ.0) TTMAX='^'*NT
    IMSD=0
    IF(IPOB.EQ.-1) THEN
      IPOB=0
      IMSD=1
    END IF

```

```

60 FORMAT(11I5,F10.0)
65 FORMAT(/,'INDICES',/' IPROB=',I5,'      IDIS =',I5/
1  ' IPL  =',I5,'      INJ  =',I5/
2  ' IBND =',I5,'      INIT  =',I5/
2  ' ISOL =',I5,'      IRAD  =',I5/
3  ' IGRID=',I5,'      NN   =',I5/
4  ' NT   =',I5,'      ISOL  =',I5/' AT   =',F10.4)
      IF(11.EQ.1) RETURN
*
*** PHYSICAL DESCRIPTION(CARD 3)
*
50 READ(IR,40) RI,RW,Q,THK,RAQ,XMS
   WRITE(IP,45) RI,RW,Q,THK,RAQ
   WRITE(IP,47)XMS
40 FORMAT(6F10.0)
45 FORMAT(/,'DIST. TO SAMPLING WELL.....=',F10.3/
1  ' RADIUS OF INJECTION WELL.....=',F10.3/
2  ' INJECTION RATE.....=',F10.3/
3  ' AQUIFER THICKNESS.....=',F10.3/
4  ' EFFECTIVE AQUIFER RADIUS.....=',F10.3)
47 FORMAT(' INJECTED MASS.....=',F10.3)
      IF(11.EQ.1) RETURN
*
*** HYDRODYNAMIC PARAMETERS(CARD 4)
*
70 IF(IPROB.EQ.1) THEN
      POR=.1
      GOTO 90
      END IF
      READ(IR,40) POR,ALP,XMS,DISEX,DMOL
      WRITE(IP,85) POR,ALP,XMS,DMOL
      WRITE(IP,86) DISEX
86 FORMAT(' VELOC. EXPONENT FOR DISPERSIVITY=',F10.3)
85 FORMAT(/,'POROSITY.....=',F10.3/
1  ' DISPERSIVITY.=',F10.3/
2  ' INJ.MASS.....=',F10.3/
3  ' MOL.DIFFUSION=',F10.3)
      IF (DISEX.NE.1.0)ISOL=0
      IF(11.EQ.1) RETURN
*
*** EXP. DECAY AT INJ. WELL(CARD 5)
*
90 IF(INJ.GE.2) GOTO 110
      READ(IR,91) CO,INJBC
91 FORMAT(F10.0,I5)
      WRITE(IP,100) CO,INJBC
100 FORMAT(/,'CONCENTRATION AT INJ WELL.=',F10.3/
1  ' INJBC.....=',I5)
      IF(11.EQ.1) RETURN
*
*** ARBITRARY B.C. AT SAMPLING WELL(CARD 6)
*
110 IF(INJ.NE.2) GOTO 130
      READ(IR,40) (CI(N),N=1,NT)
      WRITE(IP,120) (CI(N),N=1,NT)
120 FORMAT(/,'B.C. AT INJECTION WELL'//50(8F10.3//))
      IF(11.EQ.1) RETURN
*
*** VOLUME OF INJECTION WELL BOREHOLE(CARD 7)
*
130 IF(IBND.NE.2) GOTO 150
      READ(IR,40) RM ,HM,QS
      WRITE(IP,140) RM,HM,QS
140 FORMAT(/,'SAMP. BOREHOLE RADIUS=',F10.3/' HEIGHT OF WATER=',

```

```

1          F10.3,/, ' SAMP RATE='F10.5,/)
  IF(I1.EQ.1) RETURN
*
*** ARBITRARY INITIAL CONDITIONS(CARD 8B)
*
*
*** INITIAL CONDITIONS(CARD 8)
*
150 DO 205 N=1,NNA
      C1(N)=0.
205 CONTINUE
*
*** IF NOT A SLUG TEST
*
  IF(INIT.NE.0) THEN
    READ(IR,175) N1,N2
    READ(IR, 40) (C1(N),N=N1,N2)
    WRITE(IP,165) (C1(N),N=1,NN)
165   FORMAT(/,' INITIAL CONDITIONS'/50(8F10.3/))
    END IF
  IF(I1.EQ.1) RETURN
*
*** TYPE CURVES PARAMETERS(CARD 9)
*
170 IF(IPROB.NE.1) GOTO 190
  READ(IR,175) NCM,ITC,TRMIN,TRMAX,PCIN,FAC,DMOL,DISEX
  WRITE(IP,180) NCM,ITC,TRMIN,TRMAX,PCIN,FAC,DMOL,DISEX
175 FORMAT(2I5,6F10.3)
180 FORMAT(/,'TYPE CURVES PARAMETERS'/
1  ' NCM  =',I5,'   ITC  =',I5/
2  ' TRMIN=',F10.3/' TRMAX=',F10.3/
3  ' PCIN  =',F10.3/' FACTR=',F10.3/
4  ' DMOL  =',F10.3/' DISEX=',F10.3)
  IF(ITC.EQ.0) THEN
    NCM=12
    PE(1)=1.
    PE(2)=2.
    PE(3)=4.
    PE(4)=6.
    DO 182 I=1,2
      U=10.**I
      DO 181 N=1,4
        PE(N+4*I)=U*PE(N)
181    CONTINUE
182    CONTINUE
    ELSE IF(ITC.EQ.1) THEN
      PE(1)=PCIN
      DO 183 N=2,NCM
        PE(N)=FAC*PE(N-1)
183    CONTINUE
    ELSE
      READ(IR,40) (PE(N),N=1,NCM)
    ENDIF
    WRITE(IP,185) (PE(N),N=1,NCM)
185 FORMAT(/,'PECLET NUMBERS FOR TYPE CURVES'/
1 2(6F10.3/))
  IF(I1.EQ.1) RETURN
*
*** PLOTTING PARAMETERS(CARD 10)
*
190 IF(IPL.EQ.0) GOTO 210
  READ(IR,191) SMAX,SMIN,TMIN,TMAX,IFLPL,ILOG,IMASS,ISCAL
191 FORMAT(4F10.0,4I5)
  WRITE(IP,195) SMAX,SMIN,TMIN,TMAX,IFLPL,ILOG,IMASS,ISCAL

```

```

195 FORMAT(/,'PLOTTING PARAMETERS'/' SMAX =',F10.3,' SMIN=',F10.3/
1 ' TMIN=',F10.3,' TMAX=',F10.3/' IFLPL=',I2,' ILOG=',I2,
2 ' IMASS=',I2,' ISCAL=',I2)
IF(IFLPL.EQ.1) CALL P10_SAVE
IF(I1.EQ.1) RETURN
*
*** PARAMETERS ESTIMATION INDICES(CARD 11)
*
210 IF(IPROB.NE.2.AND.IMSD.EQ.0) RETURN
READ(IR,215) NINT,IW,MB,IALP,IPOR,IMAS,ITMAX,OBMIN,RATIO,AUTOC
215 FORMAT(7I5,3F10.3)
IF(NINT.GT.NMA) THEN
WRITE(6,217) NINT,NMA
WRITE(IP,217) NINT,NMA
217 FORMAT(' ERROR !!!!!!!!!!!...NUMBER OF DATA POINTS (',I5,
1 ' ) CANNOT BE LARGER THAN NMA (',I5,')....I STOP')
STOP
END IF
IF(IW.EQ.0) MB=1
IF(IW.EQ.2) MB=2
IF(ITMAX.EQ.0) ITMAX=20
WRITE(IP,220) NINT,IW,MB,IALP,IPOR,IMAS,ITMAX,OBMIN,RATIO,AUTOC
220 FORMAT(/,'ITERATIVE PROCESS PARAMETERS'/
1 ' NINT =',I5,' IW =',I5/
2 ' MB =',I5,' IALP =',I5/
3 ' IPOR =',I5,' IMAS =',I5/
4 ' ITMAX=',I5/
5 ' OBMIN=',F10.3/
6 ' RATIO=',F10.3/' AUTOC=',F10.3)
IF(I1.EQ.1) GOTO 250
230 IF(NINT.EQ.0) RETURN
*
*** MEASURED CONCENTRATION VS. TIME (PARAMETER EST.)(CARD 12)
*
DO 240 N=1,NINT
READ(IR,235) TM(N),CM(N),(W(N,M),M=1,MB)
240 CONTINUE
235 FORMAT(8F10.3)
250 IF(IW.EQ.0) THEN
DO 260 N=1,NINT
W(N,1)=1.
260 CONTINUE
ELSE IF(IW.EQ.2) THEN
C***** AUTORREGRESSIVE PROCESS!!!!!!!!!!!!!!
W(1,1)=AUTOC
END IF
IF(INP.EQ.11) RETURN
WRITE(IP,270)
270 FORMAT(/,'MEASURED CONCENTRATIONS'/11X,'TIME CONCENTRATION',
1 5X,'WEIGHT'/11X,'-----')
DO 280 N=1,NINT
WRITE(IP,235) TM(N),CM(N),(W(N,M),M=1,MB)
280 CONTINUE
RETURN
END
*****
SUBROUTINE SAUTY(STAY,GONE,A,R,C,CT,C1,CI,NNA,NTA,ISCR,PI,PC)
*****
*** COMPUTES CW(T), GIVEN Q,RI,RW,ALP,POR,XMS,AT,NN,NT,NC
*****
IMPLICIT DOUBLE PRECISION(A-H,O-Z)
DIMENSION A(NNA,3),R(NNA)
DIMENSION C(NNA),CT(NTA),C1(NNA),CI(NTA),STAY(NTA),GONE(NTA)
COMMON /DATA/ IRAD,IFLPL,THK,RI,RW,POR,ALP,XMS,Q,AT,NN,NT,NC

```

```

1 CO, NCM, ITC, TRMIN, TRMAX, SMAX, SMIN, TMIN, TMAX, TTMAX, NN1, NT1,
2 AT1, IDIS, IMASS, ILOG, DISEX, ISCAL, INJBC, IMSD, RM, RAQ, MULT, HM, QS
3 , DMOL
COMMON /INDI/ ISOL, IR, IP, IPROB, IPL, INJ, IBND, IGRID, INIT
*
*** SETS UP MESH, CONTROL BY AT IF IGRID=0, BY NN OTHERWISE
*
MULT=RAQ*RAQ/(RI*RI)
B=Q/(2.*PI*POR*THK)
U=(RAQ*RAQ-RW*RW)/(2.*B)
CALL MESH(IGRID, NN, NNA, NN1, NT, NTA, NT1, AT, AT1, TTMAX, U, IRAD)
CALL RADIUS(R, NNA, NN, RW, RAQ, IRAD)

WRITE(12, 3) AT, NT, NN, MULT
3 FORMAT(' AT=', E11.4, '/', ' NT=', I8, '/', ' NN=', I8, '/', ' MULT=', I8)
*
*** BUILDS F.D. MATRIX
*
IF(ISOL.EQ.0) THEN
CALL MATDIS(ALP, A, R, NNA, NN, B, AT, IDIS, DISEX, DMOL)
ELSE
CALL MATREL(A, R, ALP, B, AT, NNA, NN)
ENDIF
*
*** INITIAL CONDITIONS
*
111 DO 200 N=1, NN
C(N)=C1(N)
200 CONTINUE
* INJ .LE. 1 PULSE THEN CONSTANT CONCENTRATION
IF(INJ.LE.1.AND.INIT.NE.2) C(1)=C1(1)+XMS/(Q*AT)
* INJ .EQ. 3 CONSTANT CONCENTRATION (STEP INCREASE)
IF(INJ.EQ.3.AND.INIT.NE.2) THEN
CO=XMS/(Q*AT*NT)
C(1)=C1(1)
ENDIF
*
*** MODIFY A FOR B.C.
*
IF(IBND.EQ.1) THEN
CALL MODBND(A, NNA, NN, ISOL)
END IF
IF(INJBC.EQ.1) THEN
A(1,1)=1.
XXX=A(2,2)
A(2,2)=0.
END IF
*
*** TRIANGULAR DECOMPOSITION
*
IF(ISOL.EQ.0) THEN
CALL DECTRI(A, NNA, NN)
ELSE
CALL DETRUN(A, NNA, NN)
END IF
*
****STARTS SOLUTION
*
TIME=0.
ISTP=0
GONV=0.
CELVOL=Q*AT
300 TIME=TIME+AT

```

```

*
  ISTEP=ISTP+1
*** MASS BALANCE(GONE)
*
  GONM=GONM+C(NN)*CELVOL
  GONE(ISTP)=GONM/(XMS)
  IF(IRAD.EQ.1) CT(ISTP)=C(NN/MULT)
*
*** MOVES FORWARD (START ADVECTION)
*
  DO 310 I=1,NN-1
    C(NN-I+1)=C(NN-I)
  310 CONTINUE
*
*** INJECTION WELL B.C.
*
  IF(INJ.EQ.0 .OR. INJ.EQ.3) THEN
    C(1)=CO
  ELSE
    C(1)=CI(ISTP)
  END IF
  IF(INJBC.EQ.1) C(2)=C(2)-XXX*C(1)
*
*** MASS BALANCE (STAY)
*
  N1=1
  N2=NN
  CALL MBLC(C,NN,CELVOL,STY2,N1,N2,XMS)
*
*** SOLVE
*
  IF(ISOL.EQ.0) THEN
    CALL SOLTR1(A,C,NNA,NN)
  ELSE
    CALL SOTRUN(A,C,NNA,NN)
  END IF
  STAY(ISTP)=STY2
  IF(IRAD.EQ.0) CT(ISTP)=C(NN/MULT)
  IF(ISTP.LT.NT) GOTO 300
  RETURN
  END
*****
  SUBROUTINE MBLC(C,NN,CELVOL,STYM,N1,N2,XMS)
  IMPLICIT DOUBLE PRECISION(A-H,O-Z)
  DIMENSION C(NN)
*
*** MASS BALANCE (STAY)
*
  STYM=0.
  DO 315 I=N1,N2
    STYM=STYM+C(I)*CELVOL
  315 CONTINUE
  STYM=STYM/XMS
  RETURN
  END
*****
  SUBROUTINE MESH(IGRID,NN,NNA,NN1,NT,NTA,NT1,AT,AT1,TMAX,U,IRAD)
  IMPLICIT DOUBLE PRECISION(A-H,O-Z)
*
*** DECIDES ON THE VALUES OF NN, NT, AND AT
*
  IF(IGRID.EQ.0) THEN
    NT=NT1
    IF(IRAD.EQ.0) THEN

```

```

      NN=1+U/AT1
      AT=U/(NN-1)
    ELSE IF(IRAD.EQ.1) THEN
      NN=U/AT1
      AT=U/NN
    END IF
    IF(NN.GT.NNA) THEN
      NN=NNA
      IF(IRAD.EQ.0) THEN
        AT=U/(NN-1)
      ELSE IF(IRAD.EQ.1) THEN
        AT=U/NN
      END IF
      NT=TIMAX/AT
    END IF
  ELSE
    NN=NN1
    IF(IRAD.EQ.0) THEN
      AT=U/(NN-1)
    ELSE IF(IRAD.EQ.1) THEN
      AT=U/NN
    END IF
    NT=1+TIMAX/AT
    IF(NT.GT.NTA) THEN
      NT=NTA
      AT=TIMAX/NT
      NN=1+U/AT
      IF(IRAD.EQ.1) NN=U/AT
    END IF
  END IF
  RETURN
  END
*****
  SUBROUTINE RADIUS(R,NNA,NN,KW,RAQ,IRAD)
  IMPLICIT DOUBLE PRECISION(A-H,O-Z)
  DIMENSION R(NNA)
  *****
  *** CONSTRUCTS RADII ARRAY
  *****
  R2=KW**2
  IF(IRAD.EQ.0) THEN
    A=(RAQ**2-R2)/(NN-1)
    R(1)=RW
  ELSE IF(IRAD.EQ.1) THEN
    A=(RAQ**2-R2)/(2*NN-1)
    R2=R2+A
    R(1)=DSQRT(R2)
    A=2*A
  END IF
  DO 10 I=2,NN
    R2=R2+A
    R(I)=DSQRT(R2)
10 CONTINUE
  RETURN
  END
*****
  SUBROUTINE DERIV (A,R,C,CT,C1,CI,X,TM,CC,H,NNA,NTA,NMA,STAY,GONE,
  1 PI)
  IMPLICIT DOUBLE PRECISION(A-H,O-Z)
  DIMENSION A(NNA,3),R(NNA),STAY(NTA),GONE(NTA)
  DIMENSION C(NNA),CT(NTA),C1(NNA),CI(NTA),
  1 X(NTA),TM(NMA),CC(NMA),H(NMA,3)
  *****
  *** COMPUTES CONCENTRATIONS AND DERIVATIVES RESP. PARAMETERS

```

```

*****
COMMON /DATA/ IRAD, IFLPL, THK, RI, RW, POR, ALP, XMS, Q, AT, NN, NT, NC,
1 CO, NCM, ITC, TRMIN, TRMAX, SMAX, SMIN, TMIN, TMAX, TTMAX, NN1, NT1,
2 AT1, IDIS, IMASS, ILOG, DISX, ISCAL, INJBC, IMSD, RM, RAQ, MULT, HM, QS
3 , DMOL
COMMON/INDI/ ISOL, IR, IP, IPROB, IPL, INJ, IBND, IGRID, INIT
COMMON/EST/ P(5), P1(5), AA(5,5), B(5), IALP, IPOR, IMAS, MB, ITMAX,
1 NINT, OBMIN, RATIO, AUTO
*** COMPUTED CONCENTRATIONS (ARRAY CT)
CALL SAUTY(STAY, GONE, A, R, C, CT, C1, CI, NNA, NTA, ISCR, PI)
I1=0
IF(IALP.EQ.0) GOTO 200
*** SENSITIVITY TO DISPERSIVITY
AL1=ALP
AAA=.001*ALP
ALP=ALP+AAA
CALL SAUTY(STAY, GONE, A, R, C, X, C1, CI, NNA, NTA, ISCR, PI)
ALP=AL1
DO 100 I=1, NT
X(I)=(X(I)-CT(I))/AAA
100 CONTINUE
*** BOREHOLE MIXING
IF(IBND.EQ.2) CALL BOREHL(X, NTA, NT, Q, AT, RM, RI, HM, QS, PI)
*** TIME INTERP
CALL TMINT(X, CC, TM, NTA, NMA, NINT, NT, AT)
*** BUILDS IN SENS MATRIX
I1=1
DO 110 I=1, NINT
H(I, I1)=CC(I)
110 CONTINUE
*** SENSITIVITY TO POROSITY
200 IF(IPOR.EQ.0) GOTO 300
U=1.
IF(INJ.GT.0) U=0.
X(1)=- (U*CT(1)+CT(2))/POR
X(NT)=- (U*CT(NT)+(CT(NT)-CT(NT-1))*NT)/POR
DO 210 I=2, NT-1
X(I)=- (U*CT(I)+.5*(CT(I+1)-CT(I-1))*I)/POR
210 CONTINUE
*** BOREHOLE MIXING, TIME INTERP, AND SENS MATRIX
IF(IBND.EQ.2) CALL BOREHL(X, NTA, NT, Q, AT, RM, RI, HM, QS, PI)
CALL TMINT(X, CC, TM, NTA, NMA, NINT, NT, AT)
I1=I1+1
DO 230 I=1, NINT
H(I, I1)=CC(I)
230 CONTINUE
*** SENS TO INJECTED MASS
300 IF(IMAS.EQ.0) GO TO 400
IF(INJ.EQ.1) THEN
XXX=XMAS
XMAS=0.
CALL SAUTY(STAY, GONE, A, R, C, X, C1, CI, NNA, NTA, ISCR, PI)
DO 303 I=1, NT
X(I)=X(I)/XMS
303 CONTINUE
XMAS=XXX
ELSE
DO 310 I=1, NT
X(I)=CT(I)/XMS
310 CONTINUE
END IF
*** BOREHOLE MIXING, TIME INTERP, AND SENS MATRIX
IF(IBND.EQ.2) CALL BOREHL(X, NTA, NT, Q, AT, RM, RI, HM, QS, PI)
CALL TMINT(X, CC, TM, NTA, NMA, NINT, NT, AT)

```

```

      I1=I1+1
      DO 320 I=1,NINT
        H(I,I1)=CC(I)
320 CONTINUE
*** TIME INTERP. AND BOREHOLE MIXING ON COMP. CONCS.
400 CALL BOREHL(CT,NTA,NT,Q,AT,RM,RI,HM,QS,PI)
      CALL TMINT(CT,CC,TM,NTA,NMA,NINT,NT,AT)
      RETURN
      END
*****
      SUBROUTINE BOREHL(C,NTA,NT,Q,AT,RM,RI,HM,QS,PI)
      IMPLICIT DOUBLE PRECISION(A-H,O-Z)
      DIMENSION C(NTA)
*****
*** COMPUTES MIXING EFFECT IN INJECTION WELL BOREHOLE
*****
      IF(RM.LE. 0.0 .OR. HM.LE. 0.0)RETURN
      ALPHA=2.*Q*AT/(PI*PI*RI*RM*HM)
      BETA=QS*AT/(PI*RM*RM*HM)
      CONST=1.+ALPHA+BETA
      C(1)=ALPHA*C(1)/CONST
      DO 100 I=2,NT
        DUM=C(I)
        C(I)=(C(I-1)+ALPHA*DUM)/CONST
100 CONTINUE
      RETURN
      END
*****
      SUBROUTINE TMINT(C,CC,TM,NTA,NMA,NINT,NT,AT)
      IMPLICIT DOUBLE PRECISION(A-H,O-Z)
      DIMENSION C(NTA),CC(NMA),TM(NMA)
*****
*** TIME INTERPOLATION
*****
      DO 50 I=1,NINT
        U=TM(I)/AT
        N=U
        IF(N.EQ.0) THEN
          CC(I)=C(1)*U
        ELSE IF(N.LT.NT) THEN
          CC(I)=C(N)+(U-N)*(C(N+1)-C(N))
        ELSE
          CC(I)=C(NT)+(U-NT)*(C(NT)-C(NT-1))
        END IF
50 CONTINUE
      RETURN
      END
*****
      SUBROUTINE ESTIM(A,R,C,CT,C1,CI,X,CM,TM,CC,W,CW,HW,H,NNA,NTA,
1 NMA,STAY,GONE)
*****
*** COMPUTES ALP, POR, AND XMS SO AS TO FIT CM
*****
      IMPLICIT DOUBLE PRECISION(A-H,O-Z)
      DIMENSION A(NNA,3),R(NNA),STAY(NTA),GONE(NTA)
      DIMENSION C(NNA),CT(NTA),C1(NNA),CI(NTA),
1 X(NTA),CM(NMA),TM(NMA),CC(NMA),W(NMA,3),CW(NMA),HW(NMA,3),
2 H(NMA,3)
      COMMON /DATA/ IRAD,IFLPL,THK,RI,RW,POR,ALP,XMS,Q,AT,NN,NT,NC,
1 CO,NCM,ITC,TRMIN,TRMAX,SMAX,SMIN,TMIN,TMAX,TTMAX,NN1,NT1,
2 AT1,IDIS,IASS,ILOG,DISEX,ISCAL,INJBC,IMSD,RM,RAQ,MULT,FM,QS
3 ,DMOL
      COMMON /INDI/ ISOL,IR,IP,IPROB,IPL,INJ,IBND,IGRID,INIT
      COMMON /EST/ P(5),P1(5),AA(5,5),B(5),IALP,IPOR,IMAS,MB,ITMAX,

```

```

1          NINT,OBMIN,RATIO,AUTOC
*** INITIALIZATION
ITER=0
OBP=1D+40
IFIN=0
NDV=3
NDB=3
IV=1
IF(IALP.EQ.0) IV=0
P(1)=ALP
IV=IV+1
P(IV)=POR
IF(IPOR.EQ.0) IV=IV-1
IV=IV+1
P(IV)=XMS
IF(IMAS.EQ.0) IV=IV-1
IF(IV.EQ.0) RETURN
NVAR=IV
RED=.3
ITT=1
IRR=0
WRITE(IP,50)
50 FORMAT('0'/' ITERATIVE PROCESS'/1X,17('-')//
1 ' ITER ITT OBJ.FTN. DISPRST POROSITY IN.MASS'/
2 ' -----' )
*** STARTS ITERATIONS
100 ITER=ITER+1
150 CALL DERIV(A,R,C,CT,C1,CI,X,TM,CC,H,NNA,NTA,NMA,STAY,GONE,PI)
CALL WIDRES(W,CC,CM,CW,NMA,NDB,OBJ)
IF(IFIN.EQ.1) GOTO 300
IF(OBJ.LE.OBP) THEN
  OBP=OBJ
ELSE
  RR=RR*RED
  ITT=ITT+1
  IF(ITT.LT.3) GOTO 200
END IF
WRITE(IP,160) ITER,ITT,OBJ,ALP,POR,XMS
160 FORMAT(16,15,4E10.4)
RR=1.
ITT=1
CALL CFMTR(W,H,HW,NMA,NDB,NDV,NVAR)
CALL RHS(W,H,CW,CC,NMA,NDB,NDV,NVAR)
CALL CHOLE(AA,NVAR,NVAR,NDV,NDV,IEROR)
IF(IEROR.EQ.1) STOP
CALL FORBAC(AA,B,NVAR,NVAR,NDV,NDV)
*** UPDATES PARAMETERS
200 IREP=0
BET=1.
DO 210 I=1,NVAR
  IF(DABS(BET*B(I)/P(I)).GT.RR) BET=RR*DABS(P(I)/B(I))
210 CONTINUE
DO 220 I=1,NVAR
  IF(ITT.EQ.1) P1(I)=P(I)
  P(I)=P1(I)-BET*B(I)
  IF(DABS((P(I)-P1(I))/P1(I)).GT.RATIO) IREP=1
220 CONTINUE

I=0
IF(IALP.NE.0) THEN
  I=1
  ALP=P(1)
END IF
IF(IPOR.NE.0) THEN

```

```

      I=I+1
      POR=P(I)
    END IF
    IF(IMAS.NE.0) THEN
      I=I+1
      XMS=P(I)
    END IF
*** STOPPING CRITERIA
    IF(ITER.GE.ITMAX.OR.OBJ.LE.OBMIN) IFIN=1
    IF(ITT.GT.1) GOTO 150
    IF(IREP.EQ.0) THEN
      IRR=IRR+1
      IF(IRR.EQ.3) IFIN=1
    ELSE
      IRR=0
    END IF
    GOTO 100
*** PRINTS RESULTS, ETC
300 WRITE(IP,310) HED
310 FORMAT('1'//1X,60('-')/1X,15A4/1X,60('-'))
    WRITE(IP,320) ALP,POR,XMS
320 FORMAT('0',20('-'),' SUMMARY OF RESULTS ',20('-')//
1 1X,'COMPUTED PARAMETERS'/1X,19('-')//
2 ' LONG. DISPERSIVITY.....=',F10.3/
3 ' POROSITY.....=',F10.3/
4 ' INJECTED MASS OF TRACER...=',F10.3)
    U1=0
    U2=0.
    DO 330 N=1,NINT
      U=CC(N)-CM(N)
      U1=U1+U
      U2=U2+U*U
330 CONTINUE
    U1=U1/NINT
    U=U2/NINT
    WRITE(IP,340) U1,U2,U
340 FORMAT('0'/' SOME STATISTICS'/1X,15('-')//
1 ' MEAN RESIDUAL.....=',F10.3/
2 ' SUM SQ. RESIDUALS.....=',F10.3/
3 ' AVG. SQ. RESIDUAL.....=',F10.3)
    IF(IW.NE.0) WRITE(IP,350) OBJ,OBJ/NINT
350 FORMAT(1X,'SUM SQ. WEIGTHED RSDLS...=',F10.3/
1 ' AVG. SQ. WEIGTHED RSDL...=',F10.3)
    WRITE(IP,360)
360 FORMAT(///' COMPUTED CONCENTRATIONS AND RESIDUALS'/1X,37('-')//
1 6X,'TIME COMPUTED MEASURED RESIDUAL WGT.RSDL ACC.COMP',
2 ' ACC.MEAS'/6X,'----',6(2X,8('-')))
    XM=XMS
    IF(INJ.EQ.1) XM=XM+XMAS
    XMC=Q*TM(1)*CC(1)/2
    XMM=Q*TM(1)*CM(1)/2
    DO 380 N=1,NINT
      WRITE(IP,370) TM(N),CC(N),CM(N),CC(N)-CM(N),CW(N),XMC,XMM
370   FORMAT(7F10.3)
      X(N)=XMM/XM
      IF(N.EQ.NINT) GOTO 380
      XMM=XMM+(TM(N+1)-TM(N))*(CM(N+1)+CM(N))*Q/2.
      XMC=XMC+(TM(N+1)-TM(N))*(CC(N+1)+CC(N))*Q/2.
380 CONTINUE
    RETURN
  END
*****
SUBROUTINE CHOLES(A,NUMNP,MBAND,NG,MG,IEROR)

```

```
*****
*** CHOLESKY DECOMPOSITION. IF FAILS, IEROR IS SET TO 1, OTHERWISE 0.
*****
```

```

      IMPLICIT DOUBLE PRECISION(A-H,O-Z)
      DIMENSION A(NG,NG)
      COMMON /INDI/ ISOL, IR, IP, IPROB, IPL, INJ, IBND, IGRID, INIT
      IEROR=0
      DO 60 I=1,NUMNP
        II=NUMNP-I+1
        IF (MBAND .LT. II) II=MBAND
        DO 50 J=1,II
          JJ=MBAND-J
          IF (I-1 .LT. JJ) JJ=I-1
          SUM=A(I,J)
          IF (JJ .LT. 1) GO TO 20
          DO 10 K=1,JJ
            IK=I-K
            JK=J+K
            IF (A(IK,K+1) .NE. 0. .AND. A(IK,JK) .NE. 0.)
              SUM=SUM-A(IK,K+1)*A(IK,JK)
10          CONTINUE
20          IF (J .GT. 1) GO TO 40
            IF (SUM .GT. 0.) GO TO 30
            WRITE(IP,70) I
            IEROR=1
            RETURN
30          A(I,1)=1./DSQRT(SUM)
            GO TO 50
40          A(I,J)=A(I,1)*SUM
50          CONTINUE
60          CONTINUE
70          FORMAT (1H1,10X,36HCHOLESKY DECOMPOSITION FAILED AT ROW,14)
          RETURN
          END

```

```
*****
      SUBROUTINE FORBAC(A,B,NUMNP,MBAND,NG,NG)

```

```
*****
*** FORWARDS AND BACKWARDS SUBSTITUTION
*****
```

```

      IMPLICIT DOUBLE PRECISION(A-H,O-Z)
      DIMENSION A(NG,NG),B(NG)

```

```
*** FORWARD SUBSTITUTION
```

```

      DO 30 I=1,NUMNP
        J=I-MBAND+1
        IF (I+1 .LE. MBAND) J=1
        SUM=B(I)
        I1=I-1
        IF (J .GT. I1) GO TO 20
        DO 10 K=J,I1
          I1=I-K+1
          IF (A(K,I1) .NE. 0.) SUM=SUM-A(K,I1)*B(K)
10        CONTINUE
20        B(I)=SUM*A(I,1)
30        CONTINUE

```

```
*** BACK SUBSTITUTION
```

```

      DO 60 L=1,NUMNP
        I=NUMNP-L+1

```

```

      J=I+MBAND-1
      IF (J .GT. NUMNP) J=NUMNP
      SUM=B(I)
      K1=I+1
      IF (K1 .GT. J) GO TO 50
      DO 40 K=K1,J
        KK=K-1+1
        IF (A(I,KK) .NE. 0.) SUM=SUM-A(I,KK)*B(K)
40    CONTINUE
50    B(I)=SUM*A(I,1)
60    CONTINUE
      RETURN
      END

```

```

*****
      SUBROUTINE WIDRES(W,CC,CM,CW,NDI,NDB,OBJ)

```

```

*****
*** COMPUTES WEIGHTED RESIDUALS AND OB. FUNCTION
*****

```

```

      IMPLICIT DOUBLE PRECISION(A-H,O-Z)
      DIMENSION W(NDI,NDB),CC(NDI),CM(NDI),CW(NDI)
      COMMON /EST/ P(5),P1(5),AA(5,5),B(5),IALP,IPOR,IMAS,MB,ITMAX,
1          NINT,OBMIN,RATIO,AUTO
      OBJ=0.
      DO 200 N=1,NINT
        U=0.
        L=N
        DO 100 M=1,MB
          U=U+W(N,M)*(CC(L)-CM(L))
          IF(L.GE.NINT) GOTO 150
          L=L+1
100    CONTINUE
150    CW(N)=U
        OBJ=OBJ+U*U
200    CONTINUE
      RETURN
      END

```

```

*****
      SUBROUTINE CFMTR(W,H,HW,NDI,NDB,NDV,NVAR)

```

```

*****
*** COMPUTES MATRIX OF COEFFICIENTS
*****

```

```

      IMPLICIT DOUBLE PRECISION(A-H,O-Z)
      DIMENSION W(NDI,NDB),H(NDI,NDV),HW(NDI,NDV)
      COMMON /EST/ P(5),P1(5),AA(5,5),B(5),IALP,IPOR,IMAS,MB,ITMAX,
1          NINT,OBMIN,RATIO,AUTO
      DO 300 I=1,NVAR
        DO 200 N=1,NINT
          U=0.
          L=N
          DO 100 M=1,MB
            U=U+W(N,M)*H(L,I)
            IF(L.GE.NINT) GOTO 200
            L=L+1
100    CONTINUE
          HW(N,I)=U
200    CONTINUE
300    CONTINUE

```

```

DO 600 I=1,NVAR
  DO 500 J=1,NVAR
    U=0.
    DO 400 N=1,NINT
      U=U+HW(N,I)*HW(N,J)
400    CONTINUE
      K=J-I+1
      AA(I,K)=U
500    CONTINUE
600  CONTINUE
      RETURN
      END
*****
      SUBROUTINE RHS(W,H,CW,X,NDI,NDB,NDV,NVAR)
*****
      *** COMPUTES R.H.S. VECTOR
*****

      IMPLICIT DOUBLE PRECISION(A-H,O-Z)
      DIMENSION W(NDI,NDB),H(NDI,NDV),CW(NDI),X(NDI)
      COMMON /EST/ P(5),P1(5),AA(5,5),B(5),IALP,IPOR,IMAS,MB,ITMAX,
1          NINT,OBMIN,RATIO,AUTO
*****
      DO 200 N=1,NINT
        IO=1
        IF(N.GT.MB) IO=N-MB+1
        U=0.
        L=N-IO+1
        DO 100 I=IO,N
          U=U+W(N,L)*CW(I)
          L=L-1
100    CONTINUE
        X(N)=U
200  CONTINUE
      DO 400 I=1,NVAR
        U=0.
        DO 300 N=1,NINT
          U=U+H(N,I)*X(N)
300    CONTINUE
        B(I)=U
400  CONTINUE
      RETURN
      END
*****
      SUBROUTINE SAVEC(INC,NT,TS,AT,ISCAL,UM,UC,CT,CS,NTA,NPA)
      IMPLICIT DOUBLE PRECISION(A-H,O-Z)
      DIMENSION CT(NTA),CS(NTA,NPA),TS(NPA)
*****
      *** STORES CT(.) ON CS(.,INC)
*****
      TS(INC)=AT
      CMAX=1.
      IF(ISCAL.EQ.1.OR.ISCAL.EQ.3) CALL FMAX(CT,CMAX,NTA,NT)
      IF(ISCAL.GE.2) TS(INC)=AT*UC
      IF(ISCAL.EQ.4) CMAX=UM

      DO 10 N=1,NT
        CS(N,INC)=CT(N)/CMAX
10  CONTINUE
      INC=INC+1
      RETURN
      END
*****

```

```

SUBROUTINE FMAX(X,C,NDI,NINT)
*****
*** FINDS MAX. OF X
*****

      IMPLICIT DOUBLE PRECISION(A-H,O-Z)
      DIMENSION X(NDI)

      C=X(1)
      DO 10 N=1,NINT
        IF(X(N).GT.C) C=X(N)
10 CONTINUE
      RETURN
      END
*****
SUBROUTINE MATREL(A,R,ALP,B,AT,NNA,NN)
      IMPLICIT DOUBLE PRECISION(A-H,O-Z)
      DIMENSION A(NNA,3),R(NNA)
*
*** BUILDS F.E. MATRIX
*

      U=2*ALP*B*AT
      U2=0.
      R2=R(1)
      AR2=0.
      DO 10 I=1,NN-1
        R1=R2
        AR1=AR2
        U1=U2
        R2=R(I+1)
        AR2=R2-R1
        U2=U/AR2
        AR=(AR1+AR2)*R1
        X1=U1/AR
        X2=U2/AR
        A(I,1)=-X1
        A(I,2)=1+X1+X2
        A(I,3)=-X2
10 CONTINUE
      X1=U2/(R2*AR2)
      A(NN,1)=-X1
      A(NN,2)=1+X1
      A(NN,3)=0.
      RETURN
      END
*****
SUBROUTINE DETRUN(A,NNA,NN)
      IMPLICIT DOUBLE PRECISION(A-H,O-Z)
      DIMENSION A(NNA,3)
*** TRIANGULAR DECOMPOSITION OF TRIANGULAR NONSYMMETRIC MATRIX

      A(1,3)=A(1,3)/A(1,2)
      DO 100 N=2,NN
        A(N,2)=A(N,2)-A(N,1)*A(N-1,3)
        A(N,3)=A(N,3)/A(N,2)
100 CONTINUE
      RETURN
      END
*****
SUBROUTINE SOTRUN(A,B,NNA,NN,ISCR)
      IMPLICIT DOUBLE PRECISION(A-H,O-Z)
      DIMENSION A(NNA,3),B(NNA)

```

```

*****
*** SOLUTION FOR NONSYMMETRIC TRIDIAGONAL SYSTEM
*****
*** FORWARD SUBSTITUTION
      B(1)=B(1)/A(1,2)
      DO 100 N=2,NN
          B(N)=(B(N)-A(N,1)*B(N-1))/A(N,2)
100 CONTINUE
*** BACKWARD SUBSTITUTION
      DO 200 N=NN-1,1,-1
          B(N)=B(N)-A(N,3)*B(N+1)
200 CONTINUE
      RETURN
      END
*****
      SUBROUTINE CURDATA (CS,TS,NTA,NPA,TMIN,TMAX,SMAX,SMIN,
1          ILOG,NT,NP,ISCR,IMSD,TM,CM,NINT,IFLPL,
2          ISCAL,POR,THK)
*
* ROUTINE MANIPULATES THE DATA INTO A FORM THAT 'CURVA' ACCEPTS
*
      DOUBLE PRECISION CS,TS,TMIN,TMAX,SMAX,SMIN,CMIN,CMAX
      DIMENSION CS(NTA,NPA),TS(NPA),TM(NINT),CM(NINT)
      DIMENSION TMPCS(5000),TIME(5000)

      IF(IFLPL.EQ.2) THEN
          OPEN(UNIT=73,FILE='CS.DAT',STATUS='FRESH')
          WRITE(73,11) (TS(N),N=1,NT)
11         FORMAT(8G10.5E1)
          DO 12 I=1,NP
              WRITE(73,11) (CS(J,I),J=1,NT)
12         CONTINUE
          RETURN
      END IF

      ISYM = 0
      CMIN=0.

*
* FIND CMAX VALUE
*
      IF(ILOG.NE.2 .OR. ISCAL.NE.5)THEN
          CALL FMAX ( CS,CMAX,NTA*NPA,NTA*NPA)
          TTMAX=TMAX
          TTMIN=TMIN
          CCMAX=CMAX
          CCMIN=CMIN
      ELSE
          CCMAX=SMAX
          CCMIN=SMIN
      END IF
      CCMAX=SMAX
      CCMIN=SMIN
      DO 100 I = 1,NP
          K = 0
          J =MAX(IDINT(TMIN/TS(I)),1)
20         IF(ILOG.EQ.2.AND.CS(J,I).LT.ID-15) GOTO 21
          K = K + 1
          TIME(K) = J * TS(I)
          TMPCS(K) = CS(J,I)
21         J = J + 1
          IF ( TIME(K) .LT. TTMAX ) GOTO 20
*
*
* CALL CURVE ROUTINE WITH FOLLOWING:

```

```

*      1 = NUMBER OF POINTS
*      2 = X ARRAY
*      3 = Y ARRAY
*      4 = X MIN
*      5 = X MAX
*      6 = Y MIN
*      7 = Y MAX
*      8 = LOG VALUE: IF 1 , THEN LOGARITHMIC SCALE
*      9 = NUMBER OF CURVE BEING PLOTTED
*     10 = TYPE OF DATA POINT ( SMOOTH LINE = 0, ELSE SYMBOLS )
*
      NM=I
      CALL CURVA(K,TIME,TMPCS,TTMIN,TTMAX,CCMIN,CCMAX,ILOG,NM,
1     ISYM,ISCR,NTA,IFLPL)
100  CONTINUE
      IF(IMSD.EQ.0) RETURN
      K=0
      DO 200 N=1,NINT
          IF(TM(N).GE.TMIN.AND.TM(N).LE.TMAX) THEN
              K=K+1
              TIME(K)=TM(N)
              TMPCS(K)=CM(N)
          END IF
200  CONTINUE
      ISYM=8
      I=I+1
      CALL LINE(-4)
      CALL CURVA(K,TIME,TMPCS,TTMIN,TTMAX,CCMIN,CCMAX,ILOG,I,
1     ISYM,ISCR,NTA,IFLPL)
      RETURN
      END
*****
SUBROUTINE CURVA(IPTS,XARR,YARR,AXMIN,AXMAX,AYMIN,AYMAX,
1     ILOG,NCURV,ISYM,ISCR,NTA,IFLPL)
*
      DIMENSION XARR(700),YARR(700)
*
*** IF IFLPL=0 THEN PLOT TO SCREEN, IF FILPL=3 THEN PLOT TO PLOTTER
*** MUST BE IN <AE> MODE ON GRAPHICS TERMINAL
*** ALSO REMOVE FROM THIS MODE BY <AF> WHEN FINISHED
*
      IF(IFLPL.EQ.3)CALL ANMODE
*
* INITIALIZE PLOTTER
*
      IF ( NCURV .EQ. 1 ) THEN
          CALL INITT (240)
          CALL BINITT
          ENDIF
          CALL NPTS (IPTS)
          CALL SYMBL (ISYM)

          IF ( ILOG .NE. 0 ) GOTO 100

          IF ( NCURV .EQ. 1 ) THEN
              CALL DLIMX ( AXMIN,AXMAX )
              CALL DLIMY ( AYMIN,AYMAX )
              CALL CHECK ( XARR,YARR )
              CALL DSPLAY ( XARR,YARR )
              GOTO 200
          ENDIF
*
* ARITHMETIC SCALE
*

```

```

      CALL CHECK ( XARR,YARR )
      CALL CPLOT ( XARR,YARR )
      GOTO 200
*
*   LOGARITHMIC SCALE
*
100  CALL XTYPE (2)
      IF(ILOG.EQ.2) CALL YTYPE (2)

      IF ( NCURV .EQ. 1 ) THEN
        CALL DLIMX ( AXMIN,AXMAX )
        CALL DLIMY ( AYMIN,AYMAX )
        CALL CHECK ( XARR,YARR )
        CALL DISPLAY ( XARR,YARR )
        GOTO 200
      ENDIF

      CALL CHECK ( XARR,YARR )
      CALL CPLOT ( XARR,YARR )

200  RETURN
      END
*****
      SUBROUTINE FMIN ( X,CMIN,NDI,NINT )
*
*   FIND MINIMUM VALUE
*
      IMPLICIT DOUBLE PRECISION(A-H,O-Z)
      DIMENSION X(NDI)

      CMIN = X(1)
      DO 10 N = 1,NINT
        IF ( X(N) .LT. CMIN ) CMIN = X(N)
10  CONTINUE
      RETURN
      END
*****
      SUBROUTINE SOLTRI(A,B,NNA,NN)
      IMPLICIT DOUBLE PRECISION(A-H,O-Z)
      DIMENSION A(NNA,2),B(NNA)
*****
*** SOLUTION OF TRIDIAGONAL LINEAR SYSTEM
*****
*** FORWARD SUBSTITUTION
      B(1)=B(1)/A(1,1)
      DO 10 N=2,NN
        B(N)=(B(N)-B(N-1)*A(N-1,2))/A(N,1)
10  CONTINUE
*** BACKWARD SUBSTITUTION
      N=NN
      B(N)=B(N)/A(N,1)
20  N=N-1
      B(N)=(B(N)-B(N+1)*A(N,2))/A(N,1)
      IF(N.GT.1) GOTO 20
      RETURN
      END
*****
      SUBROUTINE DECTRI(A,NNA,NN)
      IMPLICIT DOUBLE PRECISION(A-H,O-Z)
      DIMENSION A(NNA,2)
*****
*** TRIANGULAR DECOMPOSITION OF TRIDIAGONAL SYMMETRIC MATRIX
*****
      A(1,1)=DSQRT(A(1,1))

```

```

DO 10 N=2,NN
  I=N-1
  A(I,2)=A(I,2)/A(I,1)
  A(N,1)=DSQRT(A(N,1)-A(I,2)**2)
10 CONTINUE
RETURN
END
*****
SUBROUTINE MODBND(A,NNA,NN,ISOL)
IMPLICIT DOUBLE PRECISION(A-H,O-Z)
DIMENSION A(NNA,3)
*****
*** MODIFIES A FOR BOUNDARY CONDITIONS
*****
  A(1,3)=0.
  IF(ISOL.EQ.0) THEN
    A(1,1)=1.
    A(1,2)=0.
  ELSE
    A(1,1)=0.
    A(1,2)=1.
  END IF
RETURN
END
*****
SUBROUTINE MATDIS(ALP,A,R,NNA,NN,B,AT,IDIS,DISEX,DMOL)
IMPLICIT DOUBLE PRECISION(A-H,O-Z)
DIMENSION A(NNA,2),R(NNA)
*****
*** BUILDS F.D. MATRIX FOR ARBITRARY DISPERSION
*****
  BT2=B*AT/2.
  X1=0.
  DO 10 I=1,NN-1
    R2=R(I)*R(I)+BT2
    R1=DSQRT(R2)
    IF(IDIS.EQ.1) THEN
      U=ALP*R1/B
      U=(ALP+DMOL)*R1/B
    ELSE IF(IDIS.EQ.2) THEN
      U=ALP*B/R1
    ELSE
      U=ALP*((B/R1)**(DISEX-1.))
      U=(ALP*((B/R1)**DISEX)+DMOL)*R1/B
    END IF
    X=U/(R(I+1)-R(I))
    A(I,1)=1.+X+X1
    A(I,2)=-X
    X1=X
10 CONTINUE
  A(NN,1)=1.+X1
  A(NN,2)=0.
RETURN
END

```

REFERENCES

- Barackman, M. L. (in preparation), Diverging-Flow Tracer Tests in Fractured Rock: Equipment Design and Data Collection, Unpublished Master's Thesis, University of Arizona, Tucson, Arizona.
- Bear, J., 1979, Hydraulics of Groundwater, McGraw-Hill, Inc.
- Brenner, H., 1962, The diffusion model of the longitudinal mixing in beds of finite length: Numerical values, Chem. Eng. Sci., vol. 17, pp. 229-243.
- Carrera, J., G. R. Walter (in preparation), An Application of Convergent Flow Tracer Tests: Numerical Studies of Design Parameters and Sensitivity of Convergent Flow Tracer Tests, Hydro Geo Chem. Inc., Tucson, Arizona.
- Chen, C., 1985, Analytical and approximate solutions to radial dispersion from an injection well to a geological unit with simultaneous diffusion into adjacent strata, WRR, vol. 21(8), pp. 1069-1076.
- Cullen, J. J., K. J. Stetzenbach and E. S. Simpson, 1985, Field studies of solute transport in fractured crystalline rock near Oracle, Arizona, Proceedings of 17th International Congress of the International Association of Hydrogeologists--Hydrogeology of Rocks of Low Permeability, pp. 332-344, Tucson, Arizona.
- DaCosta, J. A. and R. R. Bennett, 1960, The pattern of flow in the vicinity of a recharging and discharging pair of wells in an aquifer having areal parallel flow, Int. Ass. Sci. Hydrol. Pub. 52, pp. 524-536.
- Depner, J. S., 1985, Estimation of Spatial Covariance of Log Permeability Using Directional and Non-directional Measurements, Unpublished Master's Thesis, University of Arizona, Tucson, Arizona.
- Domenico, P. A. and G. A. Robbins, 1984, A dispersion scale effect in model calibrations and field tracer experiments, J. Hydrol., vol. 70, pp. 123-132.
- Ebach, E. A. and R. R. White, 1958, Mixing of fluids flowing through beds of packed solids, J. Am. Inst. Chem. Eng., vol. 2(4), pp. 161-164.

- Freeze, R. A. and J. A. Cherry, 1979, Groundwater, Prentice-Hall, Englewood Cliffs, New Jersey.
- Fried, J. J., 1975, Groundwater Pollution, Elsevier, Amsterdam.
- Gelhar, L. W. and M. A. Collins, 1971, General analysis of longitudinal dispersion in nonuniform flow, WRR, vol. 7(6), pp. 1511-1521.
- Gershon, N. D. and A. Nir, 1969, Effects of boundary conditions of models on tracer distribution in flow through porous mediums, WRR, vol. 5(4), pp. 830-839.
- Grisak, G. E., K. J. Stetzenbach, G. M. Thompson, S. Jenson, W. Stensrud, J. Fabryka-Martin, and P. A. Hsieh, 1982, Multiple tracer tests in granite using field HPLC methods, in: Field and Theoretical Investigations of Mass and Energy Transport in Sub-surface Materials, progress report to the U. S. Nuclear Regulatory Commission, Contract No. NRC-04-78-275, prepared by E. S. Simpson, S. P. Neuman, and G. M. Thompson.
- Grove, D. B. and W. A. Beetem, 1971, Porosity and dispersion constant calculations for a fractured carbonate aquifer using the two well tracer method, WRR, vol. 7(1), pp. 1287-134.
- Harleman, D. R. F. and R. R. Rumer, 1962, Longitudinal and lateral dispersion in an isotropic porous medium, J. Fluid Mech., vol. 16(3), pp. 385-394.
- Hoopes, J. A. and D. R. F. Harleman, 1967, Dispersion in radial flow from a recharging well, J. Geoph. Res., vol. 72(14), pp. 3595-3607.
- Huyakorn, P. S. and G. F. Pinder, 1983, Computational Methods in Sub-surface Flow, Academic Press.
- Jones, J. W., E. S. Simpson, S. P. Neuman and W. S. Keys, 1985, Field and Theoretical Investigations of Fractured Crystalline Rock near Oracle, Arizona, NUREG/CR-3736 Report to Nuclear Regulatory Commission, Department of Hydrology and Water Resources, University of Arizona, Tucson, Arizona.
- Lau, L. W., W. J. Kaufman and D. K. Todd, 1959, Dispersion of a water tracer in radial laminar flow through homogeneous porous media, Prog. Rep. 5, Canal Seepage Res., University of California, Berkeley.

- Mandel, S., Y. Bachmat, W. Drost and M. Bugayevsky, 1985, Estimation of longitudinal dispersivity, effective porosity and flow velocity by a single well tracer technique, Scientific Basis for Water Resources Management, Proceedings of the Jerusalem Symposium, IAHS pub. 153, pp. 219-229.
- Mercado, A., 1966, Recharge and mixing tests at Yavne 20 well field, Underground Water Storage Study Tech. Rep. 12, Publ. 611, TAHAL-Water Planning for Israel Ltd., Tel Aviv.
- Messer, A. (in preparation), Fracture permeability investigations using a heat-pulse flow meter, Unpublished Master's Thesis, University of Arizona, Tucson, Arizona.
- Novakowski, K. S., G. V. Evans, D. A. Lever and K. G. Raven, 1985, A field example of measuring hydrodynamic dispersion in a single fracture, WRR, vol. 21(8), pp. 1165-1174.
- Ogata, A., 1970, Theory of dispersion in granular medium, U. S. Geol. Surv. Prof. Paper 411-I.
- Ogata, A. and R. B. Banks, 1961, A solution of the differential equation of longitudinal dispersion in porous media, U. S. Geol. Surv. Prof. Paper 411-A.
- Pickens, J. F. and G. E. Grisak, 1981, Scale-dependent dispersion in a stratified granular aquifer, WRR, vol. 17(4), pp. 1191-1211.
- Raimondi, P., G. H. F. Gardner and C. B. Petrick, 1959, Effect of pore structure and molecular diffusion on the mixing of miscible liquids flowing in porous media, A.I.Ch.E., Soc. Petrol. Eng. Joint Symp., "Oil Recovery Methods," San Francisco, Preprint 43.
- Rifia, M. N. E., W. J. Kaufman and D. K. Todd, 1956, Dispersion phenomena in laminar flow through porous media, Inst. Eng. Res. Ser. 90, Rep. 3, University of California, Berkeley.
- Rouse, H., 1938, Fluid Mechanics for Hydraulic Engineers, McGraw-Hill Book Company, Inc.
- Sauty, J. P., 1977, Contribution a l'Identification des Parameters de Dispersion dans les Aquifers par Interpretation des Experiences de Tracage, Unpublished Ph.D. Dissertation, L'University Scientifique et Medicale et Institute National Polytechnique de Grenoble, France.
- Sauty, J. P., 1980, An analysis of hydrodispersive transport in aquifers, WRR, vol. 16(1), pp. 145-158.

- Silliman, S. E., 1985, unpublished field data, University of Arizona, Tucson, Arizona.
- Silliman, S. E., M. Barackman and A. Messer, 1985, Identification of Fracture Interconnections by Borehole Temperature Logging, AGU Fall Meeting, December December 9-13, 1985, San Francisco.
- Webster, D. S., J. F. Proctor and I. W. Marine, 1970, Two-well tracer test in fractured crystalline rock, U. S. Geol. Surv. Water-Supply Pap. 1544-I.